EUB/AGS Earth Sciences Report 2002-07

Petrographic Characteristics of Selected Kimberlitic Rocks in Northern Alberta

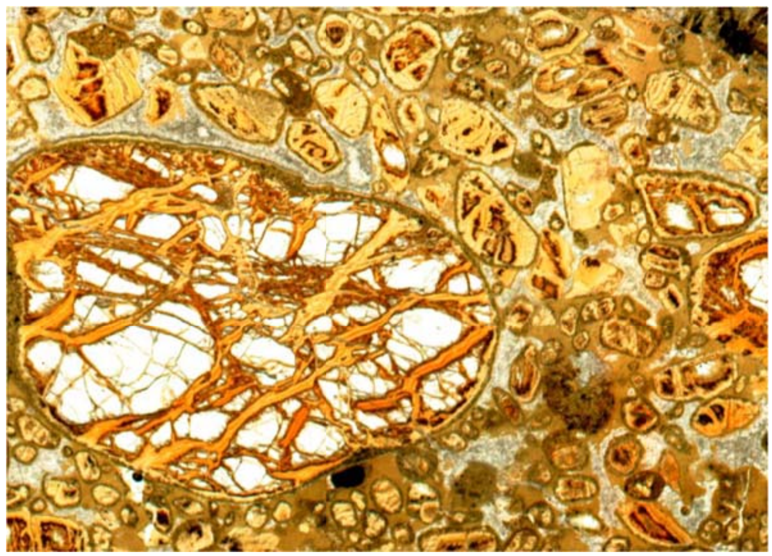

Alberta Energy and Utilities Board
Alberta Geological Survey

EUB/AGS Earth Sciences Report 2002-07

Petrographic Characteristics of Selected Kimberlitic Rocks in Northern Alberta

D. Roy Eccles

Alberta Geological Survey

February 2004

ISBN 0-7785-1509-5

Eccles, D.R. (2004): Petrographic characteristics of selected kimberlitic rocks in northern Alberta; Alberta Energy and Utilities Board, EUB/AGS Earth Sciences Report 2002-07.

Published February 2004 by:
Alberta Energy and Utilities Board
Alberta Geological Survey
4th Floor, Twin Atria Building
4999 – 98th Avenue
Edmonton, Alberta
T6B 2X3

Tel: (780) 422-3767 (Information Sales)
Fax: (780) 422-1918

E-mail: EUB.AGS-Infosales@gov.ab.ca
Web Site: www.gov.ab.ca

Contents

Acknowledgments.. vi
Abstract.. vii
1 Introduction 1
2 Selection Criteria for Detailed Petrography 2
3 Kimberlite Nomenclature and Classification 4
3.1 Nomenclature... 4
3.2 Classification.. 6
4 Petrographic Descriptions of Selected Samples 7
4.1 Samples ABK01, ABK02 and ABK03 (K4 Complex, Buffalo Head Hills) 8
4.1.1 Sample ABK01 (K4A Pipe, Buffalo Head Hills) 9
4.1.2 Sample ABK02 (K4B Pipe, Buffalo Head Hills) 9
4.1.3 Sample ABK03 (K4C Pipe, Buffalo Head Hills) 11
4.2 Samples ABK05 and ABK29 (K6 Pipe, Buffalo Head Hills) 13
4.3 Samples ABK59 and ABK68 (Legend Pipe, Birch Mountains) 20
4.4 Samples ABK75 and ABK76 (Phoenix Pipe, Birch Mountains)... 23
4.5 Samples ABK81 and ABK82 (Kendu Pipe, Birch Mountains) 27
5 Mineralogical Summary... 28
5.1 Olivine 32
5.2 Serpentine 32
5.3 Carbonate...32
5.4 Phlogopite 34
5.5 Apatite..35
5.6 Perovskite...35
5.7 Opaque Minerals 35
6 Textural-Genetic Classification 36
7 Mineralogical-Genetic Classification 38
8 Geochemical-Petrographic Comparison...38
8.1 K4 Pipe..39
8.2 K6 Pipe 39
8.3 Legend Pipe 41
8.4 Phoenix Pipe 41
8.5 Kendu Pipe...41
9 Conclusions..41
10 References...43
Appendix 1 – Electron-Microprobe Backscatter and x-ray Elemental Images 46
Appendix 2 – Bulk-Rock x-ray Diffractograms 52

Tables

Table 1 Samples selected for detailed petrography. 2
Table 2 Mineralogical comparisons between kimberlites, orangeites and lamproites (slightly modified from Mitchell, 1995). 5
Table 3 Summary of x-ray diffraction analysis on selected whole-rock northern Alberta kimberlitic rocks. 8
Table 4 Summary of the unique properties, infilling and classification of selected northern Alberta kimberlitic rocks. 37

Figures

Figure 1 Basement domains of northern Alberta, showing the Mountain Lake, Buffalo Head Hills and Birch Mountains ultramafic diatreme fields 1
Figure 2 Major- and trace-element groupings, based on principal component analysis by Eccles and Luth (2001) 3
Figure 3 Photomicrographs of sample ABK01, K4A pipe, Buffalo Head Hills: A) scan of polished thin section; B) representative matrix; and C) radiating quartz textures indicative of secondary, hydrothermal emplacement..10
Figure 4 Photomicrographs of sample ABK02, K4B pipe, Buffalo Head Hills: A) scan of polished thin section; B) representative matrix; C) curvilinear lapillus; D) comparison between lapillus matrix and matrix that encompasses lapillus; and E) pyrite nucleating on dolomite 12
Figure 5 Backscatter image of representative area from sample ABK02, K4B pipe, Buffalo Head Hills. 13
Figure 6 Photomicrographs of sample ABK03, K4C pipe, Buffalo Head Hills: A) scan of polished thin section; B) and C) selected images of tabular serpentine under plane and crossed polars, respectively 14
Figure 7 Scanned images of polished thin sections from samples ABK05 and ABK29, K6 pipe, Buffalo Head Hills. 16
Figure 8 Variation between juvenile lapilli from the K6 pipe, Buffalo Head Hills: A) large, curvilinear lapillus; and B) ash- to lapilli-sized, juvenile pyroclasts 17
Figure 9 Ash- and lapilli-sized, juvenile pyroclasts from the K6 pipe, Buffalo Head Hills: A) in hand sample; and B) photomicrograph mosaic capturing the entire pyroclast, in plane-polarized light..18
Figure 10 Photomicrographs of sample ABK05, K6 pipe, Buffalo Head Hills: A) backscatter image of representative matrix; B) perovskite; C) skeletal crystals of ilmenite; and D) intergrown ilmenite (light grey) and chromite (dark grey)..19
Figure 11 Mantle xenolith from sample ABK29, K6 pipe, Buffalo Head Hills: A) expanded view of the xenolith in contact with kimberlite; B) clinopyroxene and orthopyroxene; and C) IUGS classification of ultramafic rocks 21
Figure 12 Basement xenolith from sample ABK29, K6 pipe, Buffalo Head Hills 22
Figure 13 Photomicrographs of sample ABK59, Legend pipe, Birch Mountains: A) scan of polished thin section; B) enlargement of image A, with lapillus; C) lapillus; D) hexagonal apatite; E) needle-textured sulphide mineral (?pyrite); and F) ilmenite 24
Figure 14 Photomicrographs of sample ABK76, Phoenix pipe, Birch Mountains: A) scan of polished thin section; B) enlargement of image A; C) lapillus; D) matrix perovskite and phlogopite; and E) and F) atoll-textured spinel 25
Figure 15 Backscatter image of representative area from sample ABK76, Phoenix pipe, Birch Mountains. 26
Figure 16 Photomicrographs of sample ABK81, Kendu pipe, Birch Mountains: A) scan of polished thin section; B) juvenile lapillus in an aphanitic matrix; C) matrix comparison between pyroclast and matrix external to lapillus; and D) magnified image of an lapillus. 29
Figure 17 Photomicrographs of the Kendu pipe, Birch Mountains: A) microphenocrystic kimberlitic rock haloes around altered basement xenoliths; B) and C) pelletal-textured lapilli with tangentially aligned phlogopite crystals; and D) matrix microsegregation textures 30

Figure 18 Photomicrographs of mantle minerals from the Kendu pipe, Birch Mountains 31
Figure 19 Modal distribution of olivine, as determined in thin section, from selected northern Alberta kimberlitic pipes.. 33
Figure 20 Comparison of MgO+FeO versus SiO_2 for samples from the Buffalo Head Hills (Eccles and Luth, 2001) and olivine macrocrysts from Mitchell (1986)................................. 40
Figure 21 Micro-image of sample ABK02, kimberlite K4B. A) and B) backscattered electron images; C) to L) x-ray elemental images... 47
Figure 22 Micro-image of sample ABK05, kimberlite K6. A) and B) backscattered electron images; C) to L) x-ray elemental images... 48
Figure 23 Micro-image of sample ABK59, Legend kimberlite. A) and B) backscattered electron images; C) to L) x-ray elemental images... 49
Figure 24 Micro-image of sample ABK76, Phoenix kimberlite. A) and B) backscattered electron images; C) to L) x-ray elemental images... 50
Figure 25 Micro-image of sample ABK81, Kendu kimberlite. A) and B) backscattered electron images; C) to L) x-ray elemental images... 51
Figure 26 X-ray diffractogram for sample ABK-01, kimberlite K4A, Buffalo Head Hills. 53
Figure 27 X-ray diffractogram for sample ABK-02, kimberlite K4B, Buffalo Head Hills. 54
Figure 28 X-ray diffractogram for sample ABK-03, kimberlite K4C, Buffalo Head Hills. 55
Figure 29 X-ray diffractogram for sample ABK-05, kimberlite K6, Buffalo Head Hills. 56
Figure 30 X-ray diffractogram for sample ABK-29, kimberlite K6, Buffalo Head Hills. 57
Figure 31 X-ray diffractogram for sample ABK-59, Legend kimberlite, Birch Mountains..................... 58
Figure 32 X-ray diffractogram for sample ABK-68, Legend kimberlite, Birch Mountains. 59
Figure 33 X-ray diffractogram for sample ABK-75, Phoenix kimberlite, Birch Mountains.................... 60
Figure 34 X-ray diffractogram for sample ABK-76, Phoenix kimberlite, Birch Mountains. 61
Figure 35 X-ray diffractogram for sample ABK-81, Kendu kimberlite, Birch Mountains...................... 62
Figure 36 X-ray diffractogram for sample ABK-82, Kendu kimberlite, Birch Mountains...................... 63

Acknowledgments

Rick Richardson, Reg Olson and Mark Fenton of the Alberta Geological Survey and Bob Luth, Larry Heaman, Rob Creaser and Thomas Stachel of the University of Alberta are thanked for their intuitive discussion regarding the direction and goals of this project.

No petrographic study could be completed without access to the rocks, and Ashton Mining of Canada Inc., Kennecott Canada Exploration Inc., Montello Resources Ltd., Redwood Resources Ltd. and New Blue Ribbon Resources Ltd. (now Blue Diamond Corporation) are thanked for their roles in the discovery of kimberlite occurrences in Alberta and for providing samples of Alberta kimberlitic rocks.

Andrew Skupinski of Tatra Mineralogical Services and Barbara Scott Smith of Scott-Smith Petrological Inc. are thanked for their insightful and patient responses to the many petrological questions.

Sergei Matveev and Diane Caird at the University of Alberta are thanked for operation of the electron microprobe and x-ray diffraction spectrometer, respectively.

Larry Heaman from the Department of Earth and Atmospheric Sciences, University of Alberta; Glen Prior from the Alberta Geological Survey; and Bob Davie from RnD Technical are all thanked for editing the manuscript.

Abstract

Five kimberlitic pipes in the northern Alberta kimberlite province were selected for detailed petrography: K4 and K6 from the Buffalo Head Hills; and Legend, Phoenix and Kendu from the Birch Mountains. Part of the selection criteria was based on the whole-rock geochemical results of Eccles and Luth (2001) who suggested a linear geochemical trend reflects the compositional evolution of northern Alberta kimberlites from primitive to evolved kimberlite magmas. The main objective, therefore, is to complement and expand upon the whole-rock geochemistry with optical mineralogical observations of selected pipes.

Volcaniclastic rock types with distinct colours, mineralogical compositions, textures, and mantle xenolith and xenocryst contents are present in the pipes studied. Crater-type pyroclastic kimberlite (PK) is by far the dominant rock type followed by less common resedimented volcaniclastic kimberlite (RVK). Based on detailed mineralogical descriptions, the rocks are classified as serpentine kimberlite to carbonate-rich serpentine kimberlite.

The PK rocks are described as juvenile, lapilli-bearing olivine tuff. The observed macrocryst suite of minerals includes rounded, typically <1 cm wide, forsteritic olivine with minor phlogopite and ilmenite. The groundmass is dominated by subhedral olivine microphenocrysts (<0.25 mm) set in a fine-grained serpentine- and often carbonate-rich groundmass together with one or more of the following primary minerals: phlogopite, perovskite, spinel, ilmenite and apatite.

The PK and RVK typically include darker, finer-grained and opaque-rich spherical- and amoeboid-shaped juvenile lapilli. Several types of lapilli may be present in the PK rocks, which may be the result of multiple eruption episodes that have subsequently mixed. Multi-generation lapilli, or lapillus that formed mantles for later generations of lapillus development support this. The recognition and description of different types of lapillus may be helpful for emplacement modeling. For example, ash- to lapilli-sized juvenile pyroclasts (i.e., variably-sized single crystal olivine coated by juvenile material), which are diagnostic of the east side of the K6 pipe surface exposure, are related to a near-vent environment.

The Kendu pipe rocks are described as volcaniclastic kimberlite, where juvenile lapilli and an abundance of basement and mantle xenoliths occur within a non-uniform, segregated matrix. In the Kendu pipe, the lapilli and xenoliths occur together with less common pelletal-textured lapilli, which have a rim of tangentially aligned, extremely fine grained (<0.01 mm long) phlogopite- and serpentine-rich (lizardite) microlitic material surrounding olivine pseudomorphs. Flow-aligned textures also form ‘haloes’ around pre-existing constituents that include some irregularly shaped, altered xenoliths.

Kimberlite K6, Buffalo Head Hills, has the highest modal amount of coarse, macrocrystic olivine, and this is one of the main petrographic criteria that separate the diamondiferous K6 pipe from barren pipes studied in this report. The Legend and Phoenix pipes, Birch Mountains, are highly carbonatized, relatively devoid of olivine macrocrysts and have much higher concentrations of late-stage minerals phlogopite, apatite and perovskite, all of which are suggestive of evolved kimberlite magma.

A petrographic-geochemical comparison shows that identification of the primary mineral assemblage, together with whole-rock geochemical interpretation that uses both major and trace elements, provides a complementary tool to successfully classify Alberta kimberlitic rocks.

1 Introduction

The northern Alberta kimberlite province (NAKP) comprises three separate areas of kimberlitic rock occurrences: Mountain Lake cluster, and Buffalo Head Hills and Birch Mountains fields, located in northwestern, north-central and northeastern Alberta, respectively (Figure 1).

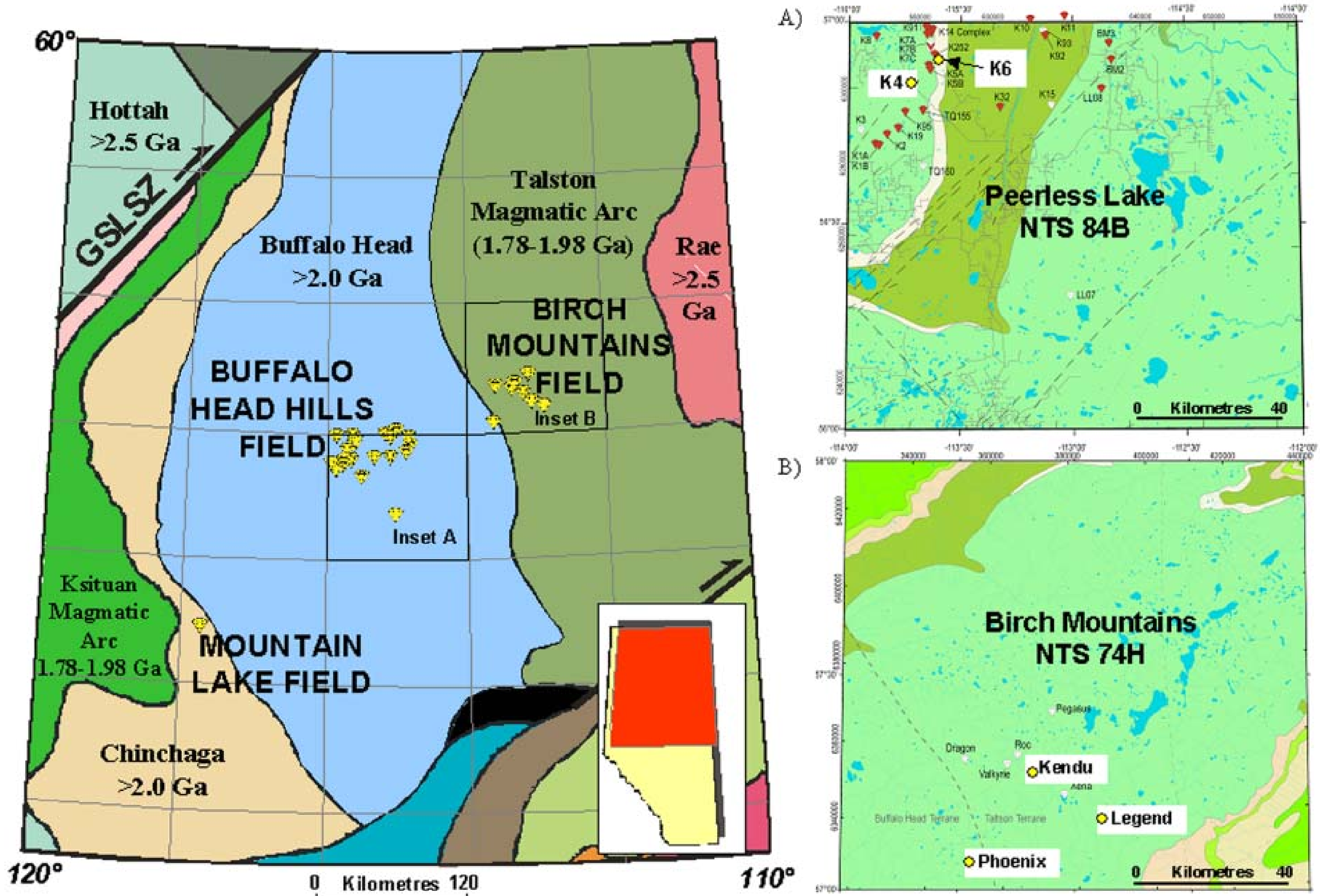

Figure 1. Basement domains of northern Alberta, showing the Mountain Lake, Buffalo Head Hills and Birch Mountains ultramafic fields. Inset A) geology of Buffalo Head Hills area, showing selected pipes K4 and K6, B) geology of Birch Mountains area, showing selected pipes Legend, Phoenix and Kendu.

This report is the second of a series intended to investigate the petrogenesis of kimberlite in Alberta. Previously, Eccles and Luth (2001) documented the major- and trace-element whole-rock geochemical content of 83 samples from the three kimberlitic fields.

On the basis of bulk-rock geochemical analyses, Eccles and Luth (2001) concluded that pipes from the Buffalo Head Hills and Birch Mountains fields have chemistries similar to South African Group I kimberlite. Of the two kimberlite fields, the Buffalo Head Hills group has the highest MgO, Cr and Ni values, the lowest Al_2O_3, SiO_2, V, Y, Pb, Sr and Ga contents, and a chemistry similar to primitive kimberlite in the Northwest Territories, Canada. The Buffalo Head Hills field may therefore be classified as containing the more primitive kimberlite rocks in this dataset. In contrast, the Birch Mountains kimberlites are more evolved, with lower SiO_2, Ni and Mg#, and higher Fe_2O_3, TiO_2, Nb, V, Sc, Zr, Hf, Y, Ba, Rb, light rare-earth elements (LREE), Ga and Pb.

This report complements and expands upon the whole-rock geochemical study of Eccles and Luth (2001), using optical mineralogical observations of selected kimberlites in the NAKP.

2 Selection Criteria for Detailed Petrography

The current report uses the results of the whole-rock geochemical report of Eccles and Luth (2001) as a basis for the selection of NAKP pipes for detailed petrographic interpretation. Eccles and Luth (2001) suggested that a kimberlite magma-evolution 'trend line' can be used to represent the compositional evolution from primitive to evolved kimberlite on Figure 2. These data were classified into five separate 'groups,' based on similar whole-rock geochemical distributions, and are interpreted to represent varying degrees of kimberlite magma evolution.

These groups form the basis for sample selection in this study. That is, a pipe from each geochemical 'group' was selected for detailed petrographic interpretation: K4 and K6 from the Buffalo Head Hills, and Legend, Phoenix and Kendu from the Birch Mountains. Hence, the sample set was selected to represent a variation of primitive to evolved kimberlite, as suggested by Eccles and Luth (2001). Two samples were collected at various depths from each of the K6, Legend, Phoenix and Kendu pipes, and one sample was collected from each of three pipes that make up the K4 complex, for a total of 11 samples (Table 1; Figures 1, 2).

Table 1. Samples selected for detailed petrography.

Sample number	Pipe name (general area)[1]	Drill hole number	Depth (m)	Easting (m)	Northing (m)	UTM zone
ABK-01	K4A (BHH)	4A-02	49.15	578380	6301519	11
ABK-02	K4B (BHH)	4B-01	140.65	578464	6300991	11
ABK-03	K4C (BHH)	4C-01	63.00	578821	6301274	11
ABK-05	K6 (BHH)	6-02	110.15	585550	6308383	11
ABK-29	K6 (BHH)	Outcrop	0 –(surface)	585317	6308651	11
ABK-59	Legend (BM)	98DH-LE01	44.00	386200	6340600	12
ABK-68	Legend (BM)	98DH-LE01	187.00	386200	6340600	12
ABK-75	Phoenix (BM)	98DH-PH01	105.00	351500	6330580	12
ABK-76	Phoenix (BM)	98DH-PH01	130.00	351500	6330580	12
ABK-81	Kendu (BM)	Kendu	102.00	368567	6353618	12
ABK-82	Kendu (BM)	Kendu	127.25	368567	6353618	12

[1] Abbreviations: BHH, Buffalo Head Hills, north-central Alberta; BM, Birch Mountains, northeastern Alberta

It is important to note that, except for one sample (ABK29 from kimberlite K6), sample descriptions from the Buffalo Head Hills are based on single, hand-sized samples, and may therefore not be representative of the overall intrusion. Specifically, not all characteristic phases may be present in a single sample, and examination of a suite of rocks or complete drillcore was not possible. Sample ABK29 is from an exposed outcrop of K6 on the southeastern flanks of the Buffalo Head Hills; a suite of samples was subsequently collected from outcrop for interpretation in consultation with Ashton Mining of Canada Inc.

Component	SiO_2	Al_2O_3	Fe_2O_3	MgO	CaO	Na_2O	K_2O	TiO_2	P_2O_5	MnO	Cr_2O_3	Ba	Ni	Ga	Nb	Rb	Sr	Th	V	Zr	Y	Pb
1	***0.88***	***0.93***	-0.68	-0.76	-0.35	***0.88***	***0.90***	-0.48	-0.46	-0.57	-0.78	***0.11***	-0.57	***0.80***	-0.69	***0.86***	-0.36	-0.59	***0.33***	-0.23	***0.39***	***0.31***
2	-0.16	***0.27***	***0.50***	-0.49	***0.52***	***0.12***	***0.23***	***0.68***	***0.69***	***0.61***	-0.08	***0.69***	-0.66	***0.47***	***0.66***	***0.31***	***0.61***	***0.65***	***0.71***	***0.79***	***0.83***	***0.76***
3	***0.20***	***0.13***	***0.35***	***0.06***	-0.50	***0.03***	-0.16	***0.44***	-0.37	-0.01	***0.11***	-0.43	-0.19	***0.30***	***0.20***	-0.15	-0.46	***0.26***	***0.20***	***0.18***	***0.09***	-0.25
4	-0.25	-0.03	-0.24	-0.33	***0.51***	-0.08	-0.15	***0.11***	-0.16	***0.11***	-0.32	-0.39	-0.29	-0.03	-0.05	-0.16	-0.05	-0.14	***0.04***	***0.10***	***0.05***	-0.29
5	***0.06***	-0.04	-0.14	***0.03***	-0.19	-0.09	-0.09	-0.07	-0.03	-0.39	-0.21	-0.10	-0.04	-0.05	***0.07***	-0.06	***0.33***	***0.12***	-0.15	***0.40***	***0.03***	***0.04***

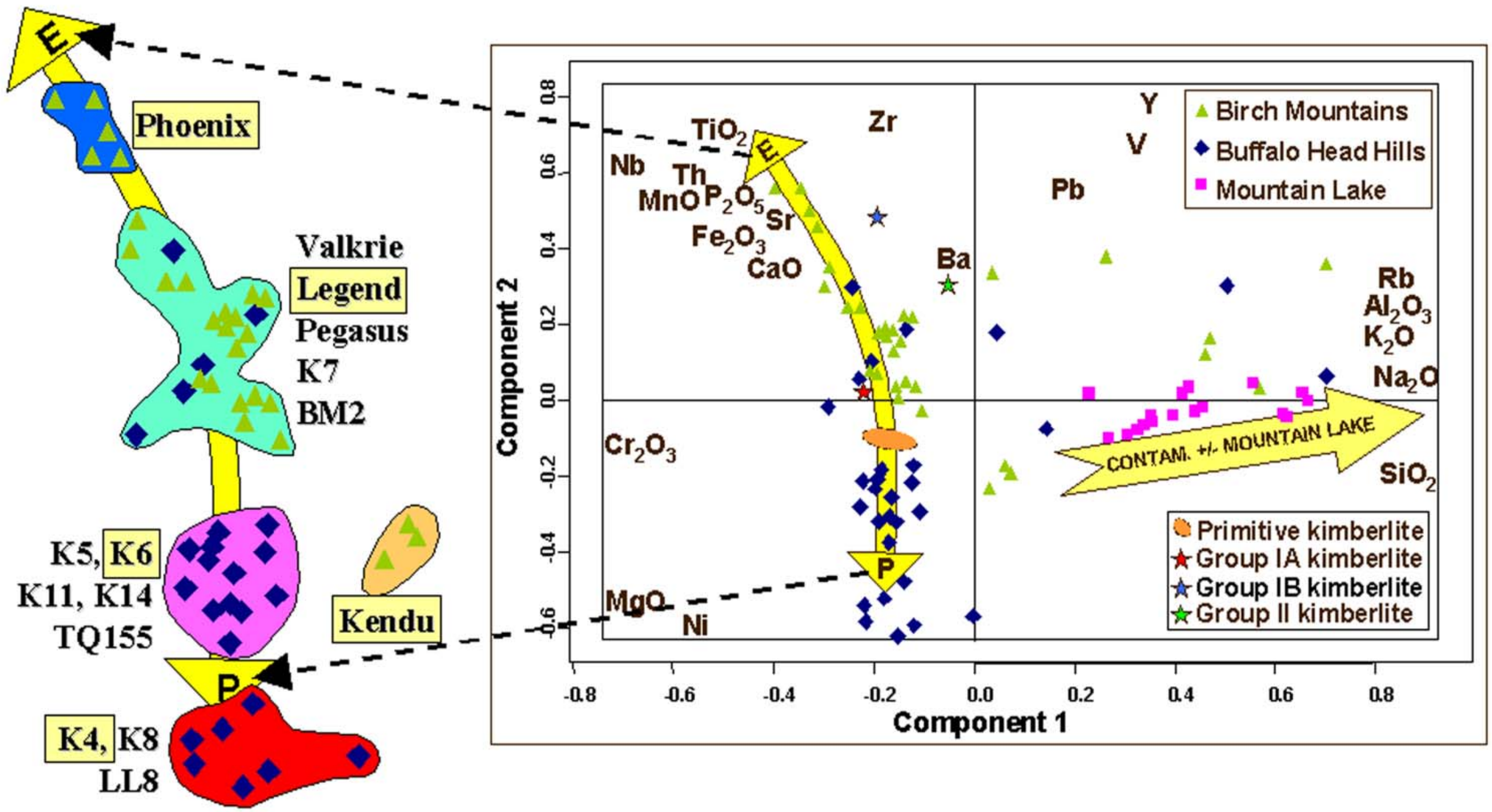

Figure 2. Major- and trace-element groupings, based on principal component analysis by Eccles and Luth (2001). Relative contributions of selected major and trace elements expressed as R-scores in table at top of figure, with positive values in bold. Solid yellow line represents Alberta kimberlite magma-evolution trend line, from primitive)p) to evolved (E) kimberlitic rocks. Geochemical groupings and pipes selected for detailed petrography are highlighted in yellow boxes on right side of figure.

In contrast, complete drillcore intersections were available for the Birch Mountains pipes by Kennecott Canada Exploration Inc., Montello Resources Ltd., Redwood Resources Ltd. and New Blue Ribbon Resources Ltd.

3 Kimberlite Nomenclature and Classification

3.1 Nomenclature

Wagner (1914) published the first comprehensive summary of kimberlite diatreme occurrences in South Africa. His important petrological observation, which remains valid today, was that South African kimberlite can be subdivided into two groups: ‘basaltic’ and ‘micaceous or lamprophyric’ kimberlite, based on the assemblage of primary minerals.

More recently, detailed studies on South African kimberlites have demonstrated that basaltic and micaceous kimberlite groups are geochemically, mineralogically and petrogenetically separate rock types that have been designated Group I and Group II kimberlites, respectively (Smith, 1983; Smith et al., 1985; Skinner, 1989).

Although petrologists actively studying kimberlites have concluded there are significant petrological differences between the two groups, opinion is divided regarding the extent to which kimberlite nomenclature needs to be revised. Some wish to retain the status quo (e.g., Skinner, 1989), whereas others (e.g., Mitchell and Bergman 1991; Mitchell, 1995) propose that the terminology should be completely revised and the nomenclature changed (*see* below).

Following a concept originally developed by Dawson (1980), kimberlite can be recognized as containing a characteristic assemblage of minerals. The following characterization of Group I kimberlites is from Mitchell (1995). The definition evolved from Mitchell (1986, 1994) and earlier ‘definitions’ by Mitchell (1979) and Clement et al. (1984):

> “Kimberlites are a group of volatile-rich (dominantly CO_2) potassic ultrabasic rocks commonly exhibiting a distinctive inequigranular texture resulting from the presence of macrocrysts (and in some instances megacrysts) set in a fine-grained matrix. The mega/macrocryst assemblage consists of anhedral crystals of olivine, magnesian ilmenite, Cr-poor titanian pyrope, diopside (commonly subcalcic), phlogopite, enstatite, and Ti-poor chromite. Olivine macrocrysts are a characteristic constituent in all but fractionated kimberlites. The matrix contains a second generation of primary euhedral-to-subhedral olivine which occurs together with one of more of the following primary minerals: monticellite, phlogopite, perovskite, spinel (magnesian ulvöspinel-Mg-chromite-ulvöspinel-magnetite solid solutions), apatite and serpentine. Many kimberlites contain late-stage poikilitic micas belonging to the barian phlogopite-kinoshitalite series. Nickeliferous sulfides and rutile are common accessory minerals. The replacement of earlier formed olivine, phlogopite, monticellite, and apatite by deuteric serpentine and calcite is common. Evolved members of the group may be poor in, or devoid of, macrocrysts and/or composed essentially of second-generation olivine, calcite, serpentinite and magnetite, together with minor phlogopite, apatite and perovskite.”

Group II kimberlite terminology is less clear. Mitchell (1995) suggested that these rocks should be termed ‘orangeite,’ in recognition of their distinct character and Wagner’s (1928) previous suggestion that the micaceous kimberlite rocks be renamed ‘orangite’ [*sic*]. The following characterization of the rocks currently described as Group II kimberlite or orangeite is that of Mitchell (1995):

"Orangeites are a clan of ultrapotassic peralkaline volatile-rich (dominantly H_2O-rich) rocks, characterized by the presence of phlogopite macrocrysts and microphenocrysts, together with groundmass micas, which vary in composition from phlogopite to tetraferriphlogopite. Rounded olivine macrocrysts and euhedral primary olivines are common, but are not always major constituents. Characteristic primary groundmass phases include diopside, commonly zoned to, and mantled by, titanian aegirine, spinels ranging in composition from Mg-chromite to Ti-magnetite, Sr- and REE-rich perovskite, Sr-rich apatite, REE-rich phosphates (monazite, daqingshanite), potassian barian titanates belonging to the hollandite group, potassium triskaidecatitanates, Nb-rutile, and Mn-ilmenite. These are set in a groundmass, which may contain calcite, dolomite, ancylite, and other rare earth carbonates, witherite, norsethite and serpentine. Evolved members of the group contain groundmass sanidine and potassium richterite. Zirconium silicates (wadeite, zircon, kimzeyitic garnets, Ca-Zr silicate) are common as late-stage groundmass minerals. Quartz may occur rarely as mesostasis mineral. Barite is a common secondary mineral."

Based on Mitchell's (1995) description, orangeites have a greater mineralogical affinity to lamproites than to Group I kimberlites. There are, however, significant differences in the compositions and overall mineral assemblage (Table 2) that permit their discrimination from lamproites.

Table 2. Mineralogical comparisons between kimberlites, orangeites and lamproites (*slightly modified from* Mitchell, 1995).

		Kimberlites	Orangeites	Lamproites
Olivine	Macrocrysts	Common	Common to rare	Rare
	Phenocrysts	Common: subhedral/ euhedral	Minor: subhedral to euhedral to dog's tooth	Common
Mica	Macrocrysts	Minor: phlogopite	Common: phlogopite	Common: phlogopite to Ti-phlogopite
	Phenocrysts	Rare: phlogopite	Common: phlogopite	Ti-phlogopite
	Groundmass	Common: phlogopite-kinoshitalite	Common: phlogopite to tetraferriphlogopite	Common: Ti-tetraferriphlogopite
Spinels		Abundant: Mg- chromite to Mg-ulvospinel (Trend 1)	Rare: Mg-chromite to Ti-magnetite (Trend 2)	Rare: Mg-chromite to Ti-magnetite
Monticellite		Common	Absent	Absent
Diopside		Primary diopside absent	Common: Al and Ti poor	Common: Al and Ti poor
Perovskite		Common: Sr and REE poor	Rare: Sr and REE rich	Rare: Sr and REE rich
Apatite		Common to rare: Sr and REE poor	Abundant euhedral prisms: Sr and REE rich	Common: Sr and REE rich
Carbonate		Common calcite; minor dolomite	Common calcite; common Sr-Mn-Fe dolomite	Absent
Serpentine		Common primary and secondary	Common: secondary	Common: secondary
Sanidine		Absent	Rare: groundmass	Common: phenocrysts and groundmass
K-richterite		Absent	Rare: groundmass	Common: phenocrysts and groundmass
K-Ba-titanates		Very rare	Common	Common
Zr-silicates		Very rare	Common	Common
Mn-ilmenite		Rare	Common	Very rare
Leucite		Absent	Rare: pseudomorphs	Common: phenocrysts
Barite		Rare	Common	Common: (?) late stage hydrothermal veins and vesicle fillings

Although the concept of a two-group classification system (Group I and Group II, or kimberlite and orangeite) seems relatively straightforward, the variable nature of a hybrid rock such as kimberlite tends to add controversy. At least two authors have described rocks that require further classification. For example, Smith et al. (1985) further subdivided South African Group I kimberlites into Group IA (on craton) and Group IB (off craton), on the basis of their chemistry. Compared to Group IA, Group IB kimberlites have lower SiO_2 and higher CaO, $FeO+Fe_2O_3$ and volatile contents, as well as somewhat higher TiO_2, P_2O_5, Nb, Zr and Y. Furthermore, Skinner et al. (1994) proposed a 'transitional' kimberlite group on the basis that rocks occurring primarily in 'domain V' of the Prieska region in South Africa have isotopic signatures that are intermediate between those of kimberlite and orangeite. Skinner et al. (1994) reported that the transitional rocks have petrographic affinities to Group I kimberlite, as they contain relatively abundant, coarse-grained, primary spinel and perovskite. In addition, Mitchell (1995) noted that the presence of amphibole and sanidine would suggest some relationship with orangeite.

To summarize, there is consensus that a single definition cannot be used to describe both kimberlite and orangeite rock types and that a simple succinct definition cannot be devised because of the mineralogical complexity of the rocks. As new discoveries of kimberlite are classified and as the techniques used to analyze these rocks improve, classification procedures for the kimberlite clan will continue to evolve.

3.2 Classification

Kimberlites are hybrid rocks that typically contain mantle- and crust-derived xenoliths and xenocrysts, as well as a variety of primary phases crystallized from kimberlitic magma, which itself may be derived from several mantle sources (Clement, 1982). Kimberlite mineralogy is further complicated by the incorporation of xenolithic material into the kimberlite magma, either at different points during its ascent from the mantle to surface, or locally as a result of final emplacement processes near the surface. Kimberlitic rocks cannot be unambiguously identified using standard igneous modal-textural classifications, either in the field or the laboratory, because 1) the contribution of any of these sources varies widely between kimberlites, and 2) kimberlites typically have similar macroscopic and petrographic appearance (Mitchell and Bergman, 1991; Scott Smith, 1992; Mitchell, 1994; Woolley et al., 1996).

Kimberlite rocks are, therefore, best characterized (at least optically) by identification and description of the given assemblage of primary minerals. Once the mineralogical assemblage of the kimberlite has been identified, it can be described by mineralogical-genetic nomenclature (Skinner and Clement, 1979). During the last 15 years, the mineralogical-genetic classification has provided petrologists with the most reliable and effective means of classifying kimberlite and lamproite (e.g., Jaques et al., 1986; Mitchell, 1986; Mitchell and Bergman, 1991; Scott Smith, 1992).

In the mineralogical-genetic classification, rock names reflect the modal abundance of major phases present. The main minerals are listed in order of increasing modal abundance before the primary rock name (e.g., kimberlite or lamproite). Skinner and Clement (1979) recommended including minerals that are two-thirds as plentiful as the dominant mineral.

Scott Smith (1995) noted, however, that caution should be exercised in the use of the mineralogical classification; it should only be used for rocks that have been determined to be kimberlite *sensu stricto* and that the classification should mainly be restricted to hypabyssal-facies rocks.

More commonly, a textural-genetic classification is employed because differences in emplacement processes result in specific products with unique textures. A generally accepted textural-genetic classification of kimberlites was devised by Clement and Skinner (1979, 1985) and Clement (1982), and expanded by Mitchell (1995). The classification relies on the generally accepted composite kimberlite-pipe model, which consists of three dominant zones: crater, diatreme and root (Hawthorne, 1975; Mitchell, 1986). Generally, specific textures define each zone and are termed crater-, diatreme- and hypabyssal-facies textures, respectively (Scott Smith, 1995). Further subdivisions of each facies may be required to describe textural-emplacement associations. For example, Field and Scott Smith (1998) divided crater-facies textures into the following subcategories:

- VK: Volcaniclastic kimberlite describes extrusively formed, fragmental kimberlite deposits for which the mode of deposition is not known.
- RVK: Resedimented, volcaniclastic kimberlite describes VK for which depositional mechanisms can be recognized and ascribed to 'normal' sedimentary processes.
- PK: Pyroclastic kimberlite describes VK for which *prima facie* evidence shows direct deposition by explosive volcanic processes.

4 Petrographic Descriptions of Selected Samples

Macroscopic and microscopic descriptions of samples from the K4 and K6 pipes in the Buffalo Head Hills, and from the Legend, Phoenix and Kendu pipes in the Birch Mountains, are described below. Macroscopic and microscopic descriptions are coupled with electron microprobe 'micro-images' (Appendix 1) and bulk-rock x-ray diffraction analysis (Appendix 2).

The micro-image combines backscattered electron and x-ray elemental images from the electron microprobe. The approximate size of each micro-image area is 410 by 410 μm. Micro-image sites were selected in areas determined to be representative of the sample. Each micro-image area was analyzed using the following specifications:

Pixels: 1024 x 1024
Pixel size: 0.02 x 0.02 μm
Dwell time: 10 milliseconds
Electron accelerating voltage: 15 kV
Current: 2.005 $x10^{-8}$ A

Individual micro-images include two backscattered images, which depict area selection and topography, and ten x-ray elemental images: MgO, SiO_2, Al_2O_3, CaO, K_2O, P, TiO_2, Cr_2O_3, FeO and S (Appendix 1). Bulk-rock x-ray spectra, from x-ray diffraction analysis on whole-rock samples, are presented in Appendix 2 and summarized in Table 3. In general, the dominant minerals are olivine (forsterite, Mg_2SiO_4), serpentine (lizardite $[(Mg,Fe)_3SiO_5(OH)_4]$ and chrysotile $[Mg_3(Si_{2-x}O_5(OH)_{4-4x}])$, calcite ($CaCO_3$), dolomite (ankerite, $Ca(Fe^{+2},Mg)(CO_3)_2$), phlogopite ($KMg_3[Si_3Al]O_{10}[OH]_2$) and magnesite ($MgCO_3$).

With respect to grain-size nomenclature of matrix minerals, this report uses a split based on size, so that microphenocrysts are <0.5 mm and macrocrysts are >0.5 mm. However, some minerals (e.g., olivine, phlogopite and ilmenite) may occur in both modes and, because of similar morphologies, it is not always possible to draw sharp distinctions between the different populations.

Table 3. Summary of x-ray diffraction analysis on selected whole-rock northern Alberta kimberlitic rocks.

Sample/pipe	Minerals (with formulas) identified in x-ray spectra
ABK01/K4A	Quartz, SiO_2; dolomite, $CaMg(CO_3)_2$; magnesite, $MgCO_3$; nimite 1MIIb, $(Ni,Mg,Al)_6(Si,Al)_4O_{10}(OH)_8$
ABK02/K4B	Dolomite, $CaMg(CO_3)_2$; forsterite, Mg_2SiO_4; lizardite 1M, $(Mg,Fe)_3Si_2O_5(OH)_4$; phlogopite 2M1, $KMg_3(Si_3Al)O_{10}(OH)_2$; pyrite, FeS_2
ABK03/K4C	Quartz, SiO_2; lizardite 6T1, $Mg_3([Si,Fe]_2O_5)(OH)_4$; dolomite, $CaMg(CO_3)_2$; magnesite, $MgCO_3$
ABK05/K6	Calcite, $CaCO_3$; lizardite 1M, $(Mg,Fe)_3Si_2O_5(OH)_4$; forsterite, Mg_2SiO_4; lizardite 6T1, $Mg_3([Si,Fe]_2O_5)(OH)_4$
ABK29/K6	Calcite, $CaCO_3$; lizardite 1M, $(Mg,Fe)_3Si_2O_5(OH)_4$; forsterite, Mg_2SiO_4
ABK59/Legend	Ankerite, $Ca(Fe^{+2},Mg)(CO_3)_2$; calcite, $CaCO_3$; lizardite 6T1, $Mg_3([Si,Fe]_2O_5)(OH)_4$ magnetite, $Fe^{+2}Fe_2^{+3}O_4$
ABK68/Legend	Ankerite, $Ca(Fe^{+2},Mg)(CO_3)_2$; magnesite, $(Mg,Fe)CO_3$; lizardite 6T1, $Mg_3([Si,Fe]_2O_5)(OH)_4$ dolomite, $CaMg(CO_3)_2$; beidellite 12A, $Na_{0.33}Al_2(Si,Al)_4O_{10}(OH)_2 \cdot 2H_2O$
ABK75/Phoenix	Ankerite, $Ca(Fe^{+2},Mg)(CO_3)_2$; annite 1M, $KFe_3^{+2}(Si,Al)_4O_{10}(OH)_2$; lizardite 6T1, $Mg_3([Si,Fe]_2O_5)(OH)_4$; magnetite, $Fe^{+2}Fe_2^{+3}O_4$
ABK76/Phoenix	Lizardite 1T, $(Mg,Al)_3([Si,Fe]_2O_5)(OH)_4$; ankerite, $Ca(Fe^{+2},Mg)(CO_3)_2$; phlogopite 2M1, $KMg_3(Si_3Al)O_{10}(OH)_2$; magnetite, $Fe^{+2}Fe_2^{+3}O_4$; hematite, Fe_2O_3
ABK81/Kendu	Lizardite 1M, $(Mg,Fe)_3Si_2O_5(OH)_4$; phlogopite 1M, $K(Mg,Fe)_3(Al,Fe)Si_3O_{10}(OH,F)_2$; lizardite 6T, $Mg_3Si_2O_5(OH)_4$; calcite, $CaCO_3$; ankerite, $Ca(Fe^{+2},Mg)(CO_3)_2$; clinochlore 1MIIb, $Mg_3Mn_2Al(Si_3Al)O_{10}(OH)_8$
ABK82/Kendu	Chrysotile, $Mg_3(Si_{2-x}O_5)(OH)_{4-4x}$; calcite, $CaCO_3$; phlogopite 1M, $K(Mg,Fe)_3(Al,Fe)Si_3O_{10}(OH,F)_2$ ankerite, $Ca(Fe^{+2},Mg)(CO_3)_2$; anorthite, $(Ca,Na)(Al,Si)_2Si_2O_8$

4.1 Samples ABK01, ABK02 and ABK03 (K4 Complex, Buffalo Head Hills)

Discovered in February 1997, the K4 'complex' comprises three separate pipes, K4A, K4B and K4C, which correspond in this study to samples ABK01, ABK02 and ABK03, respectively. Pipes in the K4 complex have distinctly separate geophysical anomalies (Skelton and Bursey, 1998), but have only been tested by relatively shallow drillholes (≤200 m). Thus, it is unknown whether the pipes are formed from three separate events or a single feeder system at depth. In contrast to the other pipes selected in the current report, which include two samples from different depths within the same pipe, the mineralogical descriptions for the three separate pipes within the K4 complex (i.e., samples ABK01, ABK02 and ABK03) are included as separate descriptions below.

4.1.1 Sample ABK01 (K4A Pipe, Buffalo Head Hills)

Drillhole 4A-2 penetrated altered, medium rusty brown to light grey-green kimberlitic rock from 26 m to the end of the hole at 52 m (Skelton and Bursey, 1998). Despite an extensively weathered, tan-brown appearance, sample ABK01, collected at 49 m, is relatively competent. Visible macrocrystalline and phenocrystalline olivine pseudomorphs constitute about 20 vol. % and appear totally altered to carbonate and/or serpentine. The dominant portion of the rock (about 75 vol. %) is composed of a granular, fine-grained matrix. Country-rock xenoliths include both subrounded carbonate and angular shale clasts, the largest of which is a blade-like, 1 by 9 mm shale xenolith. No mantle xenoliths are present. Opaque minerals occur sporadically throughout the core as 1 to 2 mm xenocrysts, along with trace (<1%) amounts of light purple-red garnets (<1 mm).

The x-ray diffraction analysis shows that sample ABK01 is composed of quartz (SiO_2), dolomite ($CaMg[CO_3]_2$), magnesite and a nickeliferous sulphide (Table 3; Appendix 2).

In thin section, sample ABK01 is almost completely altered by variable amounts of quartz and carbonate (Figure 3A, B), such that it would be difficult to optically determine if the sample is kimberlite. Quartz constitutes between 25 and 30 vol. % of the sample. Carlson et al. (1999) reported that silicification 'alteration caps' are prominent features in the upper parts of Buffalo Head Hills pipes K4A, K4B, K7A and K7C. The quartz in sample ABK01 did not crystallize from the magma; instead, it is commonly characterized by distinct radiating textures that are often associated with secondary, hydrothermal emplacement (Figure 3C). Thus, the altered but competent nature of the sample is likely the result of silicification.

Suspect olivine crystals and olivine-rich lapilli are completely altered and optically difficult to recognize. Where pseudomorphs of olivine xenocrysts are distinguishable, the olivine has been completely altered by late-stage dolomite and magnesite. The sample also includes rare opaque minerals (<2 vol. %), and phlogopite is absent.

A whole-rock x-ray diffraction spectrum from ABK01 indicates the presence of nimite ($[Ni,Mg,Al]_6[Si,Al]_4O_{10}[OH]_8$), a member of the chlorite group. This seems plausible, as nimite has been documented with ferroan trevorite, violarite, millerite, willemseite and secondary reevesite and goethite in, for example, a small body of nickeliferous rocks at the contact between quartzite and ultramafic rocks at the Scotia Tall mine in Transvaal, South Africa (Heimstra and de Waal, 1968; de Waal, 1970).

4.1.2 Sample ABK02 (K4B Pipe, Buffalo Head Hills)

Drillhole 4B-1 penetrated olivine-rich kimberlitic rock from 8.5 m to the end of the hole at 200.25 m (Skelton and Bursey, 1998). Macroscopically, sample ABK02, collected at 141 m, is light grey-green, competent, medium grained and dominated by relatively unaltered olivine xenocrysts. The core is bitumen stained, with the bitumen intermixed within a fractionated matrix. Black, angular shale clasts account for approximately 5 vol. % of the rock and vary in size, with the largest observed clast being 1.3 cm in length. No mantle xenoliths were observed. Trace amounts (<1%) of opaque (ilmenite) and sulphide minerals (pyrite) occur throughout the core.

The x-ray diffractogram indicates that sample ABK02 is composed of olivine (forsterite), serpentine (lizardite), dolomite, phlogopite and pyrite (FeS_2; Table 3; Appendix 2).

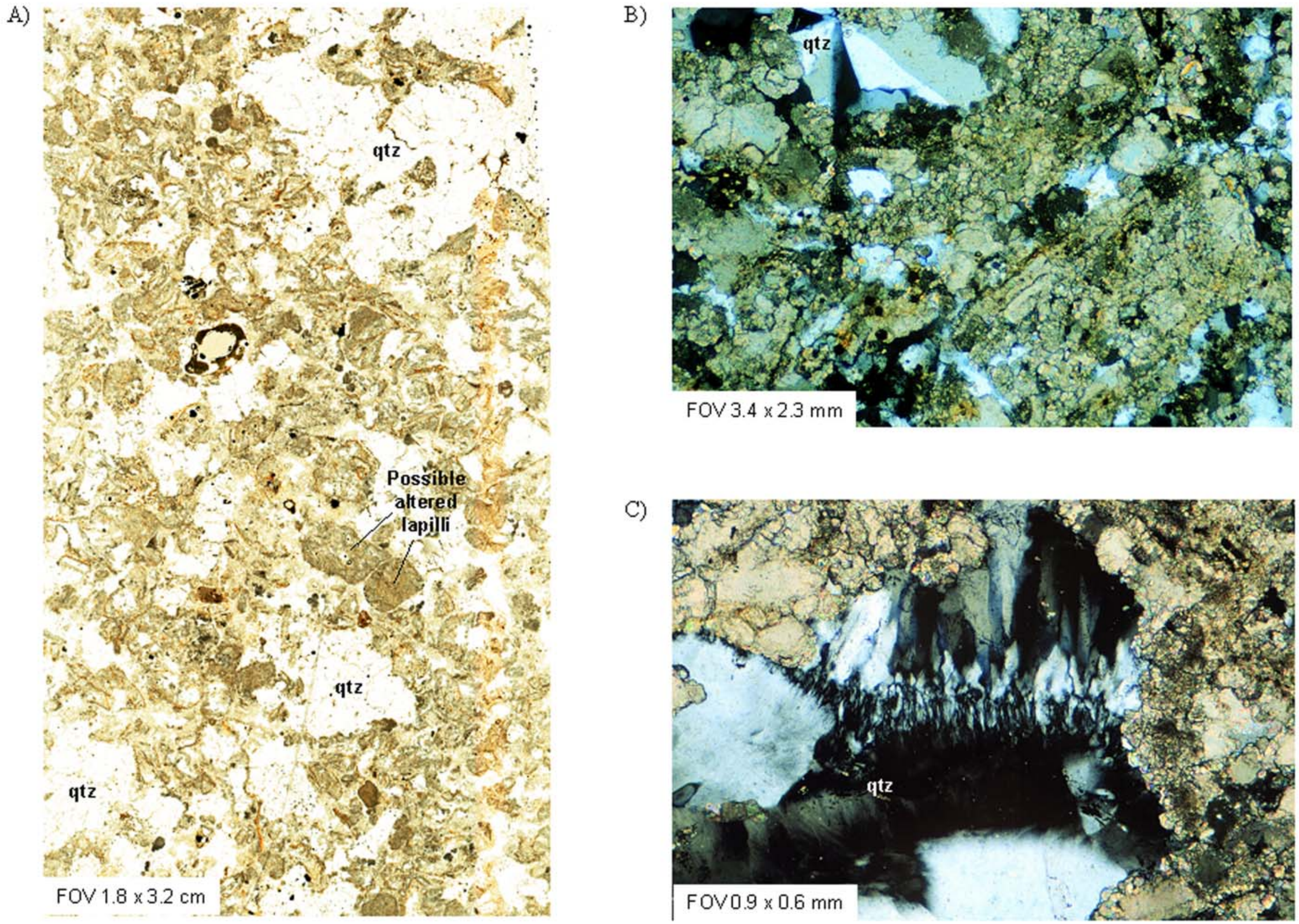

Figure 3. Photomicrographs of sample ABK01, K4A pipe, Buffalo Head Hills: A) scan of polished thin section; B) representative matrix; and C) radiating quartz textures indicative of secondary, hydrothermal emplacement. Abbreviation: FOV, field of view.

In thin section, fresh olivine microphenocrysts constitute about 60 to 65 vol. % and range in size from less than 0.25 to 0.5 mm (Figure 4A, B). Olivine macrocrysts are also present, but are rare in comparison to the microphenocryst population. The majority of the olivine crystals are preserved, and sample ABK02 is undoubtedly composed of the freshest (least altered) olivine in samples selected for this report. The subhedral to anhedral olivine crystals have a variety of shapes and are generally poorly sorted, loosely packed and have no microscopic-scale evidence of bedding. Skelton and Bursey (1998) did not report bedding in drillhole 4B-1, although they did note distinct bedding in nearby inclined drillhole 4B-2.

Juvenile lapilli are uncommon (<10 vol. %) in comparison to olivine crystals, but do occur throughout the sample. The lapilli are easily identified on account of their dark, cryptocrystalline matrix (Figure 4C, D). At least two different types of lapilli exist. The lapillus in the upper left corner of Figure 4A has a rounded margin with subhedral to anhedral olivine, similar to the olivine distribution throughout the thin section, and a matrix devoid of opaque minerals. In contrast, the lapillus in Figure 4C is darker, has slightly curvilinear margins, euhedral to subhedral olivine and up to 10 vol. % opaque minerals.

The inter-clast matrix is composed mainly of serpentine (lizardite) with less common dolomite (Figures 4E, 5; Appendix 1). The dolomite preferentially replaces olivine and occurs as blebs within the matrix. Pyrite, which is present in minor amounts (<3 vol. %), is commonly associated with the dolomite and often nucleates on the rim of the dolomite or within vugs (Figures 4e, 5). Small (<10 μm), discrete grains of apatite and chromite are rare and occur randomly in the matrix (Figure 5; Appendix 1).

Phlogopite occurs as isolated, elongate grains and is distributed throughout the thin section. The phlogopite constitutes up to 3 vol. %, with an average crystal size of 0.075 by 0.22 mm, and is randomly oriented. Irregular zoning in the phlogopite observed in ABK02 is possibly a result of tetraferriphlogopite, which may result from drastic changes in redox conditions, or the addition of groundwaters, during the final stages of crystallization (Mitchell, 1986).

4.1.3 Sample ABK03 (K4C Pipe, Buffalo Head Hills)

Drillhole 4C-1 penetrated light brown to greyish yellow, altered kimberlite from 44 to 78 m, and light green to greyish green kimberlite from 78 m to the end of the hole at 106 m (Skelton and Bursey, 1998). In hand sample, ABK03, collected at 63 m, is tan to yellow-green, medium grained and has a highly altered, incompetent and vuggy appearance. The matrix dominates the sample (up to 65 vol. %) and is characterized by elongated and randomly orientated green to black material.

The x-ray diffractogram indicates that sample ABK03 is composed of serpentine (lizardite), quartz, dolomite and magnesite (Table 3; Appendix 2).

In thin section, elongated (up to 3.5 mm long), randomly orientated material dominates the sample (Figure 6A). The grains are optically similar to phlogopite (Figure 6B, C). Element identification using the electron microprobe's energy-dispersive spectrometer (EDS) shows that these elongate grains with tabular cleavage are not phlogopite, but serpentine (lizardite). The lath-like lizardite crystals are set in dark brown, fine-grained, serpentine-carbonate cement.

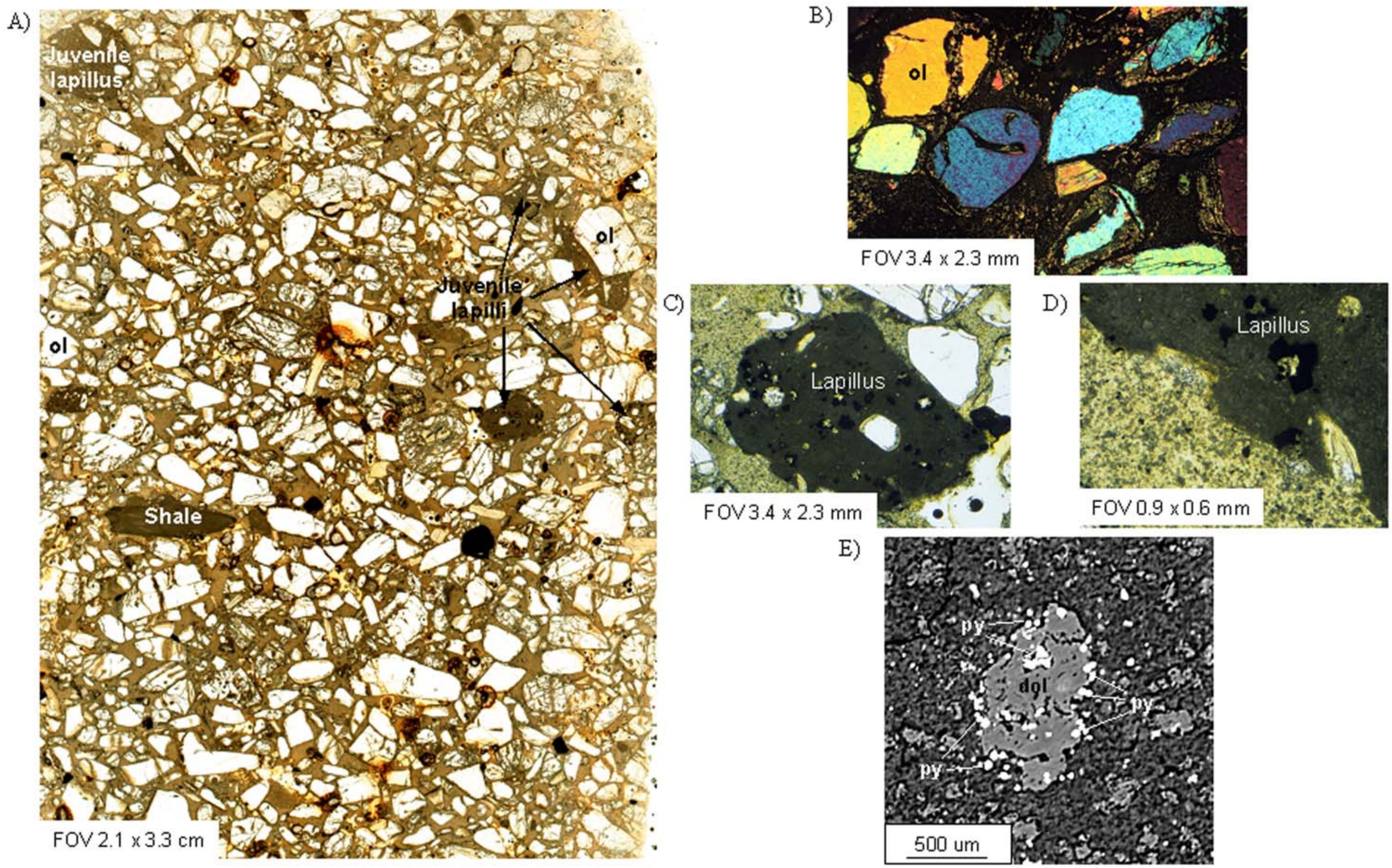

Figure 4. Photomicrographs of sample ABK02, K4B pipe, Buffalo Head Hills: A) scan of polished thin section; B) representative matrix; C) curvilinear lapillus; D) comparison between lapillus matrix and matrix that encompasses lapillus; and D) pyrite nucleating on dolomite. Abbreviation: FOV, field of view.

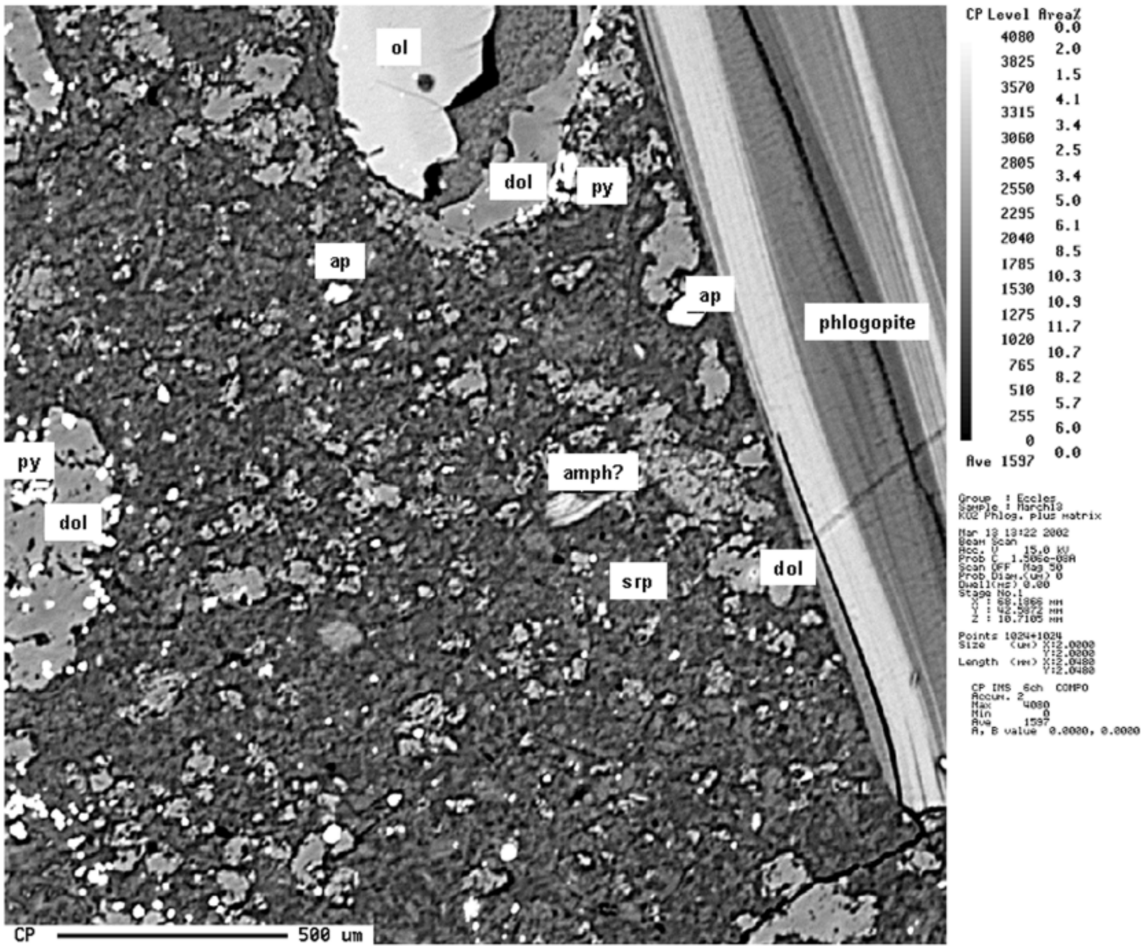

Figure 5. Backscatter image of representative area from sample ABK02, K4B pipe, Buffalo Head Hills.

4.2 Samples ABK05 and ABK29 (K6 Pipe, Buffalo Head Hills)

The K6 pipe was discovered in January 1997 when drillhole 6-1 intersected and bottomed out in 187 m of dark grey, volcaniclastic kimberlite. Sample ABK05 is from drillhole 6-2, which penetrated kimberlite from 74 to 127 m, and was collected at a depth of 100 m. Skelton and Bursey (1998) reported that several drillholes into K6 (e.g., drillholes K6-7, K6-8 and K6-10) penetrated cycles of kimberlite interlayered with mudstone with gradational contacts between kimberlite and underlying mudstone. The volcaniclastic kimberlite in drillhole 6-2 is underlain by 12 m of mudstone to the end of the hole at 139 m (Skelton and Bursey, 1998).

Macroscopically, sample ABK05 is characterized by light grey-green, competent, volcaniclastic kimberlite. Olivine macrocrysts vary in size up to 1.1 cm and typically have altered, whitish (carbonate) cores and dark green rims. The matrix is medium to coarse grained and comprises mainly serpentine and inequigranular olivine crystals. Country-rock xenoliths in sample ABK05 constitute about 5 vol. % and include altered, subangular to rounded carbonate, siltstone and shale clasts up to 2.2 cm in size. Some sedimentary clasts appear to be internally ‘sheared’ and contain calcite veinlets.

Sample ABK29 was collected from an exposure of kimberlite K6 on the southeast flank of the Buffalo Head Hills, where outcrop examinations show numerous rock subtypes based on variations in textural characteristics. In outcrop, the rock is generally composed of grey-green, competent, coarse-grained,

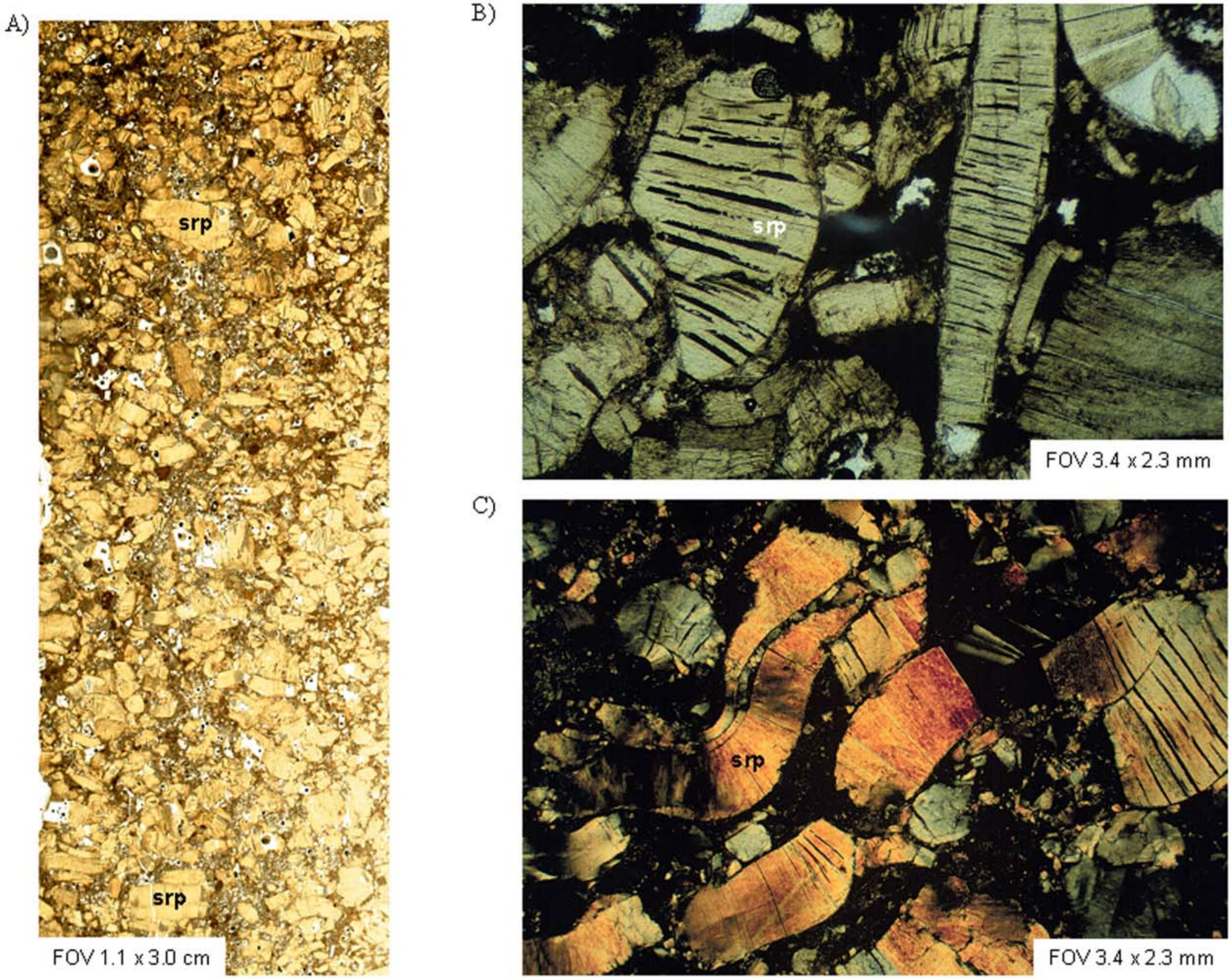

Figure 6. Photomicrographs of sample ABK03, K4C pipe, Buffalo Head Hills: A) scan of polished thin section; B) and C) selected images of tabular serpentine under plane and crossed polars, respectively. Abbreviation: FOV, field of view.

inequigranular kimberlite. The sample consists of olivine microphenocrysts and macrocrysts that constitute about 40 to 50 vol. %. Carbonate alteration is evident in outcrop, both in the matrix of the rock and preferentially in fractures, where calcite veins and stringers are up to 0.5 mm wide and typically orientated at 135° and 100°. Despite carbonate alteration being evident, the outcrop has a higher modal amount of fresh olivine compared to the core sample ABK05, which was obtained at a depth of 110 m. Dark grey to black juvenile lapilli are evident. Mantle and basement xenoliths and mantle xenocrysts are randomly distributed throughout the outcrop. Sample ABK29 was chosen as being representative of the kimberlite outcrop. In addition to this sample, and because kimberlite K6 was accessible in outcrop, a variety of material was available for study, including representative bulk-rock material and mantle and crustal xenoliths. Petrographic observations on all surface samples studied will be included below as part of sample ABK29.

The x-ray diffractograms indicate that samples ABK05 and ABK29 are composed of serpentine (lizardite), olivine (forsterite) and calcite (Table 3; Appendix 2).

In thin section, samples ABK05 and ABK29 have the classic inequigranular texture associated with kimberlite, caused by the presence of at least two generations of olivine: microphenocrysts less than 0.25 mm in size and occasional larger (up to 0.75 cm) macrocrysts (Figure 7 A, B). Together, the olivine xenocrysts constitute between 40 and 50 vol. % of the sample. The macrocrysts are rounded to subrounded, moderately fractured, and contain fresh olivine with serpentine filling the fracture spaces. The smaller olivine microphenocrysts are mostly subhedral and altered by serpentine and calcite.

At least two types of lapilli are present. Large (up to 1 cm), juvenile lapilli occur throughout and are characterized by their dark colour, fine grain size, irregular lobate to curvilinear margins, absence of larger olivine crystals, and abundance of opaque matrix minerals (spinel and possibly perovskite; Figures 7, 8A). The mineralogical groundmass compositions of lapilli and the groundmass that encompasses the lapilli are similar (serpentine and calcite), but the dark-coloured lapilli matrix is finer grained and has higher CaO and lower Fe and Al_2O_3 contents (Appendix 1). In addition to these large lapilli, ash-sized to lapilli-sized, juvenile pyroclasts (Figure 8B) occur in concentrated areas.

The juvenile pyroclasts are a significant feature of kimberlite K6, with excellent examples exposed on the eastward part of the K6 outcrop (e.g., Figure 9A). Their size varies such that they may be described as ash- to lapilli-sized juvenile pyroclasts. The pyroclasts are formed when olivine phenocrysts / microphenocrysts, and less frequently macrocrysts, act as nuclei and are coated with variably sized ‘skins’ of magmatic material (Figure 9B). The pyroclasts are not similar in petrographic character to the pelletal lapillus and/or nucleated autoliths (globular segregations) associated with some diatreme- and hypabyssal-facies kimberlites, respectively. Importantly, the material surrounding olivine kernels does not contain angular kimberlite fragments (autoliths) or microcrysts with preferred orientations, such as those typical of the diatreme facies. The rinds of the pyroclasts are optically similar to the matrix material in the larger, amoeboid lapilli, and they have obviously not travelled far. These juvenile pyroclasts, therefore, are interpreted to be textures associated with a near-vent environment.

The groundmass encompassing the lapilli and pyroclasts comprises predominantly serpentine and calcite (Figure 10A; Appendix 1). The calcite occurs as pseudomorphs of earlier phases, mainly olivine. Other groundmass minerals include perovskite, spinel, apatite, magnetite and ilmenite. Phlogopite is rare. The pinkish brown perovskite is very small (often <3 µm) and can therefore be mistaken for some other type of Ti-rich mineral (Figure 10B). Spinel and perovskite commonly form ‘necklaces’ around olivine crystals and/or psuedomorphs. Ilmenite occurs either as small skeletal crystals (Figure 10C) or together with chromite (Figure 10D).

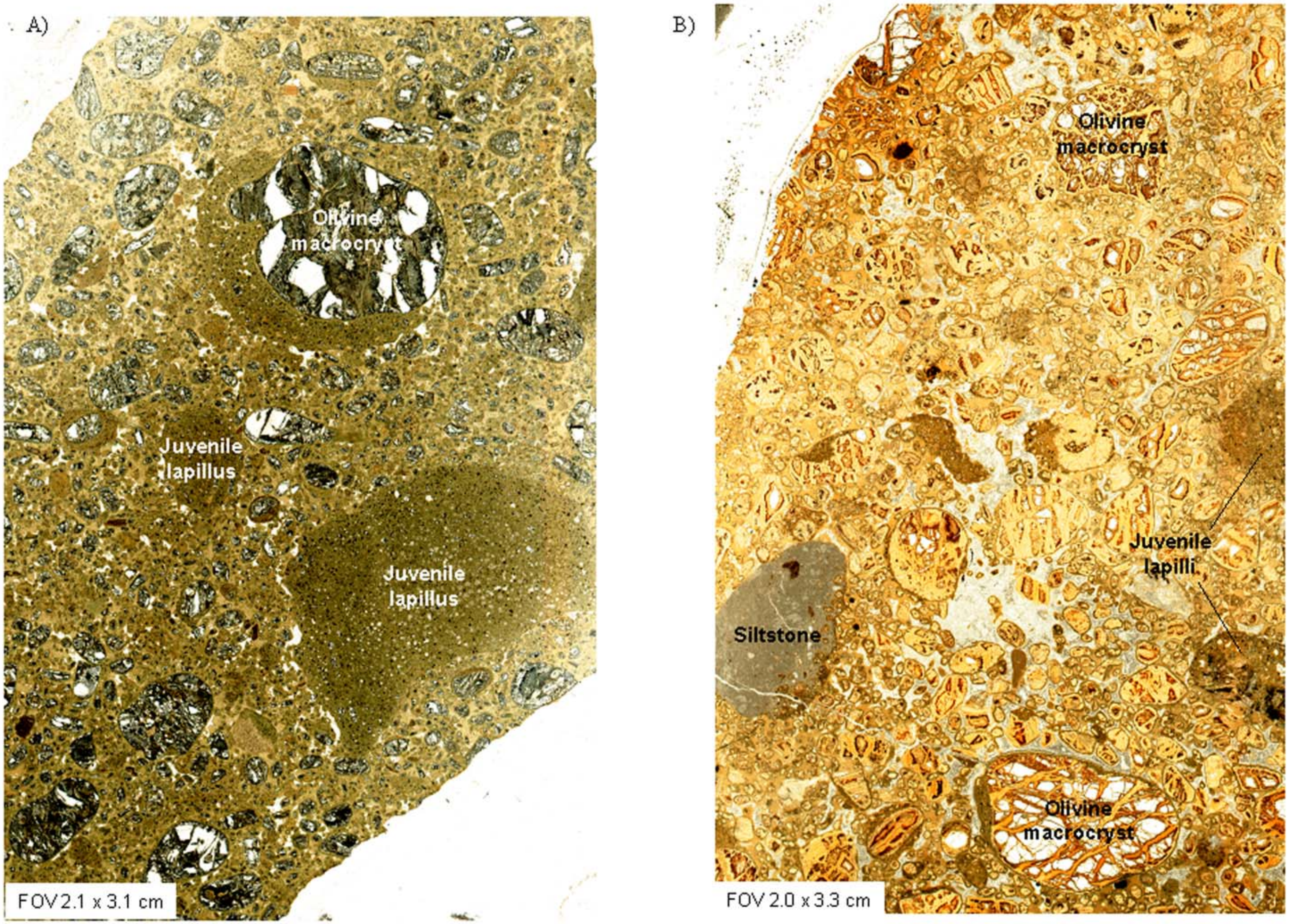

Figure 7. Scanned images of polished thin sections from samples ABK05 and ABK29, K6 pipe, Buffalo Head Hills. Abbreviation: FOV, field of view.

A)

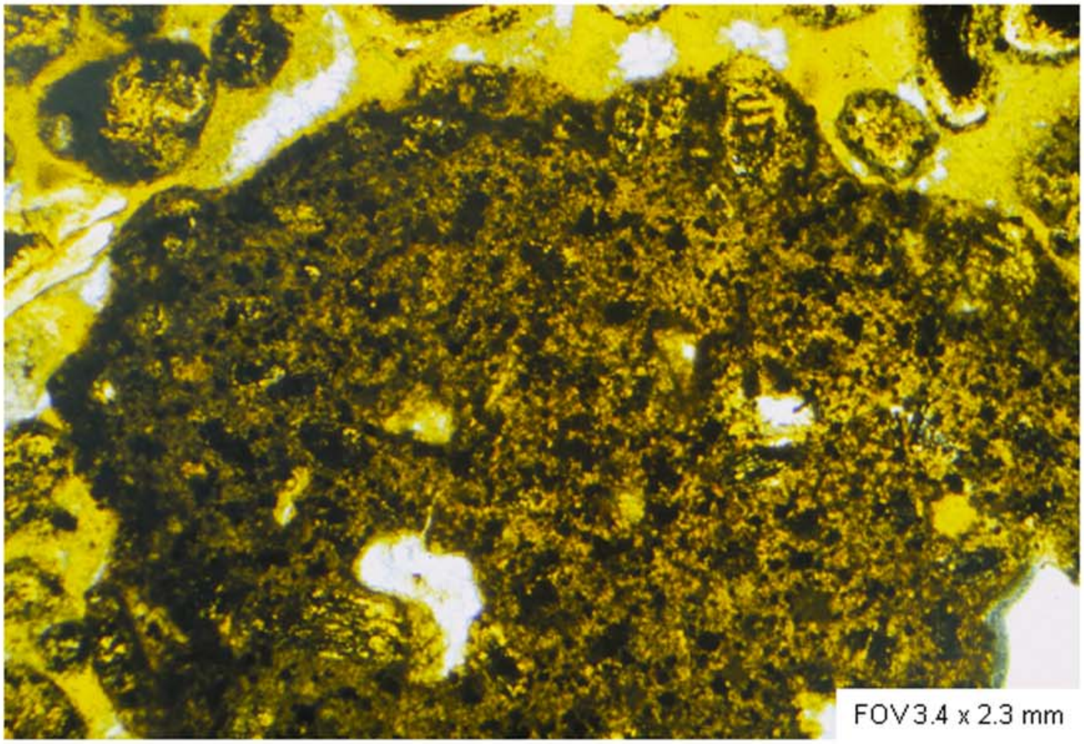

B)

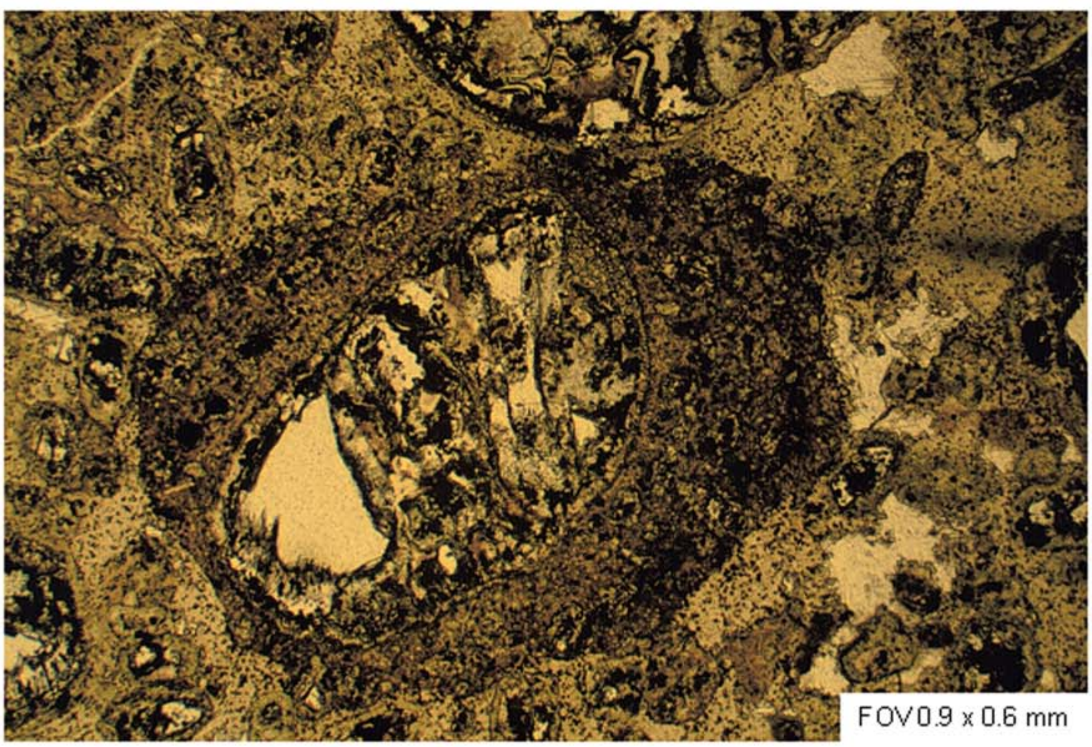

Figure 8. Variation between juvenile lapilli from the K6 pipe, Buffalo Head Hills: A) large, curvilinear lapillus; and B) ash- to lapilli-sized, juvenile pyroclasts. Abbreviation: FOV, field of view.

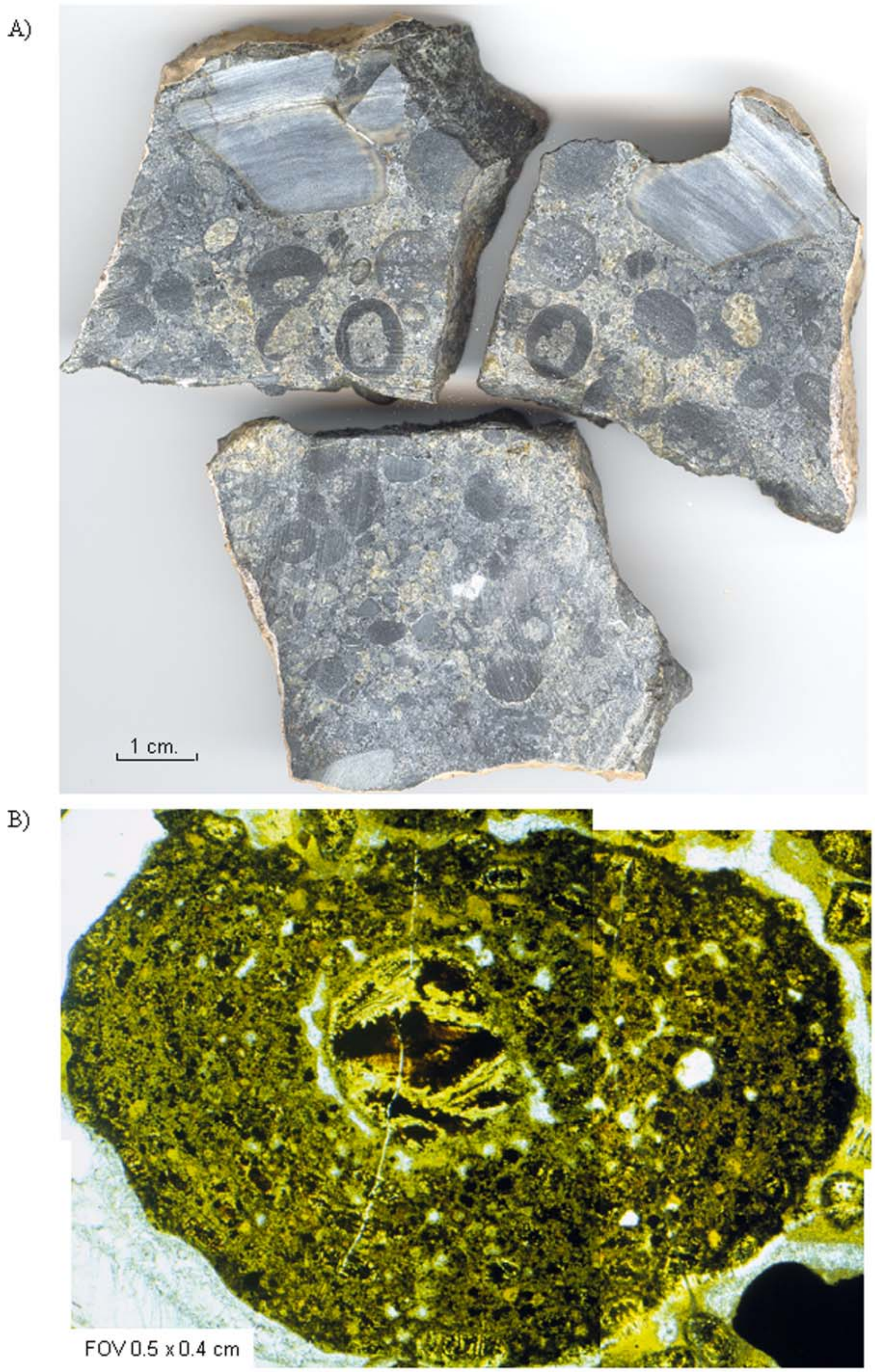

Figure 9. Ash- and lapilli-sized, juvenile pyroclasts from the K6 pipe, Buffalo Head Hills: A) in hand sample; and B) photomicrograph mosaic capturing the entire pyroclast, in plane-polarized light. Abbreviation: FOV, field of view.

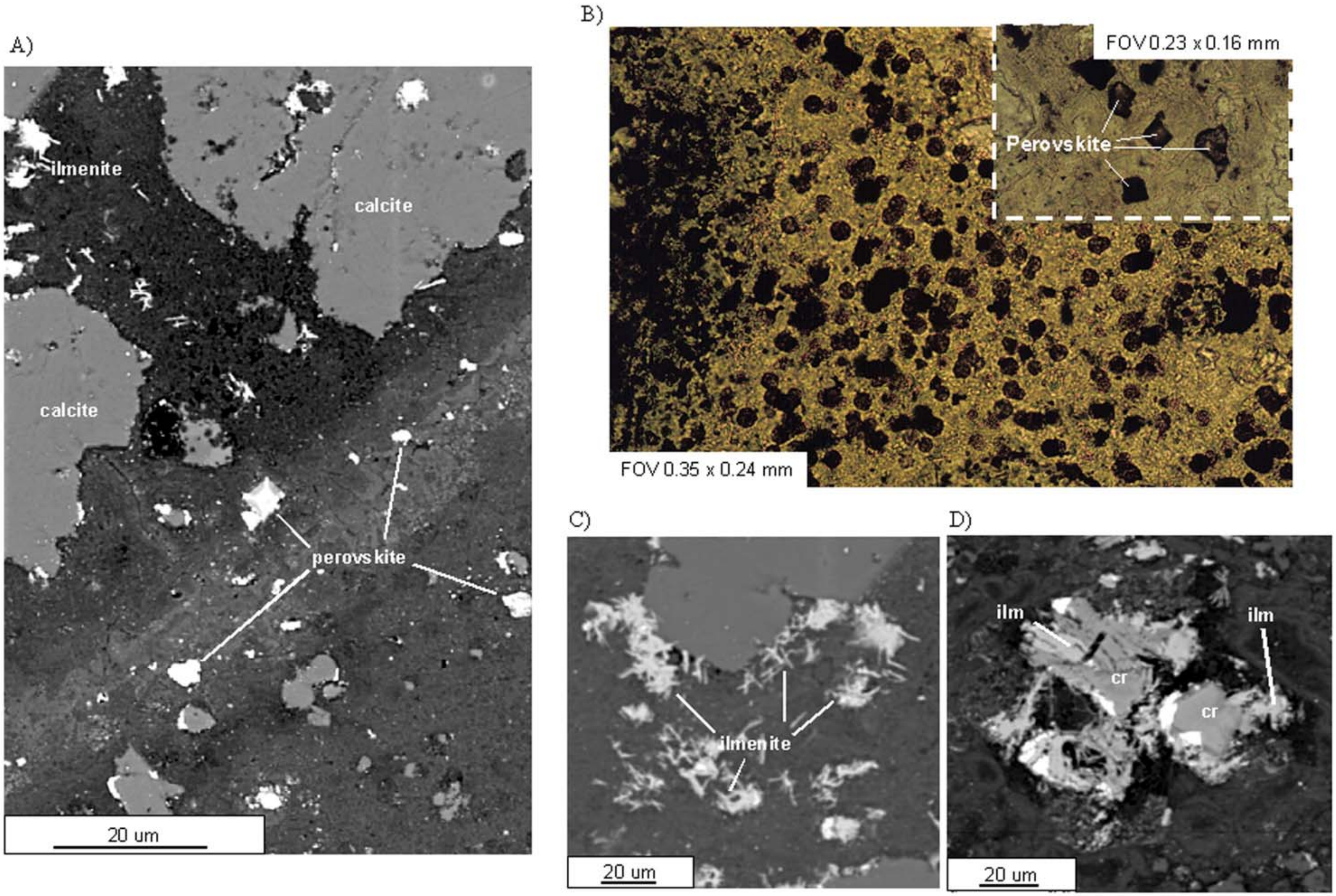

Figure 10. Photomicrographs of sample ABK05, K6 pipe, Buffalo Head Hills: A) backscatter image of representative matrix; B) perovskite; C) skeletal crystals of ilmenite; and D) intergrown ilmenite (light grey) and chromite (dark grey). Abbreviation: FOV, field of view.

Several peridotite xenoliths were observed in outcrop. The observed mantle xenoliths are typically small, averaging less than 2 cm to a maximum of 6 cm in length. A fractured, slightly altered xenolith, consisting of olivine, orthopyroxene and minor clinopyroxene in a serpentinized matrix, is shown in Figure 11. The inclusion of clinopyroxene suggests that the mantle xenoliths are dominantly lherzolitic in composition. It is, however, difficult to discern clinopyroxene in some of the observed xenoliths, which suggests that xenoliths of harzburgite are also present. The xenoliths are generally rounded and have not been severely altered, although a thin (averaging about 6 mm), calcite-rich rind separates the mantle xenolith from the kimberlite magma.

A basement xenolith (Figure 12) consists of brownish green amphibolite. The boundary of the basement clast is minimally altered or distorted, indicative of relatively cool kimberlite magma. In places, there is secondary replacement of the amphibole by biotite; the timing of the replacement is not known.

4.3 Samples ABK59 and ABK68 (Legend Pipe, Birch Mountains)

The Legend pipe was discovered in November 1998 when drillhole 98DH-LE01, which was drilled by the Kennecott Canada Exploration Ltd.–Montello Resources Ltd. joint venture in the Birch Mountains area, penetrated kimberlite. The kimberlite was intersected at a depth of 12 m and continued to the end of the drillhole at 229 m (Aravanis, 1999). Samples ABK59 and ABK68 were collected from drillhole 98DH-LE01 at depths of 44 m and 187 m, respectively. The lithology of the Legend pipes varies between alternating layers of coarse lapilli tuff and laminae of finer grained ash tuff, and bottoms out in light grey, competent kimberlite tuff.

In hand specimen, sample ABK59 is dark grey-green, competent, fine- to medium-grained and inequigranular. It comprises matrix-supported olivine xenocrysts and lapilli set in an aphanitic, dark green matrix. Probable olivine pseudomorphs dominate (about 40 vol. %); these are typically altered by carbonate, with only moderately (<10 vol. %) fresh olivine observed. Country rock xenoliths constitute about 5 vol. % and are dominated by white to whitish green, subrounded carbonate (up to 5 mm in length). Shale clasts are less common, and some have fractures filled with calcite. Other minerals include ilmenite and pyrite, which locally constitute up to 5 vol. % and 7 vol. %, respectively. Brown phlogopite macrocrysts are present, but rare.

In hand specimen, sample ABK68 is light grey, fine- to medium-grained and competent. The light colour may be related to carbonatization, as the majority of olivine phenocrysts appear to be completely altered to carbonate. The matrix is fine grained and also appears to consist of carbonate and serpentine. The core consists of about 5 vol. % country rock xenoliths, which include angular shale and rounded carbonate. Ilmenite (up to 3 vol. %) is not as common as in sample ABK59, and sulphide minerals and phlogopite are rare.

The x-ray diffractograms indicate that the Legend samples are composed mainly of serpentine (lizardite), magnesite, calcite, dolomite (ankerite) and a smectite-group clay mineral (beidellite [$Na_{0.33}Al_2(Si,Al)_4O_{10}(OH)_2 \cdot 2H_2O$]; Table 3; Appendix 2). Aravanis (1999) reported that glycolated x-ray diffractogram analysis on clay minerals from the Legend pipe identified a smectite-group mineral similar to saponite.

In thin section, the Legend pipe samples ABK59 and ABK68 are characterized by their pervasive carbonatization and high opaque-mineral (ilmenite) content. In comparison to the Buffalo Head Hills samples described above, the olivine from these samples is restricted to the microphenocryst (often <0.25 mm) phase, giving the sample a fairly homogenous appearance (Figure 13A, B). Pseudomorphed olivine microphenocrysts with relict euhedral features are by far the dominant feature and constitute

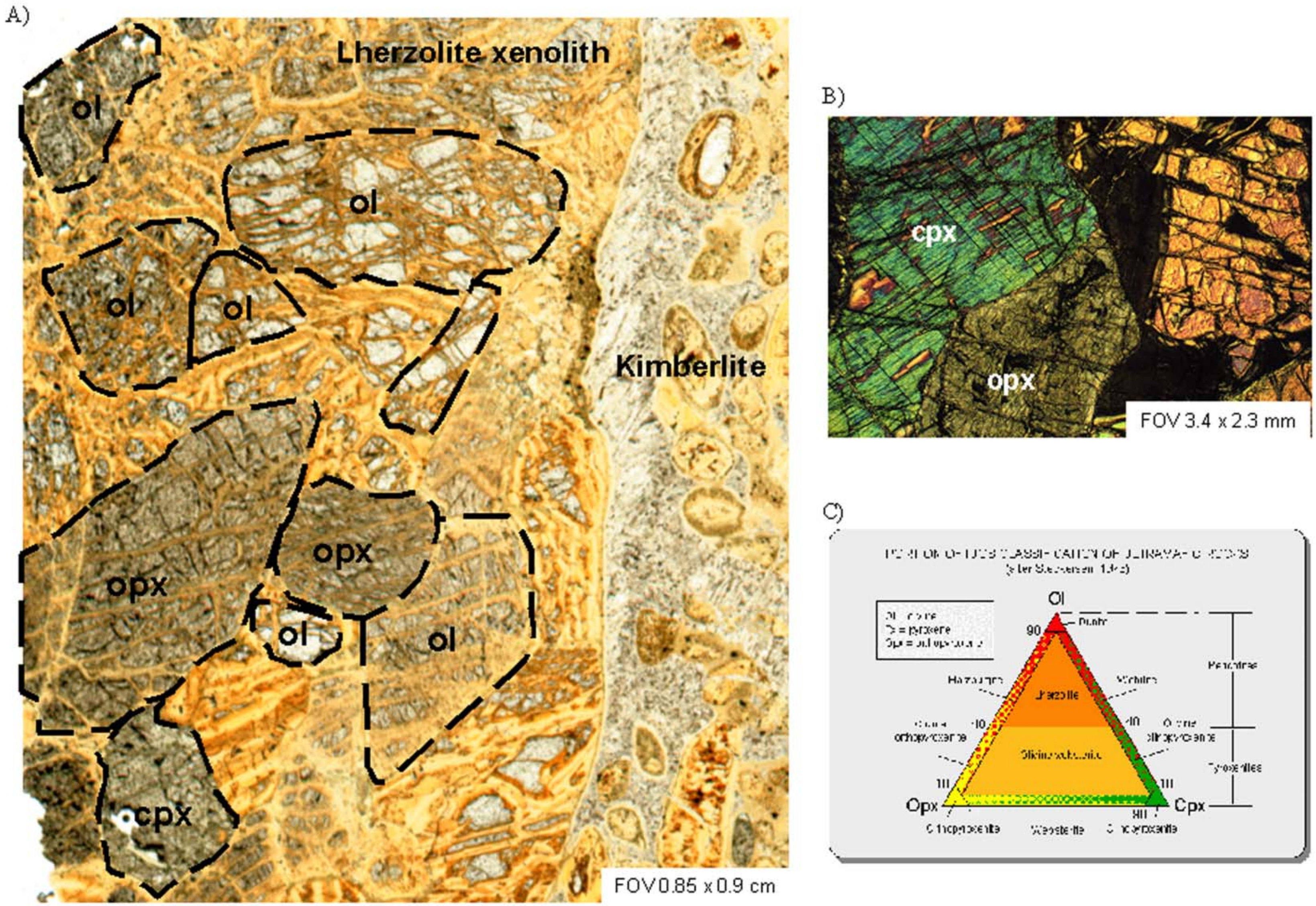

Figure 11. Mantle xenolith from sample ABK29, K6 pipe, Buffalo Head Hills: A) expanded view of the xenolith in contact with kimberlite; B) clinopyroxene and orthopyroxene; and C) IUGS classification of ultramafic rocks. Abbreviation: FOV, field of view.

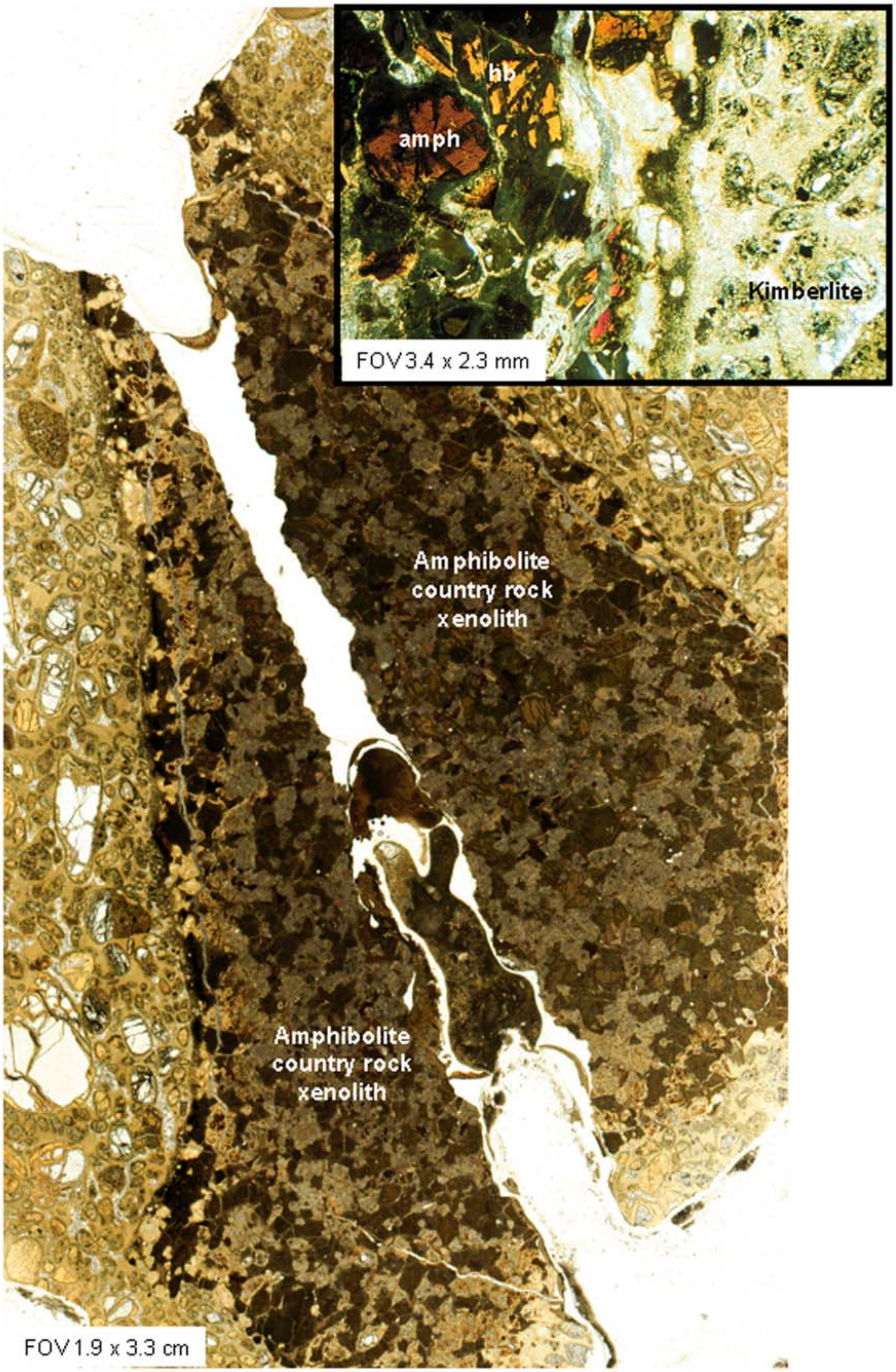

Figure 12. Basement xenolith from sample ABK29, K6 pipe, Buffalo Head Hills. Abbreviation: FOV, field of view.

about 40 to 55 vol. % of the sample. The olivine crystals have been replaced by serpentine, dolomite (ankerite) and magnesite. In rare instances, euhedral to subhedral olivine crystals are preserved and nonfractured.

Juvenile lapilli occur throughout the samples. Large lapilli have rounded to curvilinear boundaries and occur sporadically throughout the core (Figure 13B, C). Smaller ash- to lapilli-sized, accretionary pyroclasts are also present and give the rock a distinct ovoid pyroclastic texture. Both types of lapilli consist of subhedral to euhedral microphenocrysts of serpentinized olivine set in a calcite-serpentine matrix that is decidedly more calcitic than the matrix external to the clasts. Dense, lapilli-rich layers typically consist of some large and many smaller lapilli, the latter of which are interpreted to form when lava droplets are ejected into the steam above the magma column level, where the droplets are quenched and fall back to acquire a rind of new lava. The differing composition, size and shape of the lapilli result when the process is repeated, perhaps several times.

The matrix consists mainly of serpentine and calcite (Appendix 1). Large (up to 0.15 mm) hexagonal apatite grains (Figure 13D) occur throughout, and especially in calcite-rich portions of the groundmass. Needle-like acicular sulphide grains are both disseminated and form clusters (e.g., Figure 13E). Optically these sulphide grains appear to be related to sulphosalt or Ni-sulphide minerals (e.g., millerite). When tested by the electron microprobe's EDS, the 'bladed' crystals in Figure 13E are FeS-rich sulphide mineral embedded in an unknown, LREE- and Re-rich mineral.

Opaque minerals include ilmenite and chromite. The ilmenite xenocrysts (Figure 13F) vary in size up to 1 cm and constitute up to 5 vol. %. Some of the ilmenite has a reddish-coloured alteration on the borders, which may be limonite or goethite. No phenocrysts and/or macrocrysts of phlogopite or perovskite were located optically.

4.4 Samples ABK75 and ABK76 (Phoenix Pipe, Birch Mountains)

The Phoenix pipe, discovered in September 1998, was the first target drilled by the Kennecott Canada Exploration Ltd.–Montello Resources Ltd. joint venture in the Birch Mountains area. Drillhole 98DH-PH01 penetrated volcaniclastic kimberlite from 103 m to the end at 226 m (Aravanis, 1999). Samples ABK75 and ABK76 were collected at depths of 105 m and 130 m, respectively.

Macroscopically, sample ABK75 is grey-green, competent, fine- to medium-grained, volcaniclastic kimberlitic rock. The sample contains abundant amber to dark brown phlogopite (up to 5 vol. %). Country rock xenoliths are a minor component (<3 vol. %) and, when present, include grey clay and mudstone.

Macroscopically, sample ABK76 is dark grey, competent, fine- to medium-grained volcaniclastic kimberlitic rock. Olivine xenocrysts are mainly altered, but some relatively fresh olivine macrocrysts are visible. Phlogopite is quite prominent in this sample and constitutes up to 8 vol. %. The matrix is generally fine grained and appears highly carbonatized.

The x-ray diffractograms indicate that the Phoenix samples are composed mainly of dolomite (ankerite) and serpentine (lizardite), with magnetite ($Fe^{+2}Fe_2^{+3}O_4$) and phlogopite (Table 3; Appendix 2). In addition, sample ABK76 contains hematite (Fe_2O_3).

Like samples from the Legend pipe, those from the Phoenix pipe are highly carbonatized. In thin section, carbonate is present in both the fine-grained matrix and partially to completely replaced olivine microphenocrysts (Figure 14A, B). Olivine microphenocryst pseudomorphs are typically subhedral,

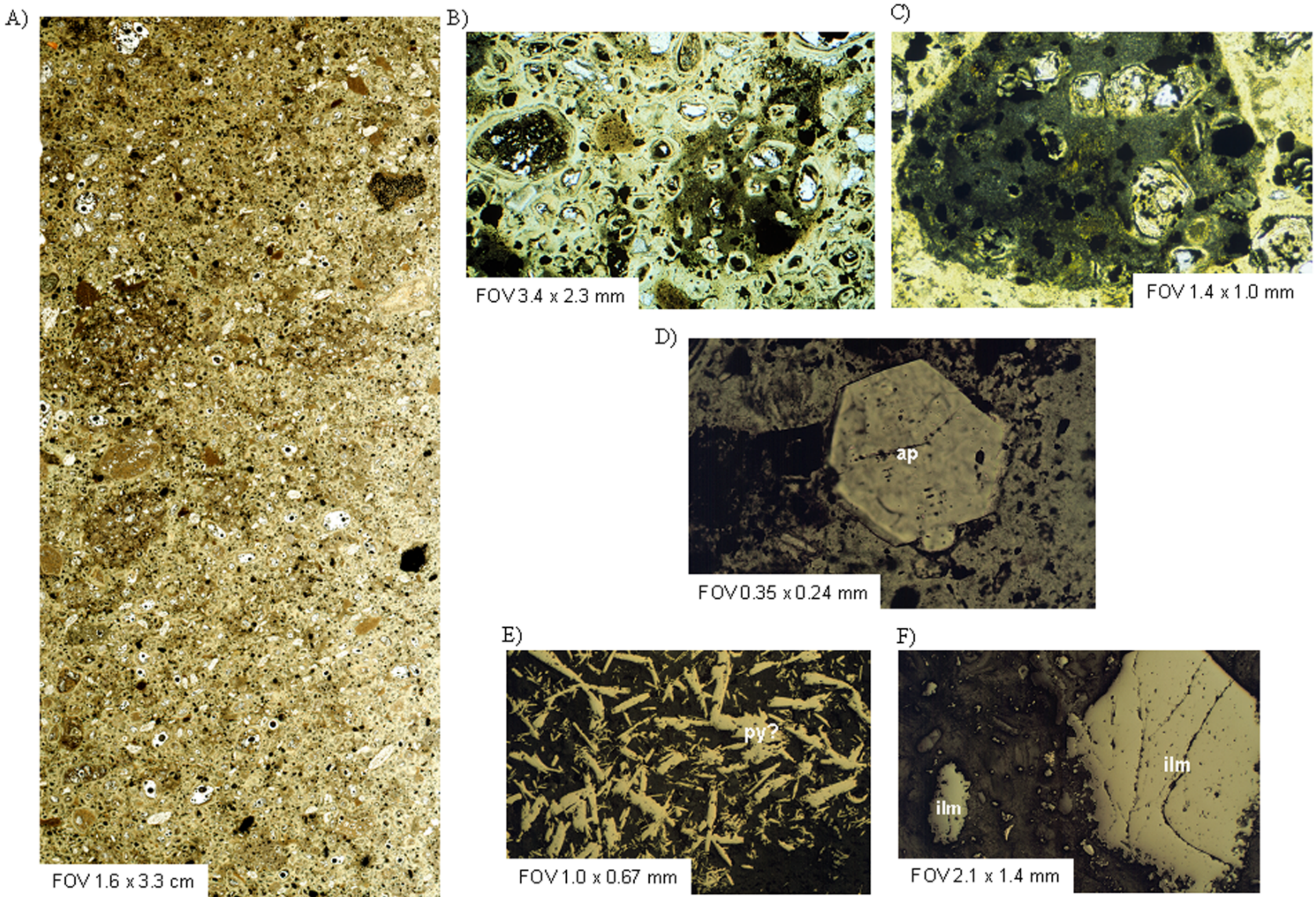

Figure 13. Photomicrographs of sample ABK59, Legend pipe, Birch Mountains: A) scan of polished thin section; B) enlargement of image A, with lapillus; C) lapillus; D) hexagonal apatite; E) needle-textured sulphide mineral (?pyrite); and F) ilmenite. Abbreviation: FOV, field of view.

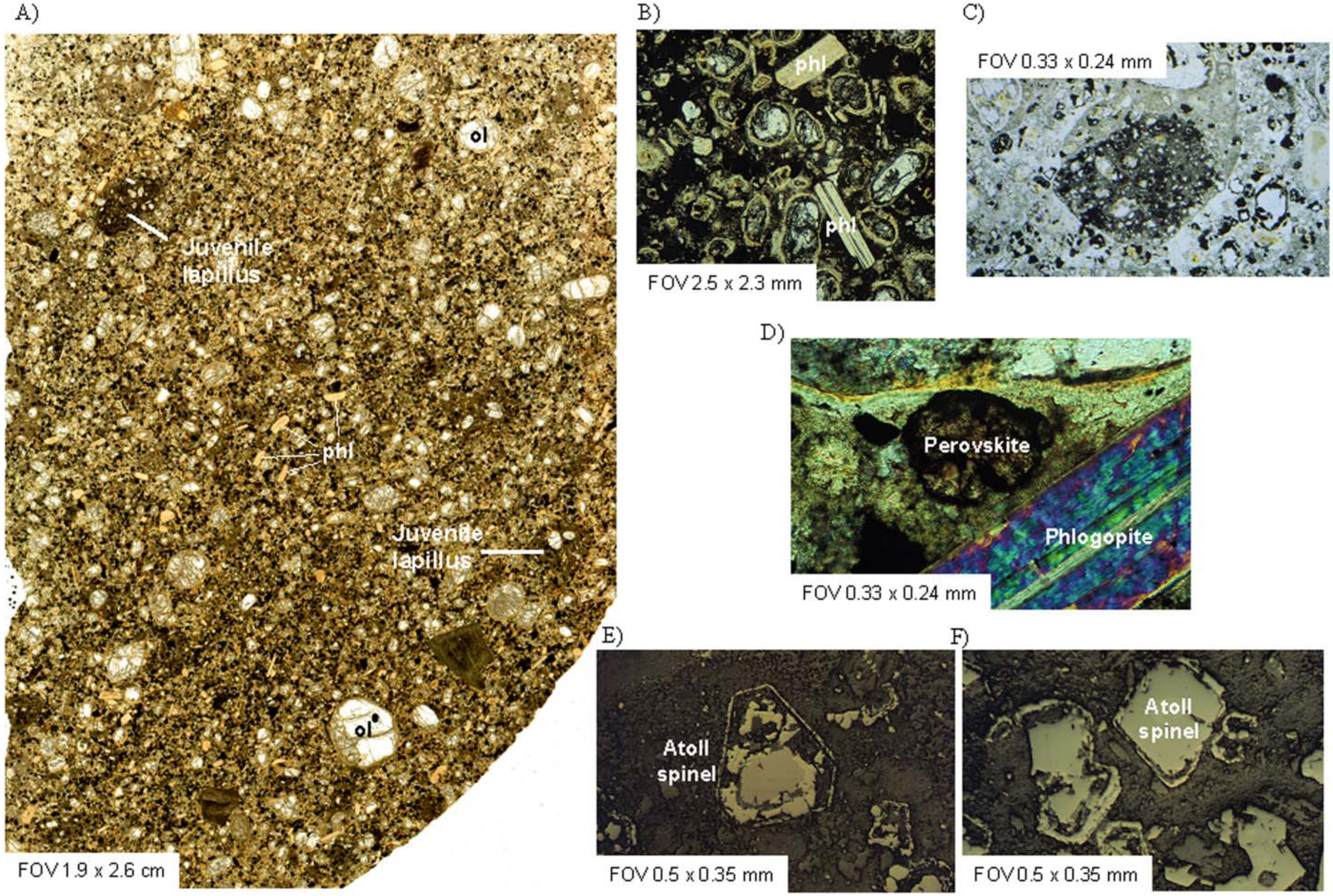

Figure 14. Photomicrographs of sample ABK76, Phoenix pipe, Birch Mountains: A) scan of polished thin section; B) enlargement of image A; C) lapillus; D) matrix perovskite and phlogopite; and E) and F) atoll-textured spinel. Abbreviation: FOV, field of view.

although some larger phenocrysts (up to 2.5 mm) are rounded. Olivine macrocrysts were not observed. Some fresh and nonfractured olivine is present in the larger phenocrysts, particularly from sample ABK76.

The samples from the Phoenix pipe contain two types of lapilli: ash-sized, single-kernel pyroclasts and larger, multi-olivine, crystal lapilli (Figures 14B,C). The lapillus in Figure 14C appears to have a secondary, lighter lapillus margin, which may suggest that the original, dark lapillus has undergone a second eruption event.

The matrix consists mainly of serpentine with some dolomite and calcite (Appendix 1; Figure 15), but overall is characterized by an abundance of phlogopite macrocrysts and perovskite phenocrysts (Figures 14B, D) relative to the K4, K6 and Legend pipes. The phlogopite constitutes between 4 and 7 vol. %. The mica grains are typically randomly orientated and isolated, although the grains, in places, appear aligned and, at significant magnification, (Figure 15), smaller (<20 μm) phlogopite grains are intergrown. A greenish hue on most phlogopite grains is likely related to chloritization. Several phlogopite grains include inclusions of either a sulphide mineral or apatite. The perovskite grains are typically large (up to 0.12 mm and average about 0.08 mm) and have altered rims (Figures 14D, 15).

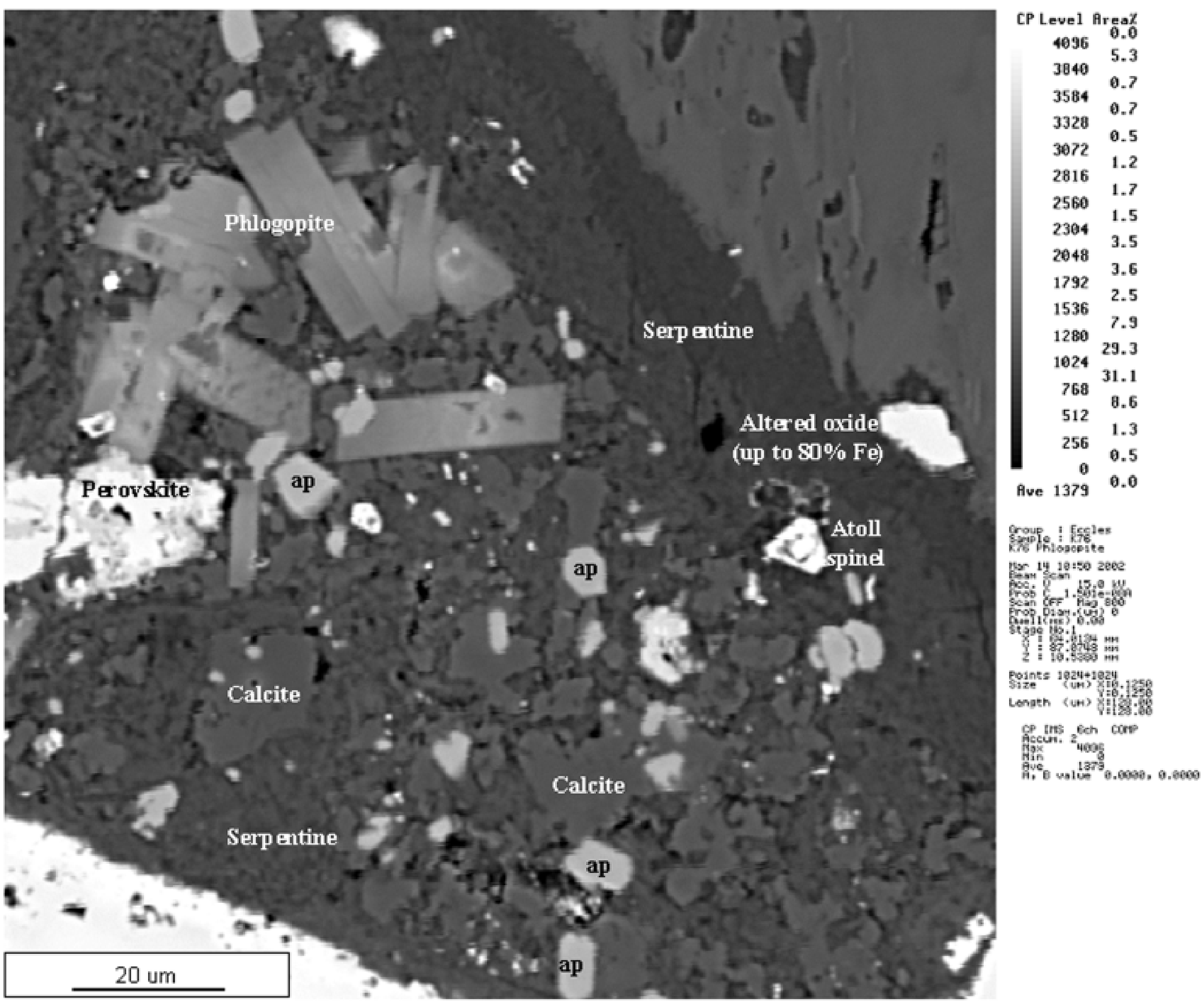

Figure 15. Backscatter image of representative area from sample ABK76, Phoenix pipe, Birch Mountains.

Atoll-textured spinel grains are distributed throughout the sample (Figure 14E, F). The term 'atoll spinel' was used by Mitchell and Clarke (1976) to describe resorbed, complexly mantled spinel grains, believed to have formed by the instability of magnesian ulvöspinel–ulvöspinel–magnetite spinel with late-stage, carbonate-rich fluids that formed the groundmass. Optically, these spinel grains have a different reflectivity from core to border. The cores of the atoll spinel grains in the Phoenix pipe are almost totally altered to magnetite, whereas the rims consist of Fe, Ti and relatively little Cr.

Other groundmass minerals include hexagonal apatite and highly altered iron-oxide minerals (Figure 15). Ilmenite xenocrysts are rare.

4.5 Samples ABK81 and ABK82 (Kendu Pipe, Birch Mountains)

Macroscopically, sample ABK81, collected at 102 m, is light to dark grey-green and fairly competent. In contrast to other samples studied in this report, the Kendu core contains abundant mantle xenolith and xenocrystic material, lapilli and segregation-type textures as defined by the agglomeration of specific minerals. The matrix is fine grained to aphanitic, dark grey-green and carbonatized. Several mantle xenoliths were observed. The largest, a possible eclogitic mantle xenolith, is about 1.65 by 1.25 cm. Fresh xenocrysts of eclogitic and pyrope garnet, phlogopite and diopside are randomly distributed throughout the sample.

Macroscopically, sample ABK82, collected at 127 m, is light to dark grey-green, fairly competent and mantle xenocryst–rich. Dark green-black, fragments (lapilli) occur throughout the sample. The matrix is grey-green and fine grained. Mantle xenoliths in this sample are up to 2.3 by 0.9 cm in size and typically consist of olivine and eclogitic garnet. There are also several smaller (<0.5 cm) xenoliths. The sample contains abundant mantle-indicator minerals (phlogopite, chrome diopside, eclogitic and pyrope garnet, ilmenite, clinopyroxene). Country rock xenoliths (possibly plagioclase) constitute up to 8 vol. %, and are variably altered.

Compared to samples from the K4, K6, Legend and Phoenix pipes, the Kendu samples can easily be distinguished macroscopically and microscopically by the relative homogeneity of the core and abundance of

- mantle xenocrysts (mainly phlogopite, chrome diopside and garnet);
- mantle xenoliths (possibly lherzolite and eclogite), which are set in a fine-grained, dark brown matrix;
- dark, black-green juvenile lapilli; and
- abundance of altered, metasomatized basement-rock xenoliths.

The x-ray diffractograms indicate that the Kendu samples are composed predominately of serpentine (lizardite and chrysotile [$Mg_3(Si_{2-x}O_5)(OH)_{4-4x}$]), dolomite (ankerite), phlogopite and calcite (Table 3; Appendix 2). The samples also contain significant contamination from bedrock material. Sample ABK81 contains clinochlore ($Mg_3Mn_2Al[Si_3Al]O_{10}[OH]_8$), which typically forms as a common hydrothermal alteration product of amphibole, pyroxene and biotite, and sample ABK82 contains anorthite ($[Ca,Na][Al,Si]_2Si_2O_8$).

Mantle xenoliths and xenocrysts may locally constitute up to 30 vol. % of the samples. The xenoliths comprise mainly lherzolite and eclogite, (determined optically as electron microprobe analysis was not completed as part of this study). Their exact size is difficult to ascertain in drillcore, but they generally are less than 10 cm in diameter, with the majority being less than 5 cm. The xenoliths are ovoid to subangular, irregularly shaped and slightly to moderately altered (Figure 16A). Alteration and irregularly shaped xenoliths suggest derivation from a deep, hot magma source. The mantle xenocryst population occurs throughout the core and includes pyrope and eclogitic garnet, clinopyroxene, orthopyroxene, phlogopite, ilmenite and spinel. Garnet grains are up to, but rarely larger than, 0.5 mm in one direction. Complete or partial kelyphite rims are present on garnet and orthopyroxene xenocrysts.

Juvenile lapilli are another diagnostic feature in the Kendu samples and locally constitute up to 40 vol. %. The dark-coloured lapilli stand out in an aphanitic, almost indistinguishable matrix, and consist of randomly orientated, microphenocrystic phlogopite (Figure 16B–D). A micro-image of a lapillus shows that phlogopite can constitute up to 40 vol. % (Appendix 1). In addition to phlogopite, the lapilli also contain serpentine (lizardite), opaque minerals (mainly ilmenite), apatite and calcite-rich anhedral to euhedral spherical structures, which likely represent altered olivine. The lapilli vary in diameter, up to 1.2 cm and more (the pyroclast in Figure 16 continues off the slide), and average about 0.25 mm. They vary drastically in shape, from rounded, spherical shapes to very irregular, but somewhat predictable shapes (*see* below).

The term 'predictable' irregular shapes is used because a phlogopite-rich microlitic material, which is very similar in mineralogy to the juvenile lapilli, coats the surface and forms 'haloes' around pre-existing constituents, such as country rock xenoliths (e.g., anorthite; Figure 17A).

Pelletal-textured lapilli are less common than juvenile lapilli, but occur throughout the sample. These lapilli consist of large (up to 0.2 mm), mostly altered olivine kernels that are surrounded by thin mantles of fine-grained cryptocrystalline kimberlitic material (mainly phlogopite, serpentine and apatite). Figure 17B and C illustrates the pelletal lapilli, complete with tangentially aligned platy shards of phlogopite and olivine microphenocrysts around a remnant olivine kernel. The lapilli rim material is similar in mineralogy to the matrix composition of larger xenoliths or juvenile lapilli.

The juvenile lapilli and pelletal lapilli are set in a commonly aphanitic, but nonuniform distribution of groundmass minerals. Based on bulk-rock x-ray diffraction analysis, the groundmass consists mainly of serpentine and calcite. The olivine xenocrysts outside the lapilli are difficult to distinguish in plane-polarized light due to pervasive replacement. In places, microsegregation textures are observed (Figure 17D) and occur when minerals segregate and crystallize both late and simultaneously and, are therefore, concentrated in certain areas of the rock. In addition, the groundmass has a wide range of silicate (e.g., garnet, clinopyroxene and orthopyroxene), semi-opaque (e.g., perovskite), and opaque (e.g., spinel, ilmenite and sulphide) minerals (Figure 18). Rutile is also common, as observed in heavy-mineral concentrates. Optically, rutile is commonly present in clinopyroxene and occurs as rod-like or needle-like rutile inclusions, which are generally oriented parallel to crystal faces, and is therefore of mantle-derived xenocrystic origin (Figure 18A, B).

Basement xenoliths consist mainly of anorthite (anorthosite xenoliths). It is possible that they have undergone contact metamorphism, as indicated by their irregular, diffuse boundaries (Figure 17A). Trace amounts of possible labradorite and/or bronzite were also observed.

5 Mineralogical Summary

The intent of this section is not to provide a discourse on the mineralogy of kimberlite rocks, which has been adequately described by several authors (e.g., Dawson, 1980; Mitchell, 1986; Scott Smith, 1995), but to describe aspects of minerals specific to selected Alberta kimberlites, particularly those that have significant paragenetic implications.

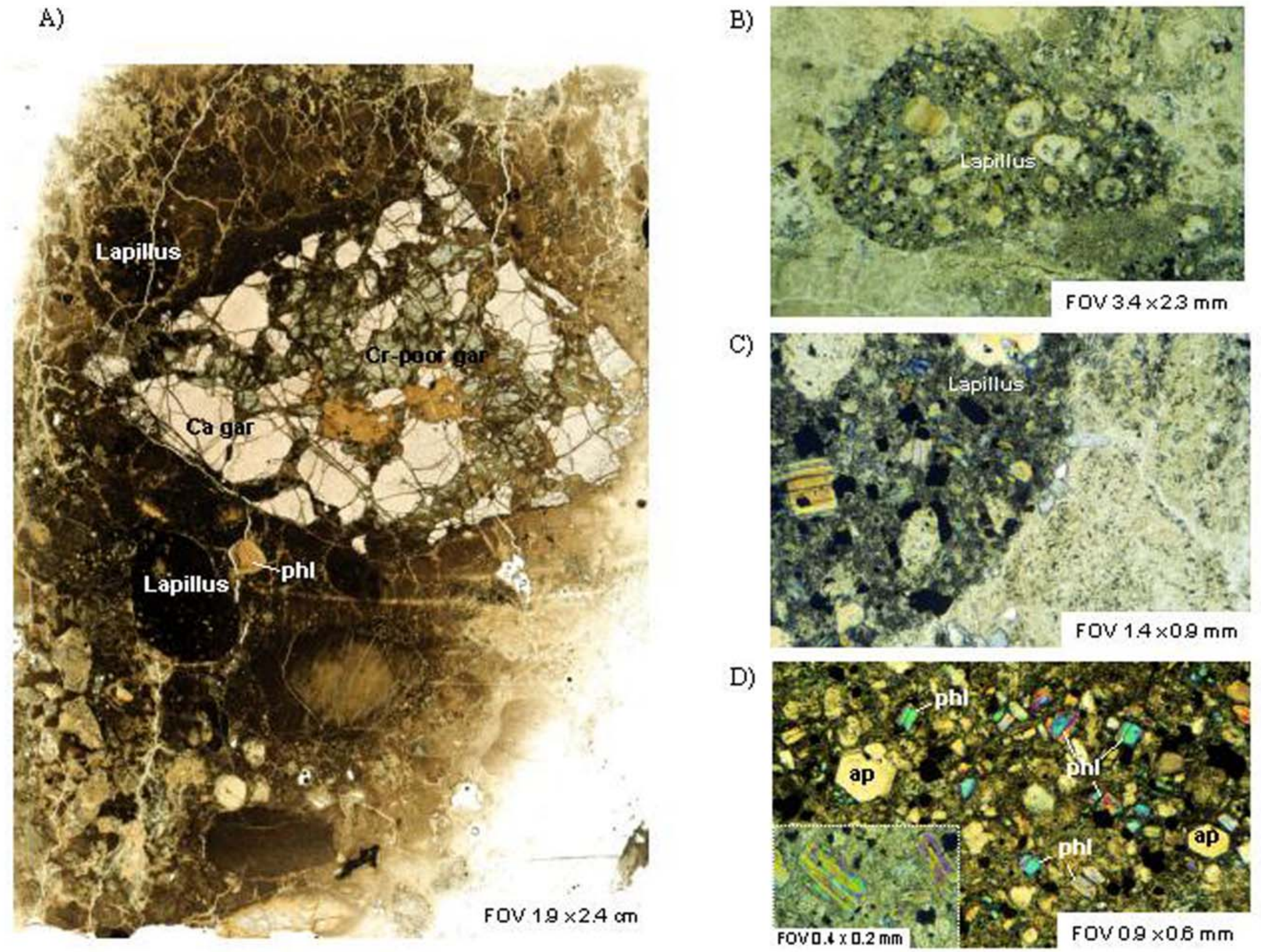

Figure 16. Photomicrographs of sample ABK81, Kendu pipe, Birch Mountains: A) scan of polished thin section; B) juvenile lapillus in an aphanitic matrix; C) matrix comparison between pyroclast and matrix external to lapillus; and D) magnified image of an lapillus. Abbreviation: FOV, field of view.

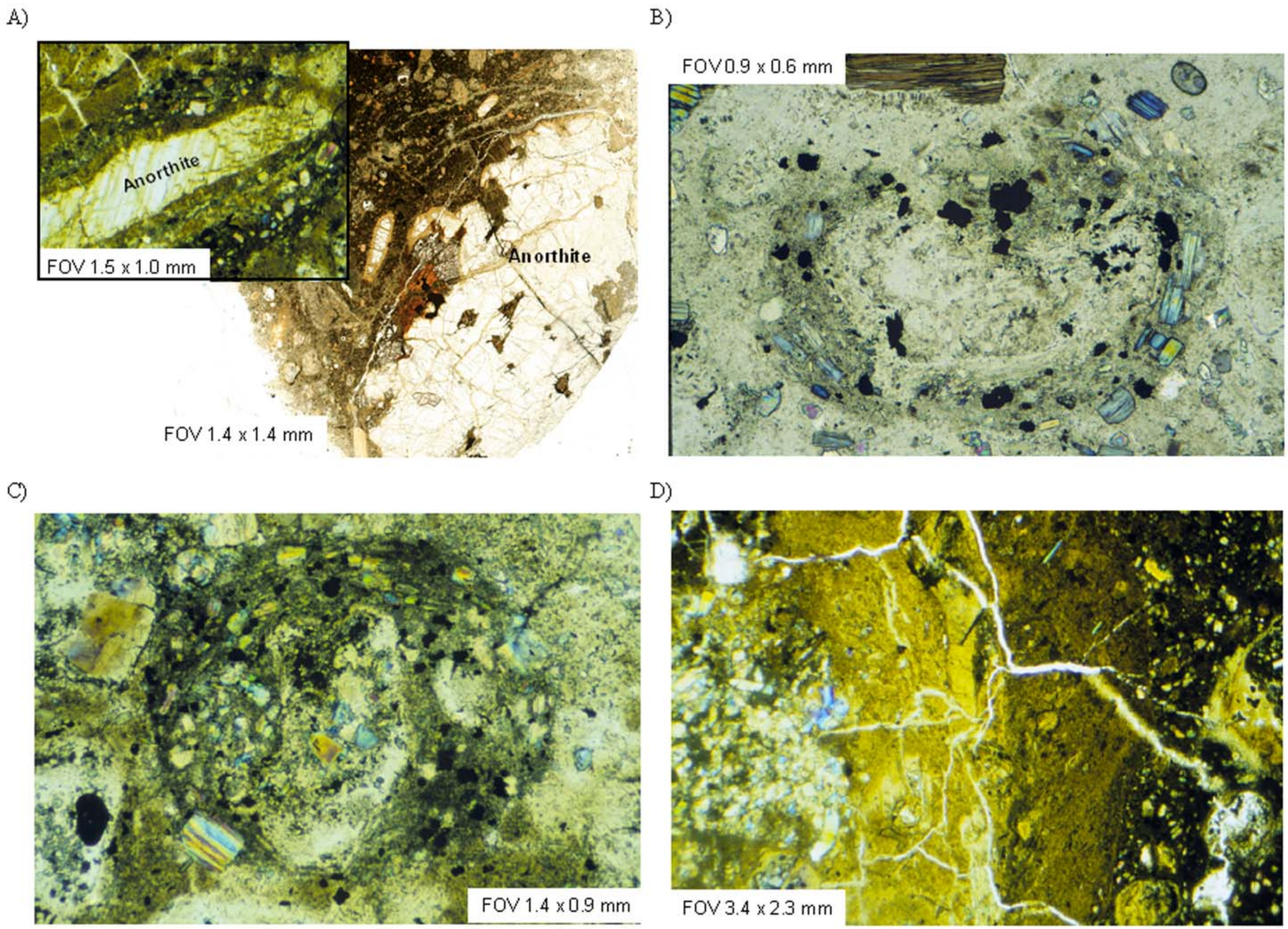

Figure 17. Photomicrographs of the Kendu pipe, Birch Mountains: A) microphenocrystic kimberlitic rock haloes around altered basement xenoliths; B) and C) pelletal-textured lapilli with tangentially aligned phlogopite crystals; and D) matrix microsegregation textures. Abbreviation: FOV, field of view.

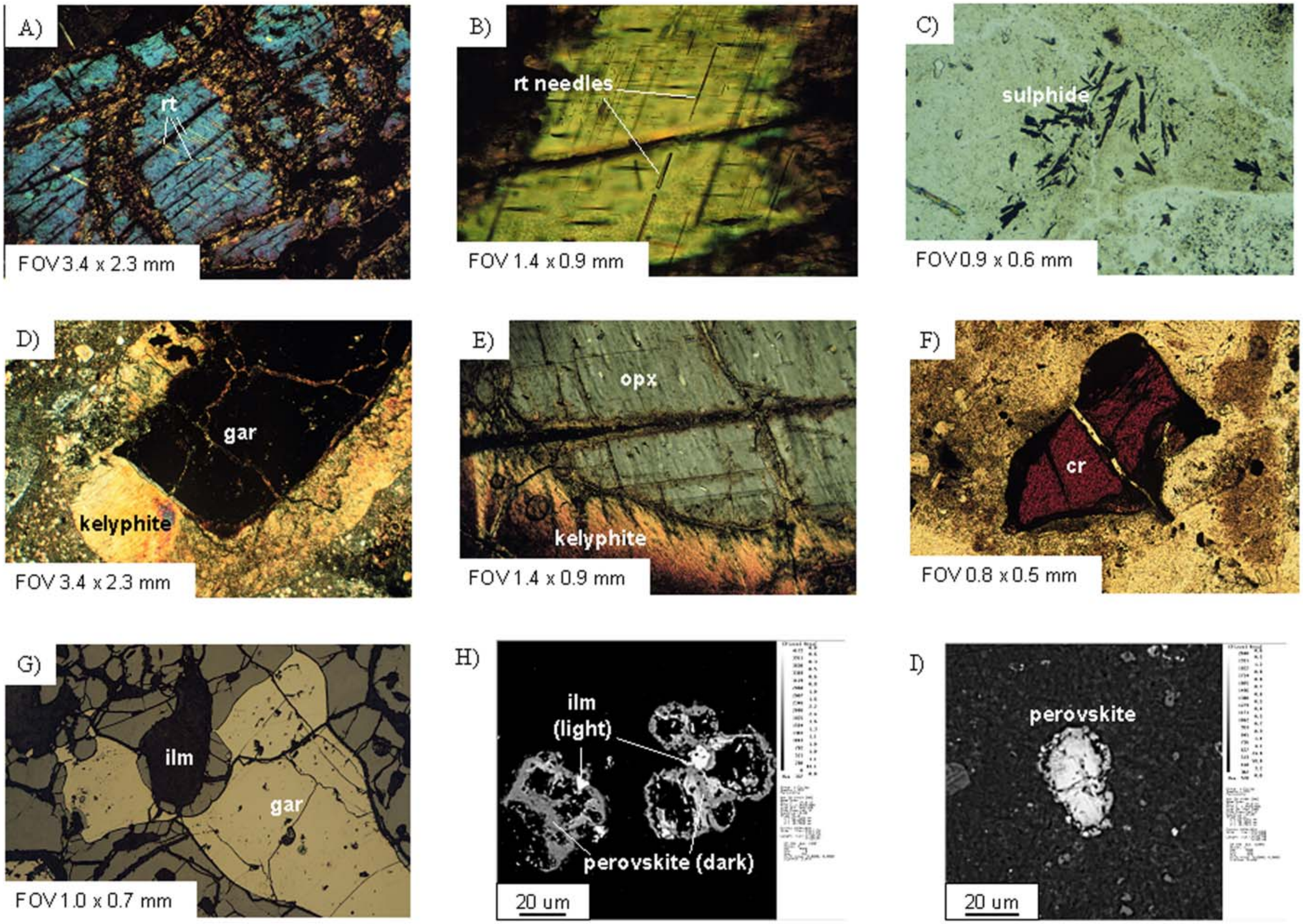

Figure 18. Photomicrographs of mantle minerals from the Kendu pipe, Birch Mountains. Abbreviation: FOV, field of view.

5.1 Olivine

Olivine is a ubiquitous and abundant mineral in the northern Alberta pipes, forming up to 65 vol. % of the total mineral content. Olivine displays a wide range in size, but is present in most samples in at least two distinct generations. Measurements of olivine in thin section show that approximately 90% of the grains occur as microphenocrysts measuring 0.5 mm or less, and typically less than 0.25 mm (Figure 19). These olivine crystals are usually subhedral, although euhedral and anhedral varieties occur in any given pipe.

Macrocrystalline olivine is not abundant and is most prominent in the K6 pipe. When present, the olivine macrocrysts are typically ovoid in shape and range in size from 0.5 to 10 mm. The relative proportion of primary microphenocrystalline to macrocrystalline olivine varies. For example, the K4 pipe is composed primarily of ash-sized olivine crystals, whereas the K6 pipe contains abundant large, ovoid olivine macrocrysts. Figure 19 shows a general lack of olivine macrocrysts in the Birch Mountains samples. The degree of alteration from olivine to serpentine, calcite and magnesite varies; therefore, the colour of the olivine grains ranges from dark green to pale green to pale greenish white. Complete pseudomorphing by serpentine is typical of many of the smaller crystals; despite serpentinization and/or carbonatization, the morphology of the olivine phenocrysts is generally well preserved. Zoned pseudomorphs are common, where serpentine and carbonate minerals form rims on olivine crystals but do not totally replace them. Many of the olivine macrocrysts contain inner cores of relict, fresh forsteritic olivine, the alteration being confined to their margins and along fractures.

5.2 Serpentine

Next to olivine, serpentine is the most abundant mineral, followed by carbonate (calcite and/or dolomite). Although intimately associated with carbonate, it dominates the groundmass and is the primary replacement mineral of olivine xenocrysts. There are several generations of serpentine, as determined by their significantly different textural variations, from pseudomorphic to relatively coarse, platy varieties. The predominant serpentine is pseudomorphic lizardite, which formed at a relatively early stage. Based on degradation and preservation of various primary minerals, the serpentine typically pseudomorphs after olivine phenocrysts and forms the groundmass along with other late-stage minerals (e.g., perovskite, apatite, phlogopite). This serpentine is oxidized and stained brown to dark brown, likely by iron oxyhydroxide.

Whole-rock x-ray diffraction shows at least three types of serpentine to be present: 1M and 1T lizardite, 6T lizardite and chrysotile. Jago and Mitchell (1985) suggested that x-ray diffraction techniques can be used to distinguish between primary groundmass serpentine (1T lizardite) and nonpseudomorphic prograde serpentine (6T lizardite), in which case both types are present in the northern Alberta pipes. The lack of vein-filling and mesh-textured serpentine suggests that serpentine is of hydrothermal or metasomatic origin, replacing primary olivine. Podvysotskiy (1985) reported that this is the most common formation mechanism for serpentine in kimberlite, where extensive serpentinization occurs when mineralized meteoric and/or hydrothermal waters from the crust enter the kimberlite. From the few micro-images obtained, serpentine in the olivine margins has higher Al_2O_3 and FeO contents, probably at the expense of MgO and SiO_2, than groundmass serpentine. This may be related to late-stage fluids or later serpentinization. In some cases, serpentine-rich pseudomorphs are accompanied by extensive development of magnetite, particularly in the Legend and Phoenix pipes. It should be noted, however, that the development of any additional minerals appears to be preceded by an initial stage of serpentinization. No chloritization of the serpentine is observed.

5.3 Carbonate

Carbonate minerals are common late-stage groundmass in kimberlite, the amounts varying from trace quantities to more than 50 vol. % in calcite kimberlites (Skinner and Clement, 1979; Dawson, 1980;

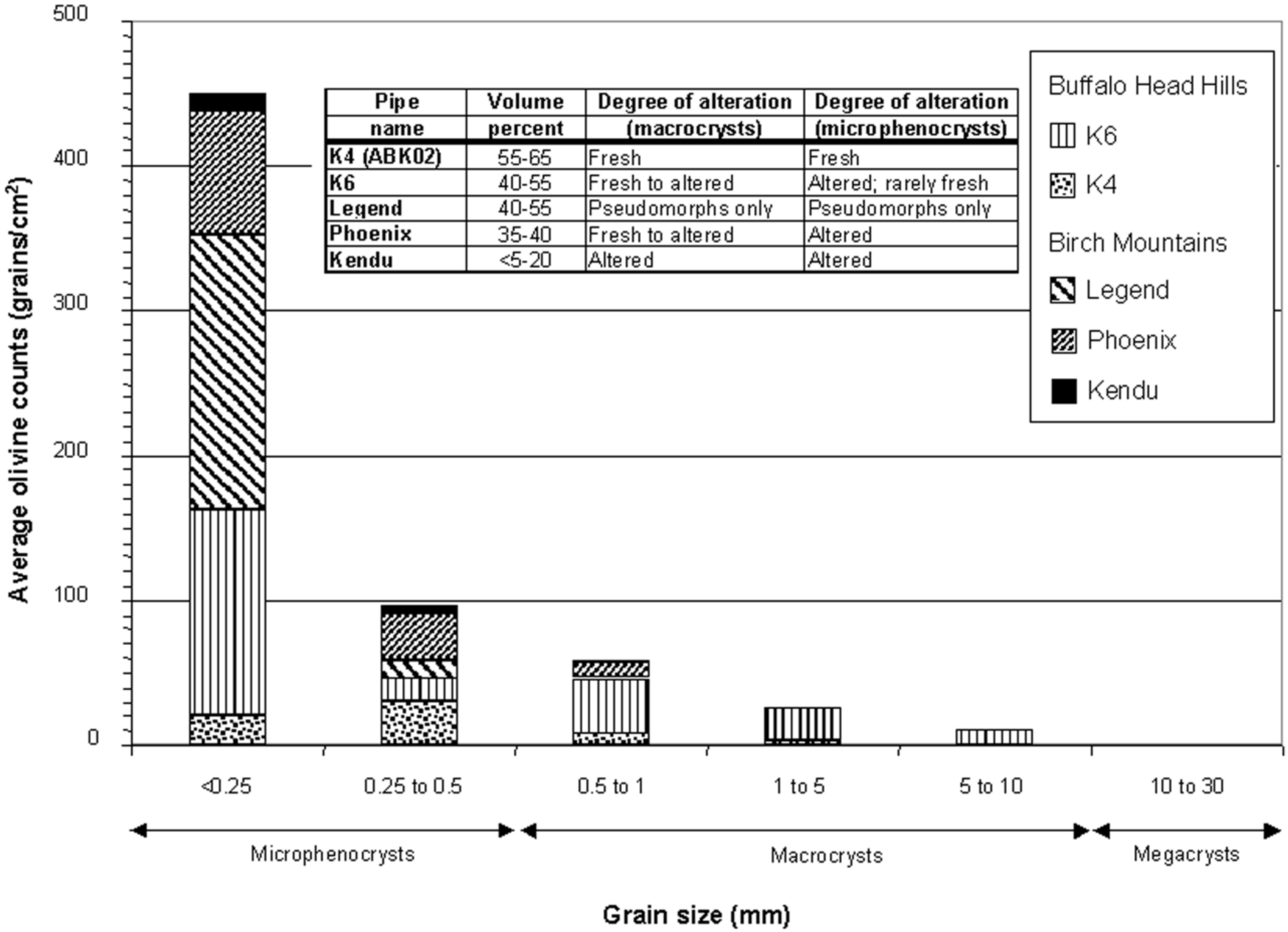

Pipe name	Volume percent	Degree of alteration (macrocrysts)	Degree of alteration (microphenocrysts)
K4 (ABK02)	55-65	Fresh	Fresh
K6	40-55	Fresh to altered	Altered; rarely fresh
Legend	40-55	Pseudomorphs only	Pseudomorphs only
Phoenix	35-40	Fresh to altered	Altered
Kendu	<5-20	Altered	Altered

Figure 19. Modal distribution of olivine, as determined in thin section, from selected northern Alberta kimberlitic pipes.

Mitchell, 1986).

In the northern Alberta pipes, carbonate typically occurs together with serpentine as fine-grained (often <0.1 mm) aggregates of xenomorphic grains in the groundmass with magnetite and phlogopite, and/or as pseudomorphs of earlier formed olivine. As such, the relation and ratio between serpentine and carbonate varies considerably from one pipe to another.

The most abundant carbonate mineral in samples studied in this report is calcite, followed by dolomite and ankerite. Calcite occurs, to some extent, in all of the pipes investigated, particularly K6, Legend, Phoenix and Kendu. Dolomite is the predominant carbonate in the K4 pipe.

Pipe-specific examples of carbonate distribution include

- concentrations of carbonate at the margins of partially serpentinized olivine grains (dolomite in K4, calcite in Legend);
- calcite filling the cores, or possibly vugs, in weathered olivine grains (K6, Legend and Phoenix);
- pool-like segregations of carbonate-rich serpentinized matrix (calcite and/or ankerite in Kendu); and
- intimate intergrowths evenly distributed throughout the serpentinized matrix (dolomite in K4, K6, Legend and Phoenix).

The origin of the carbonate in the northern Alberta pipes is speculative, but the majority is believed to be primary in origin. The reason for this is that much of the carbonate occurs in conjunction with serpentine and late-stage minerals, such as apatite and perovskite, that are well preserved despite being particularly prone to carbonatization. In addition, primary tabular carbonate crystals (microliths) in the Kendu pipe have straight extinction and rhombohedral end faces, and are sometimes twinned. These features may represent the highest temperature habit of calcite (e.g., Podvysotskiy, 1985).

In addition to primary carbonate, the pipes have undergone secondary carbonatization, probably related to groundwater circulation and/or hydrothermal solutions, as evidenced by vein calcite and infilling of small pores and cavities in the K6, Legend and Phoenix pipes. Metasomatic calcite was encountered as 1 to 3 mm, fibrous calcite veinlets in outcrop at kimberlite K6.

5.4 Phlogopite

Phlogopite mica is a minor constituent of the Buffalo Head Hills pipes, generally forming <5 vol. % of the mineral assemblage with macrocrysts up to 10 mm in length that are normally quite dispersed. The modal amount of phlogopite in the Birch Mountain pipes varies from nonexistent (Legend pipe) to moderate (up to 8 vol. % in the Phoenix pipe) to high, with local concentrations of up to 40 vol. % (Kendu pipe). Phlogopite was easily sampled from coarse-crushed material from the Phoenix and Kendu pipes.

In thin section, phlogopite typically occurs as small groundmass crystals characterized by subhedral to euhedral laths that range in length from 0.05 to 0.1 mm and have a similar length-breadth ratio (2.5 to 3.5). With the exception of the Kendu pipe, the grains are typically randomly orientated and isolated. In contrast to the olivine, which is highly altered, the phlogopite is partially altered and its idiomorphic character is only slightly modified by varied degrees of corroded margins. This may be related to the late-stage development of the phlogopite. When present, the alteration occurs along cleavage planes and is dominated by chloritization.

Zoning is common and typically confined to core-rim relationships, where the rims may be thick or thin relative to the cores. Some zoning, however, appears erratic or random so that a clear distinction between the core and rims is not always possible. Zoning irregularities may be due to reactions with late liquids and with local microenvironments that may have influenced the nature and extent of the reactions.

No sieve-textured phlogopite mica was encountered, although inclusions of pyrite and apatite in phlogopite from the Phoenix pipe demonstrate the late-crystallizing nature of some phlogopite.

5.5 Apatite

Apatite is a late-crystallizing groundmass phase, ranging from trace amounts (≤1 vol. %) in the Buffalo Head Hills pipes (K4 and K6) and up to about 5 vol. % in the Birch Mountains pipes. The apatite is relatively unaltered, and the few partially replaced grains have a slightly irregular, corroded appearance. As such, apatite usually forms as euhedral, prismatic crystals with distinct hexagonal base sections. The euhedral crystals are commonly scattered fairly evenly throughout the groundmass, but are more prevalent in calcite- or carbonate-rich portions. Thus, the apatite is larger (up to 0.9 mm in diameter in the Phoenix pipe) and better formed in carbonate-rich Birch Mountains pipes compared to those in the Buffalo Head Hills, where the apatite is predominantly small (about 0.01 mm) and forms as anhedral grains. Based on the observation of these samples, apatite may be used for petrographic discrimination between the Buffalo Head Hills and Birch Mountains pipes.

5.6 Perovskite

Perovskite was optically observed in the K6, Phoenix and Kendu pipes as pinkish brown, subhedral, rounded crystals. The perovskite grains are typically isolated, but also occur within mantles on xenocrystic ilmenite. The size of perovskite crystals varies appreciably between pipes. In kimberlite K6, perovskite occurs as very small (typically <3 µm), rounded crystals that, in places, dominate the opaque mineral suite. In the Phoenix pipe, abundant (up to 5 vol. %), unusually large perovskite averages 0.08 mm in diameter and ranges up to 0.12 mm.

Chakhmouradian and Mitchell (2000) reported that perovskite is unstable in a carbonate-rich environment and, during the final stages of kimberlite evolution, commonly undergoes cation leaching and replacement by other Ti-bearing minerals. Euhedral perovskite, however, is known to occur in some carbonatite bodies (L. Heaman, pers. comm., 2002). Regardless, perovskite in the Phoenix pipe is easily large enough for its core to survive alteration, but the very small perovskite crystals in the K6 and Kendu pipes may be altered, possibly to a titanium dioxide (TiO_2) phase (e.g., rutile, anatase) or ilmenite. Mineral separates of perovskite from the Phoenix pipe are coated by a whitish, carbonate-rich alteration material that, when combined with ilmenite, has a salt-and-pepper appearance. Pervasively altered perovskite has a corroded, ‘spongy’ appearance.

5.7 Opaque Minerals

Spinel is ubiquitous and occurs in all samples. It often forms subhedral to euhedral, cubic to corroded grains that range in size from 0.001 to 0.1 mm. It typically occurs as a primary groundmass mineral and varies in abundance from 1 to 5 vol. %. Spinel, in conjunction with perovskite and ilmenite, may form ‘necklace textures’ around discrete olivine crystals or around pseudomorphed, subhedral olivine. Spinel is typically altered, particularly in the Birch Mountains pipes, where ‘cloudy fringes’ of amorphous iron hydroxide/oxide characterize the crystals. Atoll-textured spinel (i.e., resorbed, complexly mantled spinel that resembles an island surrounded by a barrier reef; Mitchell and Clarke, 1976) is common in the Legend pipe, where chromite cores are surrounded by multiple atolls of resorbed spinel (dominantly magnetite).

Ilmenite is present in all of the pipes and may constitute up to 5 vol. %, as it does in the Legend pipe, where ilmenite xenocrysts are a predominant feature and range up to 9 mm in diameter. Ilmenite typically occurs as

- small (<20 µm), euhedral, single-crystal matrixes;
- disseminated macrocrysts, consisting of large (up to 9 mm), rounded, single crystals and polycrystalline aggregates; and
- intergrowths with groundmass spinel and perovskite.

Sulphide minerals are present, albeit only as a minor component, in all of the pipes investigated. Minor (1–3 vol. %) to moderate (up to 7 vol. %) quantities of sulphide minerals are restricted to the K4 and Legend pipes, respectively. Sulphide minerals typically occur as anhedral disseminations in the groundmass and, possibly, as replacements of various biota. In the K4 pipes, the sulphide minerals are primarily associated with dolomite. Carlson et al. (1999) reported that, in addition to pyrite, the sulphide minerals chalcopyrite, sphalerite and millerite, and an unidentified Ca-REE phosphate mineral have been identified in trace amounts in the Buffalo Head Hills pipes.

Serpentinization may be accompanied by the formation of nickel sulphide as acicular crystals (e.g., Lattavaram kimberlite, southern India; Akella et al., 1979). In the Legend and Kendu pipes, euhedral acicular 'needles' of an iron-rich sulphide mineral occur in clusters and disseminations**.** Aravanis (1999) identified the sulphide mineral greigite [$Fe^{2+}Fe_2^{3+}S_4$] from either the Jason target (magnetic anomaly with no kimberlitic rocks intersected) or the Legend pipe in the Birch Mountains area.

6 Textural-Genetic Classification

Selected pipes in this report comprise volcaniclastic rocks, particularly pyroclastic kimberlite. An overview of the textural and mineralogical highlights of each selected pipe is presented in Table 4.

Microscopically, the samples are crater volcaniclastic rocks because they

- contain juvenile spherical and amoeboid lapilli;
- lack true glass, glass shards and scoriaceous lapilli;
- do not contain abundant xenoliths and quenched acicular microlites of diopside (clinopyroxene) in the rims of the lapilli and their interclast matrix;
- are poorly sorted, with loosely packed, clast-supported textures; and
- contain common primary microcrystalline (quenched) carbonate.

Megascopic (i.e., drillcore) properties that support this contention include the following:

- The Birch Mountain cores show bedding and graded layers, particularly stratified tuff with alternating layers of coarse lapilli-sized (2–64 mm) and laminae of finer ash-sized (<2 mm) tuff.
- Drillholes K6-7, K6-8 and K6-10 from the K6 pipe penetrated cycles of kimberlite interlayered with mudstone, with gradational lower contacts between the kimberlite and the underlying mudstone (Skelton and Bursey, 1998).
- The Legend and Phoenix holes bottom out in 'kimberlite tuff' (Aravanis, 1999).

The fragile lapilli (often curvilinear) and shale clasts (often angular and unaltered) lack of breakage on fresh olivine grains, lack of sedimentary rocks in the matrix, lack of sorting and sedimentary structures, loosely packed and clast-supported textures, and nature of bedding (or lack or it) are all strong indicators that the selected pipes should be classified as PK deposits. The coexistence of variably sized lapilli, some with different groundmass mineralogies, may result from different eruptions or variations in the conditions during eruptions, with the extrusive tephra having been subsequently mixed together in their current host. Multi-generation lapilli, or lapillus that formed mantles for later generations of lapillus development support this.

Table 4. Summary of the unique properties, infilling and classification of selected northern Alberta kimberlitic rocks.

Pipe name	Unique properties	Mantle xenoliths	Infilling[1]	Mineralogical-genetic classification
K4	K4A – silicification; K4B – abundant, fresh, ash-sized olivine (olivine crystal tuff); K4C – elongated-platy serpentine	Rare	Juvenile lapilli-bearing, olivine tuff; VK where PK is greater than RVK	Serpentine kimberlite
K6	Juvenile pyroclasts; abundant, fresh olivine macrocrysts (>0.5 mm) and phenocrysts (<0.5 mm); calcite alteration and veining	Moderate	Juvenile lapilli-bearing, olivine tuff; VK where PK is greater than RVK	Calcite serpentine kimberlite
Legend	Carbonatized; abundant ilmenite	Rare	Juvenile lapilli-bearing, olivine tuff; PK	Carbonate-bearing serpentine kimberlite
Phoenix	Carbonatized; abundant perovskite (up to 0.12 mm) and phlogopite	Rare	Juvenile lapilli-bearing, olivine tuff; PK	Carbonate-bearing serpentine kimberlite
Kendu	Abundant phlogopite-rich juvenile lapilli and basement and mantle xenoliths (mainly anorthosite); minor component of pelletal lapilli; flow-aligned and segregation textures	Abundant xenoliths and xenocrysts	VK	Phlogopite serpentine kimberlite

[1] Infilling definitions from Field and Scott-Smith (1998):

VK – volcaniclastic kimberlite describes extrusively formed fragmental kimberlite deposits for which the mode of deposition is not known

RVK – resedimented volcaniclastic kimberlite describes VK for which depositional mechanisms can be recognized and ascribed to 'normal' sedimentary processes

PK – pyroclastic kimberlite describes VK for which *prima facie* evidence shows direct deposition by explosive volcanic processes

There is, however, some evidence for RVK, particularly in the fresher, less evolved Buffalo Head Hills pipes, where the boundaries of some lapilli are curvilinear on one side and fragmented on the other, and the lapilli are 'somewhat' horizontally oriented. In addition, some olivine grains are broken and fractured. Many of the lapilli, however, are more or less preserved and the presence of highly irregular amoeboid lapilli suggests that transportation of clasts has not been extensive. In addition, little to no sedimentary rock material occurs in the matrix. Thus, it is concluded that the PK component is greater than the RVK component and these pipes should therefore be classified as PK.

The recognition and description of different types of lapillus may be helpful for emplacement modeling. For example, ash- to lapilli-sized juvenile pyroclasts (i.e., variably-sized single crystal olivine coated by juvenile material), which are diagnostic of the east side of the K6 pipe surface exposure, are related to a near-vent environment. In addition, petrographic textures from the Kendu pipe samples are suggestive of rocks originating from deeper within the volcaniclastic pile in comparison to textures observed in the majority of the NAKP pipes. The following observations support this contention:

- abundance of metasomatized basement-rock xenoliths with irregular, diffuse boundaries with the surrounding kimberlitic rock
- abundance of mantle xenoliths, some of which have nonrounded shapes and are altered
- abundance of delicate juvenile lapilli, which are predominately of earlier crystallized kimberlitic rock fragments characterized by angular phlogopite microphenocrysts
- presence of pelletal-textured lapilli, which commonly have a rim of tangentially aligned, extremely fine grained (<0.01 mm long) phlogopite and serpentine microlitic material surrounding olivine pseudomorphs; the pelletal lapilli flow-alignment textures are similar, but lack the diopside microlites described by Scott-Smith (1995) and Mitchell (1995) as a 'hallmark' texture of diatreme-facies kimberlite
- flow-aligned microcrystalline kimberlitic rock that form haloes around mantle and basement-rock xenoliths
- matrix has a nonuniform distribution with isolated 'pools' of groundmass minerals

7 Mineralogical-Genetic Classification

Scott Smith (1995) suggested that application of this classification scheme should be restricted to hypabyssal-facies rocks and cannot readily be used for other textural types because they lack primary groundmass minerals. Nevertheless, a mineralogical-genetic classification is attempted for the selected samples in this report because 1) of the level of description of mineralogical assemblages identified earlier in this report; and 2) Eccles and Luth (2001) suggested that, despite deposition in a crater environment, the whole-rock geochemical signature of Alberta kimberlitic rocks can be used to evaluate the extent of contamination and that some samples from the NAKP are geochemically similar to 'fresh,' hypabyssal-facies kimberlite documented in the Northwest Territories.

The modal abundances of xenocrystic (e.g., olivine and phlogopite) and groundmass constituents (phlogopite, calcite, serpentine, opaque oxides, perovskite and apatite) were used to classify the samples. Where primary minerals have been replaced, regardless of process, a petrographic assessment of the original mineralogy is used to satisfy criteria for the mineralogical-genetic classification.

Selected pipes in this report are volumetrically dominated by olivine and serpentine, such that most of the samples can be described as serpentine kimberlite. Variable proportions of carbonate may be high enough to further classify the samples as carbonate-bearing or calcite-serpentine kimberlite.

8 Geochemical-Petrographic Comparison

Part of the criteria for sample selection in this study was based on the whole-rock geochemical interpretations of Eccles and Luth (2001). They suggested that a low component 2 score (negative load) is related to high MgO, Ni and Cr_2O_3 (primitive kimberlite), and a high component 2 score (positive load) is related to high TiO_2, P_2O_5, MnO, Fe_2O_3, Nb, Th and Zr (*see* Figure 2).

Contamination problems aside, past arguments against whole-rock compositional variation in kimberlites pointed out that linear trends on certain variation diagrams (e.g., CaO versus MgO) simply reflect differing proportions of olivine to calcite in the samples, and can be interpreted as olivine control lines. This argument is valid, especially since much (approximately 50 vol. %) of the geochemical character of kimberlite (high MgO, Cr and Ni) is attributable to the presence of olivine, which typically forms about half of the mineral mode, with at least half of that olivine (approximately 25 vol. %) considered to be of mantle-derived xenocrystic origin (Scott Smith, 1995). The evaluation of whole-rock geochemical data, however, is clearly more complicated. For example, Kendu is interpreted to have a primitive geochemical signature (high MgO and Ni; Eccles and Luth, 2001); it should therefore have abundant olivine, but Kendu contains the smallest amount of fresh olivine by volume (<20 vol. %) of all the samples in this study.

Furthermore, kimberlite often contains different distributions of primary, euhedral olivine phenocrysts, which suggests that many erupting kimberlites probably represent mixed batches of different primitive liquids that formed in the mantle (Clement, 1982). The resulting mixed kimberlite liquids then become extensively contaminated by mantle xenoliths and xenocrysts, which are dominated by single grains of olivine (i.e., macrocrysts) and so-called groundmass minerals that can crystallize at different stages during ascent. The later minerals typically influence the incompatible element component of kimberlite, where some elements can be increased by the presence of specific xenocrystic minerals, such as Zr and Hf from ilmenite and zircon, and Ba and Rb from phlogopite. For example, based on major-element data, the Legend pipe has higher CaO and lower MgO than the Phoenix pipe (i.e., Legend is the more evolved kimberlite), yet incompatible element compositions led Eccles and Luth (2001) to conclude that the Phoenix pipe represents the most evolved Alberta kimberlite magma. Thus, comparisons between the petrographic character and the geochemical results of samples selected from five separate ‘groupings’ along the Alberta kimberlite magma-evolution trend line are discussed below.

8.1 K4 Pipe

Samples ABK01, ABK02 and ABK03 form a tight cluster, together with samples from kimberlites K8 and LL8, at the most primitive end of the Alberta kimberlite trend line (*see* Figure 2). Of the 83 samples analyzed by Eccles and Luth (2001), those from the K4 pipes are characterized by the lowest Al_2O_3, TiO_2 and REE, and the highest Ni and Mg#.

The K4B pipe has the highest abundance of olivine (up to 65 vol. %), relative to this dataset, possibly as a result of subaerial winnowing of olivine from ash. A plot of MgO+FeO versus SiO_2 (Figure 20) shows a relatively linear correlation between whole-rock Buffalo Head Hills data of Eccles and Luth (2001) and olivine macrocrysts from Mitchell (1986). Samples from pipes K4B, K8 and LL8 plot nearest to the Mitchell (1986) olivine macrocryst field. This suggests the primitive geochemical signature of this grouping is directly related to high olivine content.

8.2 K6 Pipe

Whole-rock samples from K6 plot near the primitive end of the kimberlite magma-evolution trend line. Incidentally, this grouping includes most of the samples from pipes with elevated contents of diamonds (e.g., K5, K6, K11 and K14 in the Buffalo Head Hills).

Petrographically, the abundant olivine-macrocryst population and general lack of minerals associated with high field-strength elements (HFSE) in K6 distinguish it from other samples in this dataset. Phlogopite is rare, and semi-opaque to opaque minerals, including perovskite, chromite and ilmenite, are present but in minor amounts.

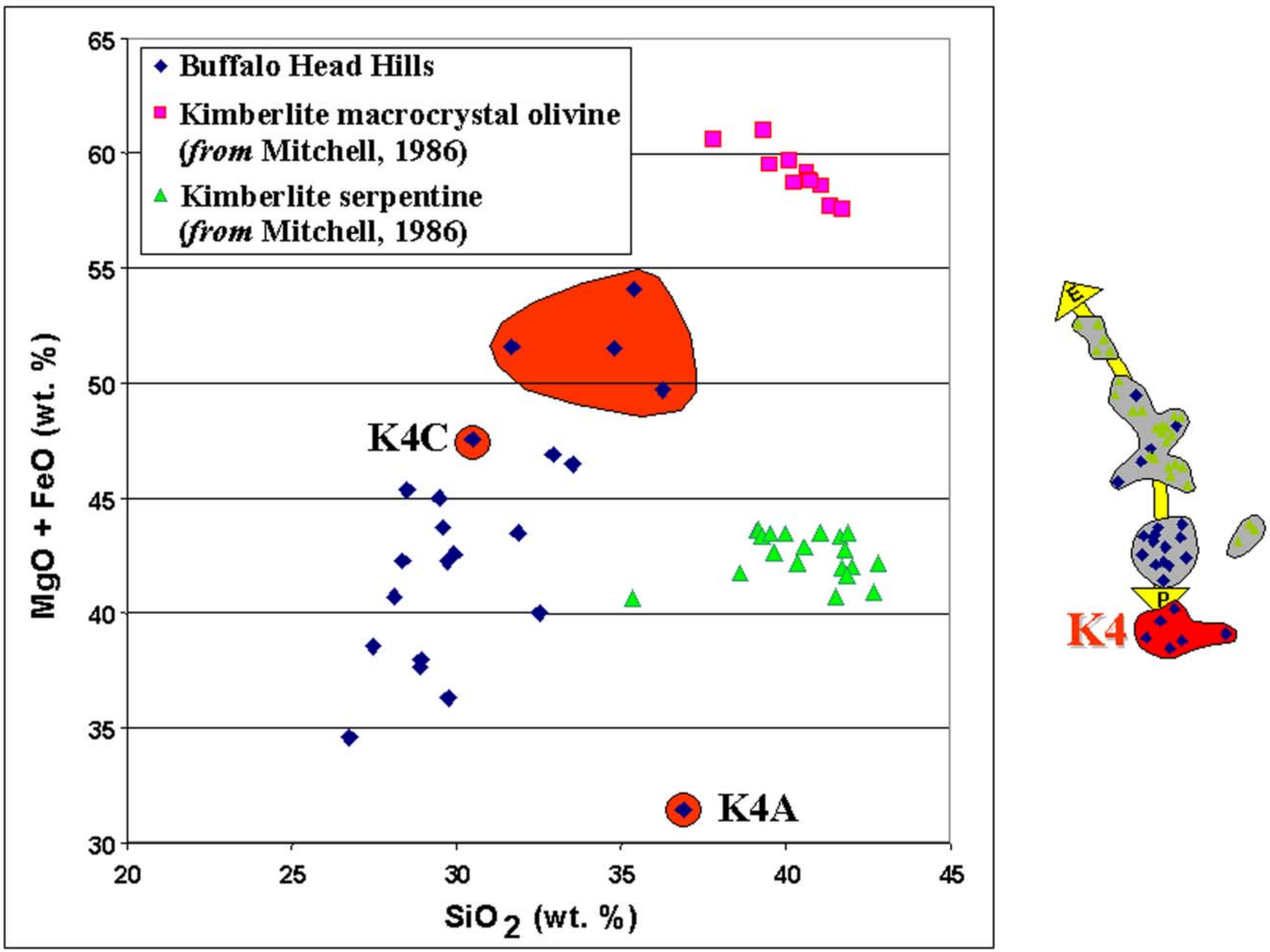

Figure 20. Comparison of MgO+FeO versus SiO_2 for samples from the Buffalo Head Hills (Eccles and Luth, 2001) and olivine macrocrysts from Mitchell (1986).

8.3 Legend Pipe

Whole-rock samples from the Legend pipe plot toward the evolved end of the trend line. Microscopically, the samples are generally devoid of olivine macrocrysts, the microphenocrystic olivine population is highly altered, and the late-stage minerals include ilmenite, calcite and apatite.

Ilmenite and apatite occur throughout the samples and may constitute up to 8 vol. %. Consequently, the Legend pipe has the highest TiO_2 (up to 4.1 wt. %), Fe_2O_3 (up to 13.6 wt. %) and P_2O_5 (up to 0.8 wt. %). The Legend samples, therefore, plot toward the evolved end of the trend line.

8.4 Phoenix Pipe

Whole-rock samples from the Phoenix pipe plot as the most evolved geochemical group in the dataset. Like the Legend pipe, the samples are generally devoid of macrocrysts, the olivine microphenocryst population is highly altered, and the matrix is composed of late-stage minerals, including perovskite, phlogopite and calcite.

The Phoenix kimberlite contains a high modal abundance of perovskite and late-stage phlogopite. Perovskite is relatively well preserved and large (up to 0.12 mm) relative to kimberlite perovskite worldwide. Consequently, the Phoenix pipe has the highest concentrations of Nb (up to 509 ppm), Hf (7.9 ppm), LREE (up to 488 ppm La and 883 ppm Ce), Zr (311 ppm) and Th (up to 97.3 ppm).

8.5 Kendu Pipe

The heterolithic composition (juvenile lapilli, and basement and mantle xenoliths) and groundmass segregation textures in Kendu indicate atypical and modally extreme mineralogy in the context of this dataset.

Samples from the Kendu pipe plot near the K6 grouping, but have higher intermediate compositions of SiO_2, Al_2O_3, K_2O and Na_2O than most NAKP kimberlite samples. Petrographic interpretation attribute the higher silica and alkali content to an abundance of basement xenoliths (predominantly anorthite) and to the mantle xenolith-xenocryst component for Kendu having the most primitive kimberlite composition in the Birch Mountains.

9 Conclusions

Petrographic examination of selected cores from Alberta kimberlite showed that volcaniclastic kimberlitic rocks are comprised of dominantly pyroclastic kimberlite (PK) with a minor component of resedimented volcaniclastic kimberlite (RVK).

The PK rocks are described as juvenile, lapilli-bearing olivine (crystal) tuff. The macrocryst suite of minerals includes rounded, less than 1 cm wide, forsteritic olivine and a minor component of phlogopite and ilmenite, which are thought to originate from the disaggregation of mantle-derived peridotite xenoliths. No megacrysts were observed. The groundmass is dominated by mostly subhedral olivine microphenocrysts (<0.25 mm) set in a fine-grained, serpentine- and sometimes carbonate-rich groundmass, and occur together with one or more of the following primary minerals: phlogopite, perovskite, spinel, ilmenite and apatite. Spherical and amoeboid juvenile lapilli are either isolated in the olivine crystal tuff, or occur together with ash- to lapilli-sized juvenile pyroclasts; their coexistence may result from multiple eruptions that have subsequently been mixed together.

The K6 pipe in the Buffalo Head Hills exhibits a distinctive inequigranular texture resulting from the presence of macrocrysts set in a fine-grained matrix and best fits the petrographic definition of kimberlite. The K4B pipe, Buffalo Head Hills, contains an unusual amount (up to 65 vol. %) of individual olivine crystals, possibly the result of subaerial winnowing of olivine. In contrast to the Buffalo Head Hills samples, the Legend and Phoenix kimberlites are highly carbonatized, relatively devoid of olivine macrocrysts, and have much higher concentrations of the late-stage minerals phlogopite, apatite and perovskite, all of which are suggestive of evolved kimberlite magma.

The Kendu samples display features consistent with volcaniclastic kimberlite. Juvenile lapilli and an abundance of basement and mantle xenoliths occur within a non-uniform, segregated matrix. The juvenile lapillie and xenoliths occur together with pelletal-textured lapilli, which commonly have a rim of tangentially aligned, extremely fine grained (<0.01 mm long) phlogopite- and serpentine-rich (lizardite) microlitic material surrounding olivine pseudomorphs. Flow-aligned textures also form 'haloes' around pre-existing constituents that include irregularly shaped, altered xenoliths.

A comparison between the mineralogy of the selected samples with the results of the multivariate geochemical analysis by Eccles and Luth (2001) show that the geochemical composition of Alberta kimberlite can be explained by the abundances of primitive and late-stage xenocrystic material. Consequently, the identification of the assemblage of primary minerals, together with whole-rock kimberlite geochemical evaluation using multivariate analysis (including both major and trace elements), can be used as a complementary tool to classify Alberta kimberlites.

10 References

Akella, J., Rao, P.S., McCallister, R.H., Boyd, F.R. and Meyer, H.O.A. (1979): Mineralogical studies of the diamondiferous kimberlite of the Wajrakharur area, southern India; *in* Proceedings of the Second International Kimberlite Conference, Volume 1. Kimberlite, Diatremes and Diamonds: Their Geology, Petrology and Geochemistry, F.R. Boyd Jr. and H.O.A. Meyer (ed.), American Geophysical Union, Washington, D.C., p. 172–177.

Aravanis, T. (1999): Legend property assessment report, Birch Mountains area, Alberta; Alberta Energy and Utilities Board, EUB/AGS, Assessment File 20000003, 23 p.

Carlson, S.M., Hillier, W.D., Hood, C.T., Pryde, R.P. and Skelton, D.N. (1999): The Buffalo Hills kimberlites: a newly discovered diamondiferous kimberlite province in north-central Alberta, Canada; *in* Proceedings of the Seventh International Kimberlite Conference, J.B. Dawson Volume, J.J. Gurney, J.L. Gurney, M.D. Pascoe and S.H. Richardson (ed.), National Book Printers, South Africa, p. 109–116.

Chakhmouradian, A.R. and Mitchell, R.H. (2000): Occurrence, alteration patterns and compositional variation of perovskite in kimberlites; The Canadian Mineralogist, v. 38, p. 975–994.

Clement, C.R. (1982): A comparative geological study of some major kimberlite pipes in the Northern Cape and Orange Free State; Ph.D. thesis, University of Cape Town, Cape Town, South Africa, 2 vol.

Clement, C.R. and Skinner, E.M.W. (1979): A textural-genetic classification of kimberlite rocks; *in* Proceedings of the Second International Kimberlite Conference, Volume 1. Kimberlite, Diatremes and Diamonds: Their Geology, Petrology and Geochemistry, F.R. Boyd Jr. and H.O.A. Meyer (ed.), American Geophysical Union, Washington, D.C., Extended Abstracts.

Clement, C.R. and Skinner, E.M.W. (1985): A textural-genetic classification of kimberlites; Transactions Geological Society South Africa, v. 88, p. 403–409.

Clement, C.R., Skinner, E.M.W. and Scott Smith, B.H. (1984): Kimberlite redefined; Journal of Geology, v. 92, p. 223–228.

Dawson, J.B. (1980): Kimberlites and their Xenoliths; Springer-Verlag, Berlin, Germany.

de Waal, S.A. (1970): Nickel minerals from Barberton, South Africa, II. nimite, a nickel-rich chlorite; American Mineralogist, v. 55, p. 18–30.

Eccles, D.R. and Luth, R.W. (2001): Major and trace element geochemistry of ultramafic diatremes in Alberta; Alberta Energy and Utilities Board, EUB/AGS Earth Sciences Report 2001-15, 52 p.

Field, M. and Scott Smith, B.H. (1998): Contrasting geology and near-surface emplacement of kimberlite pipes in Southern Africa and Canada; *in* Proceedings of the Seventh International Kimberlite Conference, Cape Town, South Africa, 1998, J.J. Gurney, J.L. Gurney, M.D. Pascoe and S.H. Richardson (ed.); Red Roof Design cc, South Africa, v. 1, p. 214–237.

Hawthorne, J.B. (1975): Model of a kimberlite pipe; Physics and Chemistry of the Earth, v. 9, p. 1–15.

Heimstra, S.A. and de Waal, S.A. (1968): Nickel minerals and Barberton, II. nimite, a nickelian chlorite; National Institute of Metallurgy (South Africa), Research Report 3444, p. 1–10.

Jago, B.C. and Mitchell, R.H. (1985): Mineralogy and petrology of the Ham kimberlite, Somerset Island, Northwest Territories, Canada, Canadian Mineralogist, v. 23, p. 619-634.

Jaques, A.L., Lewis, J.D. and Smith, C.B. (1986): The kimberlites and lamproites of Western Australia;

Geological Survey of Western Australia, Bulletin 132, 268 p.

Mitchell, R.H. (1979): The alleged kimberlite-carbonatite relationship: additional contrary mineralogical evidence; American Journal of Science, v. 279, p. 570–589.

Mitchell, R.H. (1986): Kimberlites: Mineralogy, Geochemistry and Petrology; Plenum Press, New York, 442 p.

Mitchell, R.H. (1994): Suggestions for revisions to the terminology of kimberlites and lamprophyres from a genetic viewpoint; *in* Proceedings of the Fifth International Kimberlite Conference, I. Kimberlites and Related Rocks and Mantle Xenoliths, H.O.A. Meyer and O.H. Leonardos (ed.); Companhia de Pesquisa de Recursos Minerais (Brasilia), Special Publication 1/A, p. 15–26.

Mitchell, R.H. (1995): Kimberlites, Orangeites and Related Rocks; Plenum Press, New York, 410 p.

Mitchell, R.H. and Bergman, S.C. (1991): Petrology of Lamproites; Plenum Press, New York, 447 p.

Mitchell, R.H. and Clarke, D.B. (1976): Oxide and sulphide mineralogy of the Peuyuk kimberlite, Somerset Island, N.W.T.; Contributions to Mineralogy and Petrology, v. 56, p. 157–172.

Podvysotskiy, V.T. (1985): Serpentine-carbonate mineralization in kimberlites; International Geology Review, Winston and Sons, Inc. United States, v. 27, p. 810–823 (*translated from* Serpentino-karbonatnaya mineralizatsiya v kimberliteakh; Zapiski Vsesoyuznogo Mineralogicheskogo Obshchestva, 1985, p. 234–247).

Scott Smith, B.H. (1992): Contrasting kimberlites and lamproites; Exploration and Mining Geology, v. 4, p. 127–140.

Scott Smith, B.H. (1995): Kimberlites; *in* Undersaturated Alkaline Rocks: Mineralogy, Petrogenesis and Economic Potential, R.H. Mitchell (ed.), Mineralogical Association of Canada, Short Course Series, v. 24, p. 217–243.

Skelton, D. and Bursey, T. (1998): Assessment report: Buffalo Head Hills property (AL01), Ashton Mining of Canada Inc.; Alberta EUB/AGS, Assessment File 19980015, 19 p.

Skinner, E.M.W. (1989): Contrasting group-1 and group-2 kimberlite petrology: towards a genetic model for kimberlites; *in* Proceedings of the Fourth International Kimberlite Conference (Perth), Geological Society of Australia, Special Publication 14, p. 528–544.

Skinner, E.M.W. and Clement, C.R. (1979): Mineralogical classification of southern African kimberlites; *in* Proceedings of the Second International Kimberlite Conference, I. Kimberlites, Diatremes and Diamonds: their Geology, Petrology and Geochemistry, F.R. Boyd and H.O.A. Meyer (ed.), American Geophysical Union, Washington, D.C., p. 129–139.

Skinner, E.M.W., Viljoen, K.S., Clark, T.C. and Smith, C.B. (1994): The petrography, tectonic setting and emplacement ages of kimberlites in the southwestern border region of the Kaapvaal craton, Prieska area; *in* Proceedings of the Fifth International Kimberlite Conference, Volume 1: Kimberlites and Related Rocks, H.O.A. Meyer and O.H. Leonardos (ed.), Companhia de Pesquisa de Recursos Minerals, Brazil, p. 80–97.

Smith, C.B. (1983): Pb, Sr and Nd isotopic evidence for sources of African Cretaceous kimberlite; Nature, v. 304, p. 51–54.

Smith, C.B., Gurney, J.J., Skinner, E.M.W., Clement, C.R. and Ebrahim, N. (1985): Geochemical character of southern African kimberlites: a new approach based upon isotopic constraints; Transactions Geological Society South Africa, v. 88, p. 267–280.

Wagner, P.A. (1914): The Diamond Fields of Southern Africa; Transvaal Leader, Johannesburg, South

Africa.

Wagner, P.A. (1928): The evidence of kimberlite pipes on the constitution of the outer part of the Earth; South African Journal of Science, v. 25, p. 127–148.

Woolley, A.R., Bergman, S.C., Edgar, A.D., Le Bas, M.J., Mitchell, R.H., Rock, N.M.S, Scott Smith, B.H. (1996): Classification of lamprophyres, lamproites, kimberlites and the kalsilitic, melilitic and leucitic rocks; The Canadian Mineralogist, v. 34, p. 175–186.

Appendix 1 – Electron-Microprobe Backscatter and X-Ray Elemental Images

Figure 21. Micro-image of sample ABK02, kimberlite K4B. A) and B) backscattered electron images; C) to L) x-ray elemental images.

Figure 22. Micro-image of sample ABK05, kimberlite K6. A) and B) backscattered electron images; C) to L) x-ray elemental images**.**

Figure 23. Micro-image of sample ABK59, Legend kimberlite. A) and B) backscattered electron images; C) to L) x-ray elemental images.

Figure 24. Micro-image of sample ABK76, Phoenix kimberlite. A) and B) backscattered electron images; C) to L) x-ray elemental images**.**

Figure 25. Micro-image of sample ABK81, Kendu kimberlite. A) and B) backscattered electron images; C) to L) x-ray elemental images**.**

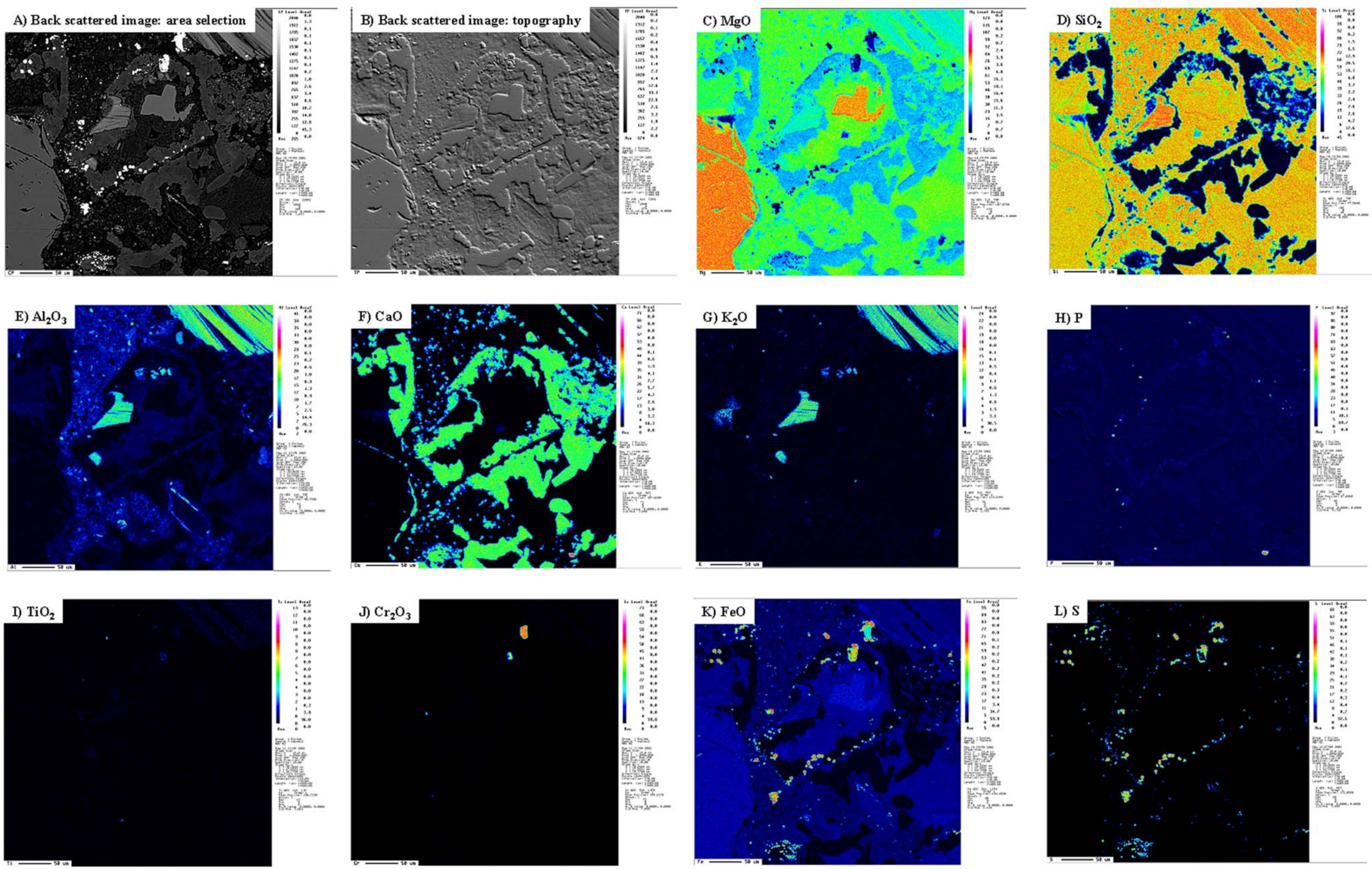

Figure 21. Micro-image of sample ABK02, kimberlite K4B. A) and B) backscattered electron images; C) to L) x-ray elemental images.

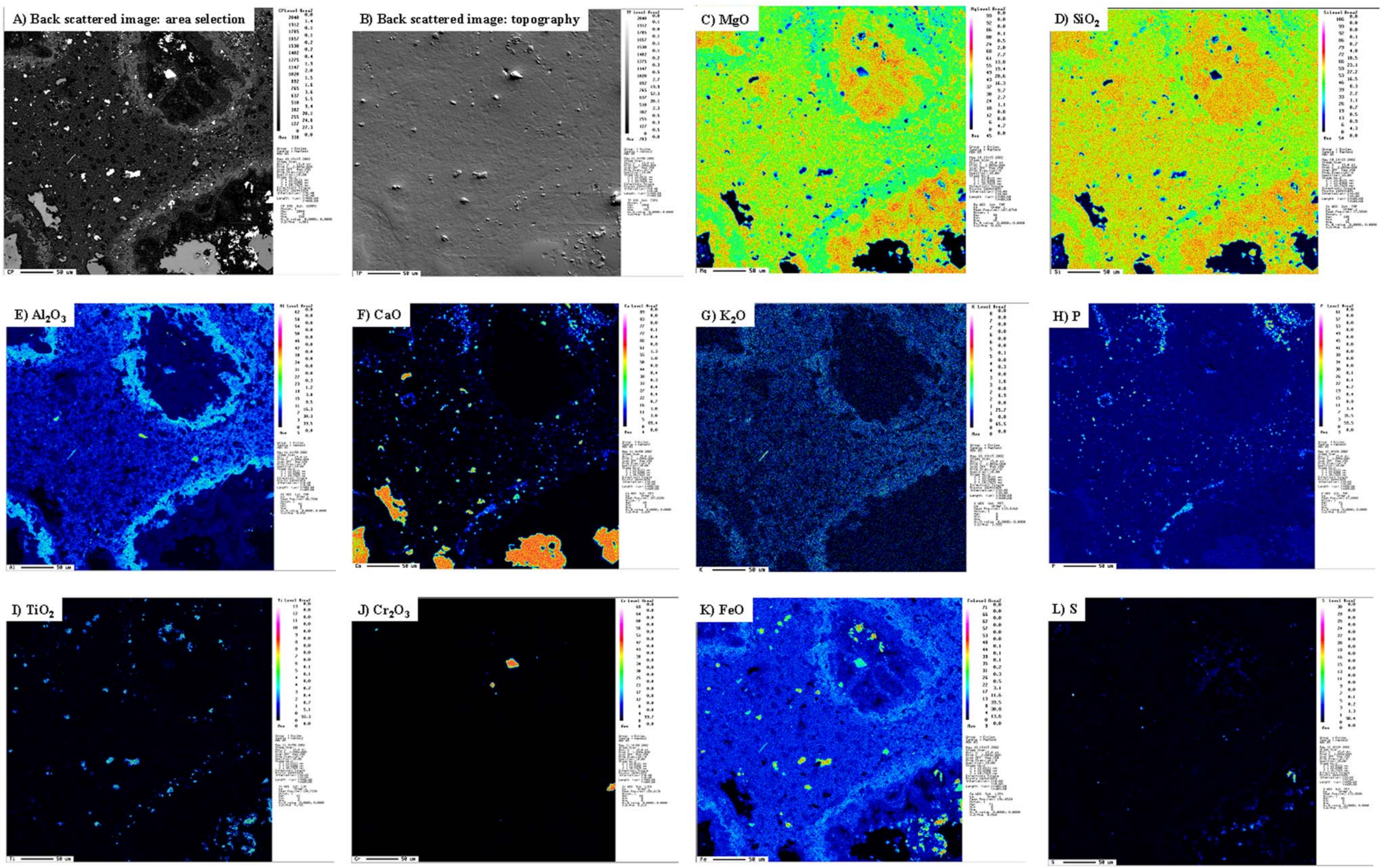

Figure 22. Micro-image of sample ABK05, kimberlite K6. A) and B) backscattered electron images; C) to L) x-ray elemental images.

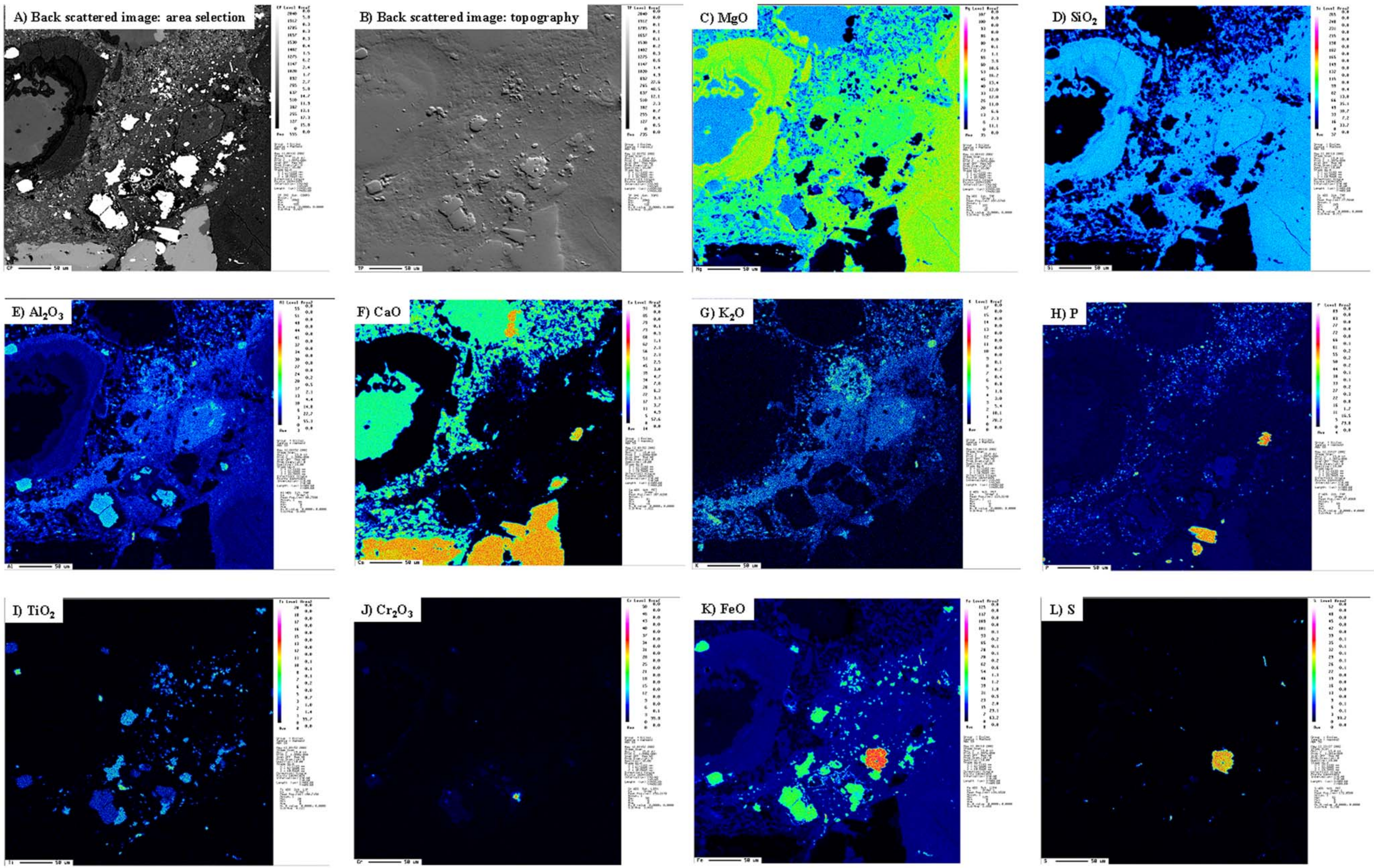

Figure 23. Micro-image of sample ABK59, Legend kimberlite. A) and B) backscattered electron images; C) to L) x-ray elemental images.

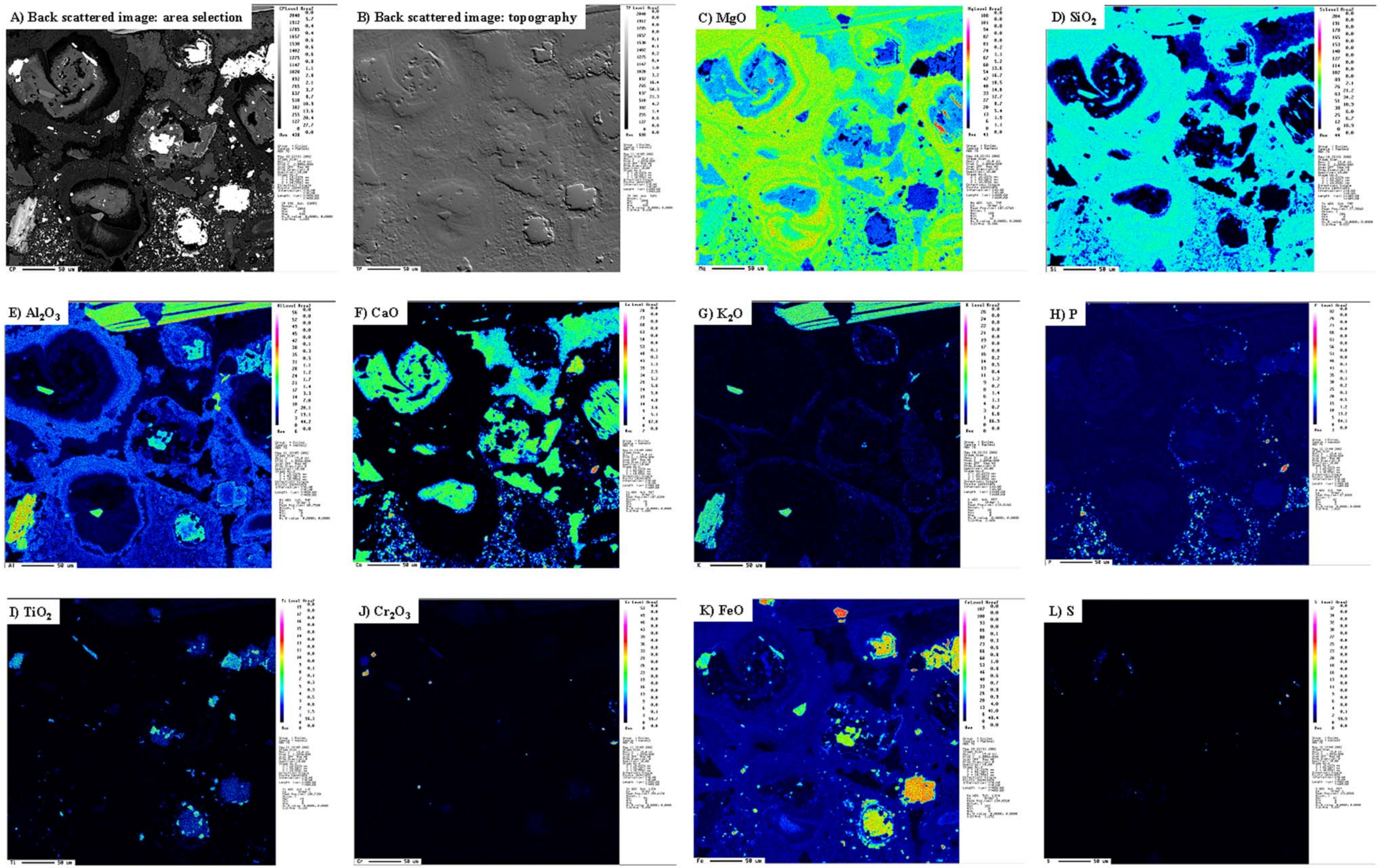

Figure 24. Micro-image of sample ABK76, Phoenix kimberlite. A) and B) backscattered electron images; C) to L) x-ray elemental images.

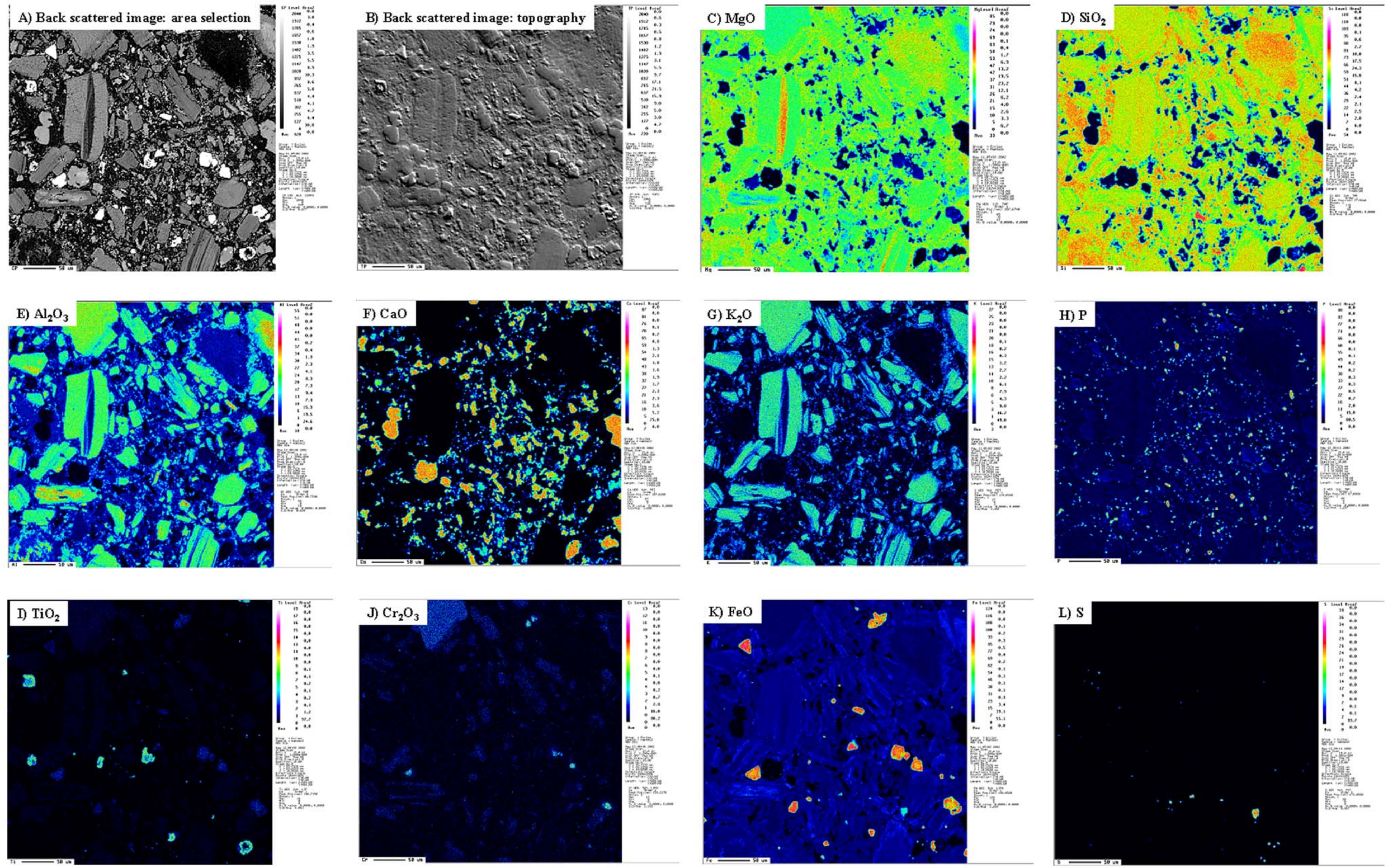

Figure 25. Micro-image of sample ABK81, Kendu kimberlite. A) and B) backscattered electron images; C) to L) x-ray elemental images.

Appendix 2 – Bulk-Rock X-Ray Diffractograms

Figure 26. X-ray diffractogram for sample ABK-01, kimberlite K4A, Buffalo Head Hills.

Figure 27. X-ray diffractogram for sample ABK-02, kimberlite K4B, Buffalo Head Hills.

Figure 28. X-ray diffractogram for sample ABK-03, kimberlite K4C, Buffalo Head Hills.

Figure 29. X-ray diffractogram for sample ABK-05, kimberlite K6, Buffalo Head Hills.

Figure 30. X-ray diffractogram for sample ABK-29, kimberlite K6, Buffalo Head Hills.

Figure 31. X-ray diffractogram for sample ABK-59, Legend kimberlite, Birch Mountains.

Figure 32. X-ray diffractogram for sample ABK-68, Legend kimberlite, Birch Mountains.

Figure 33. X-ray diffractogram for sample ABK-75, Phoenix kimberlite, Birch Mountains.

Figure 34. X-ray diffractogram for sample ABK-76, Phoenix kimberlite, Birch Mountains.

Figure 35. X-ray diffractogram for sample ABK-81, Kendu kimberlite, Birch Mountains.

Figure 36. X-ray diffractogram for sample ABK-82, Kendu kimberlite, Birch Mountains.

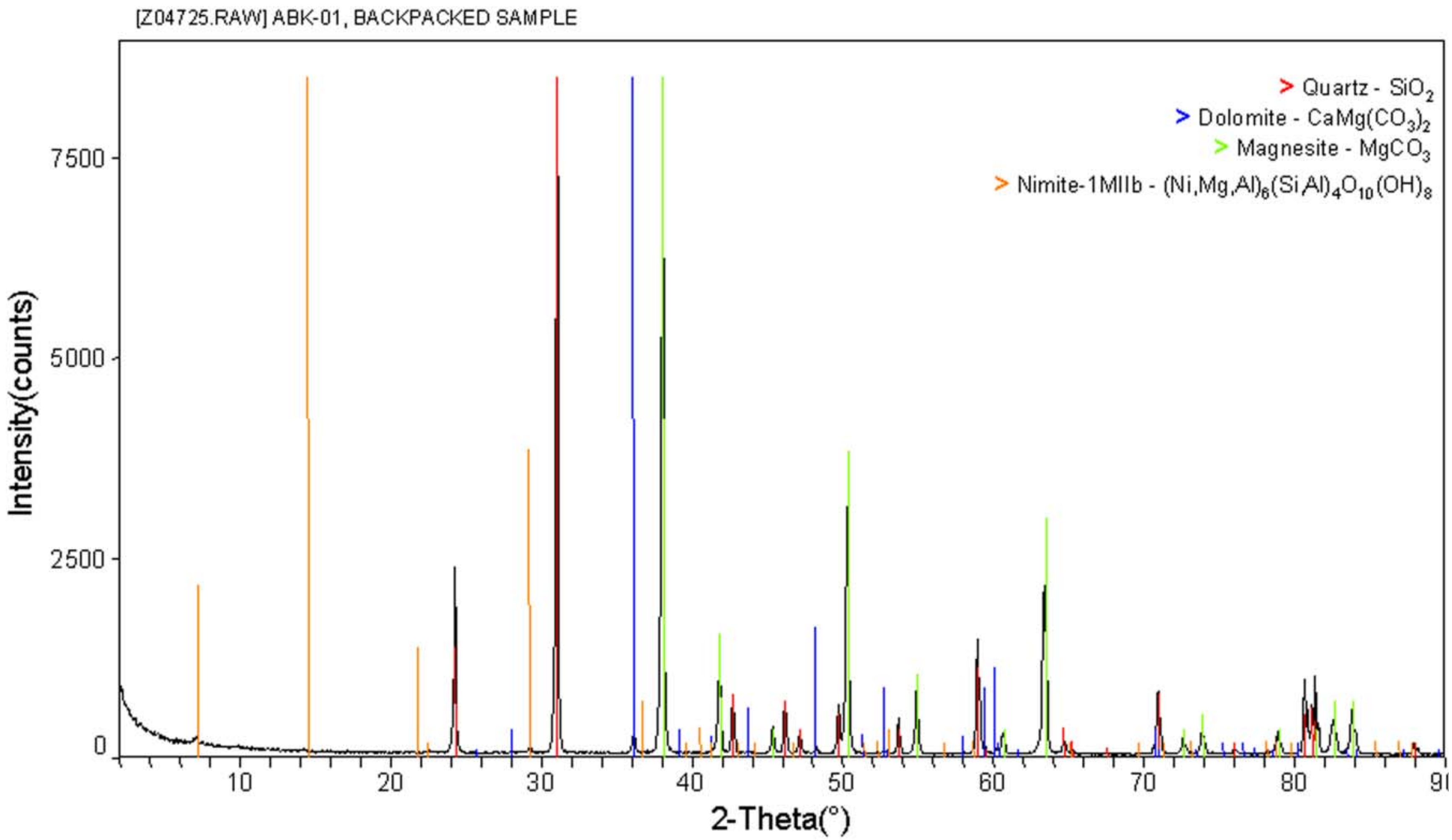

Figure 26. X-ray diffractogram for sample ABK-01, kimberlite K4A, Buffalo Head Hills.

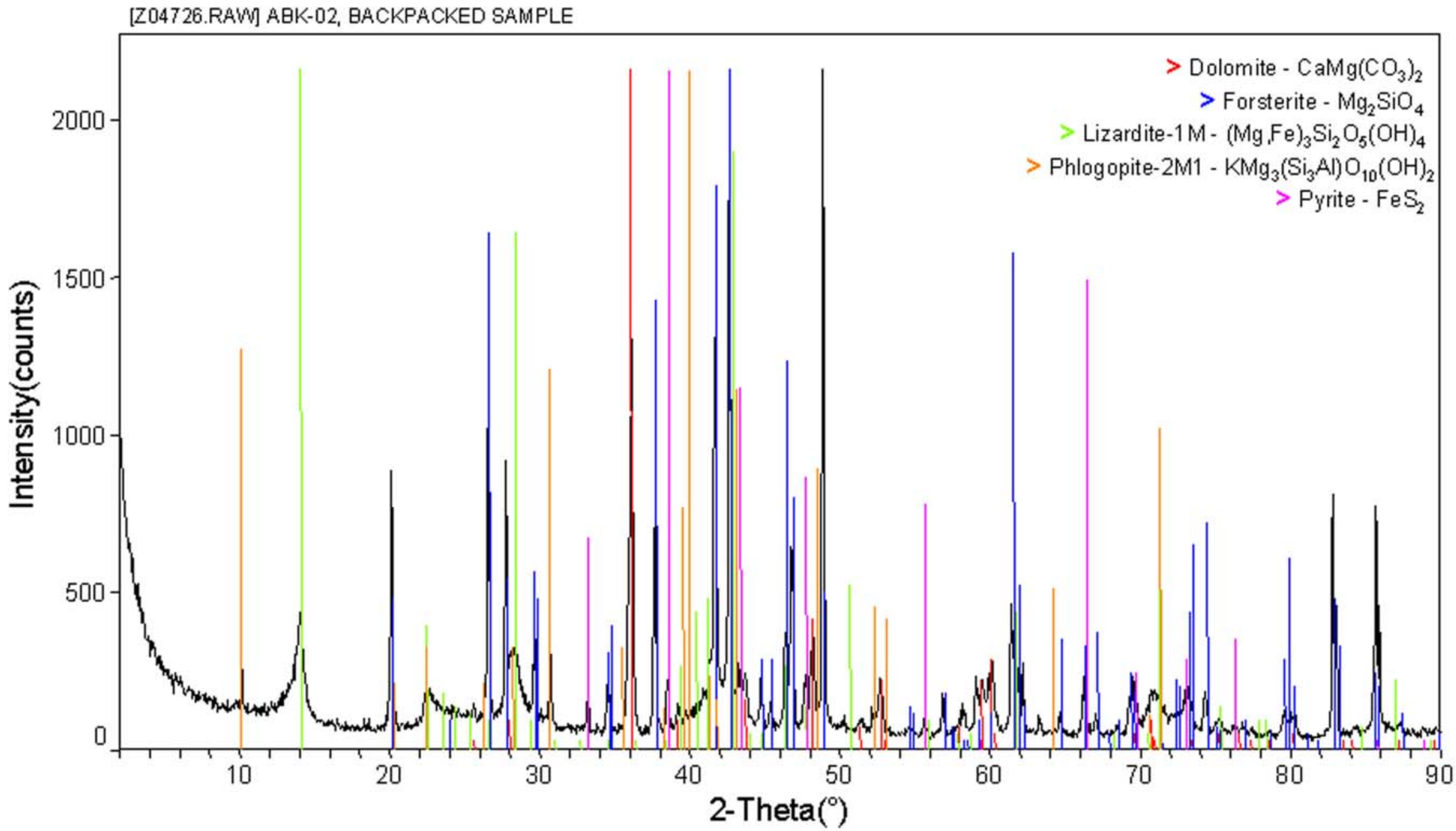

Figure 27. X-ray diffractogram for sample ABK-02, kimberlite K4B, Buffalo Head Hills.

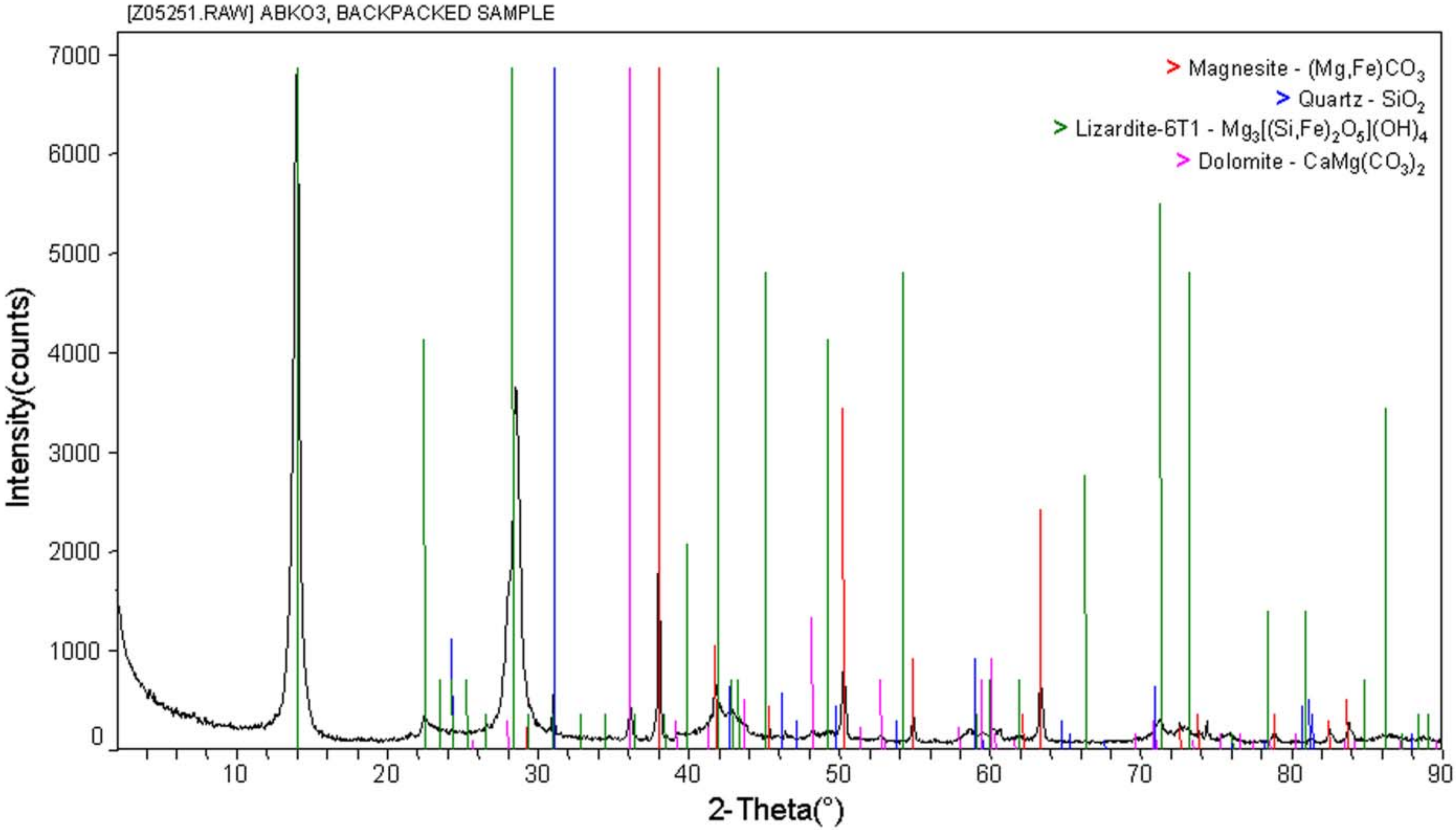

Figure 28. X-ray diffractogram for sample ABK-03, kimberlite K4C, Buffalo Head Hills.

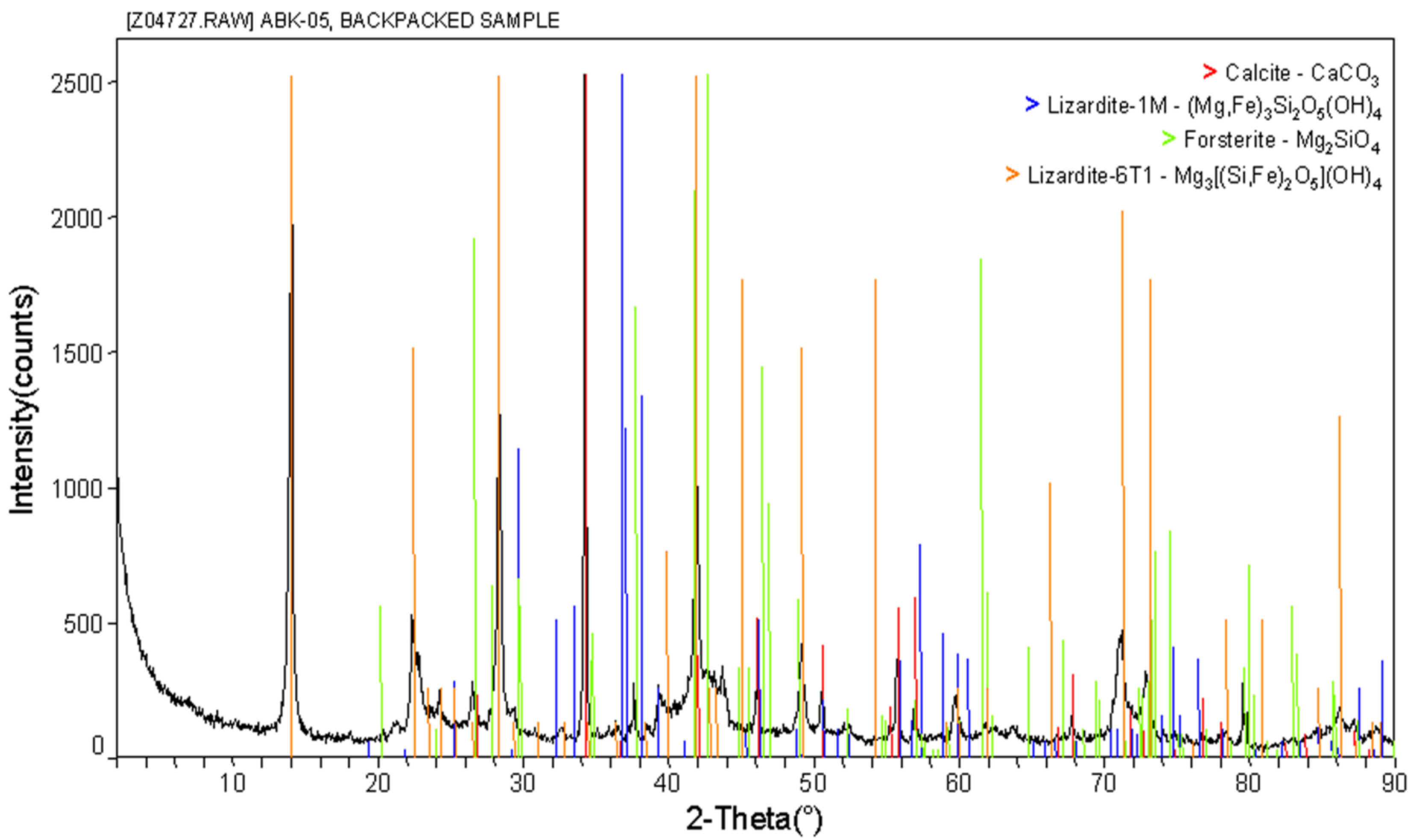

Figure 29. X-ray diffractogram for sample ABK-05, kimberlite K6, Buffalo Head Hills.

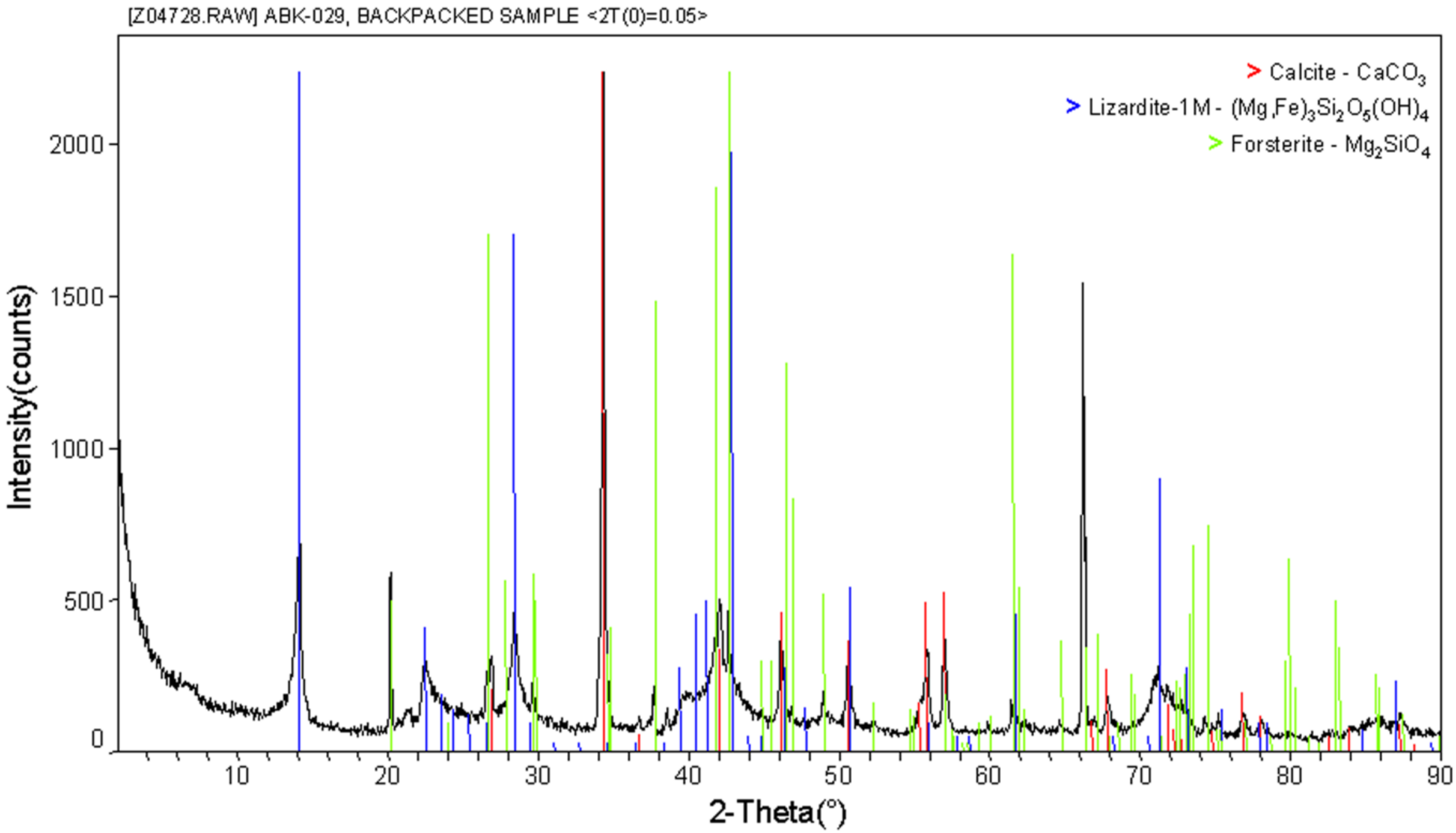

Figure 30. X-ray diffractogram for sample ABK-29, kimberlite K6, Buffalo Head Hills.

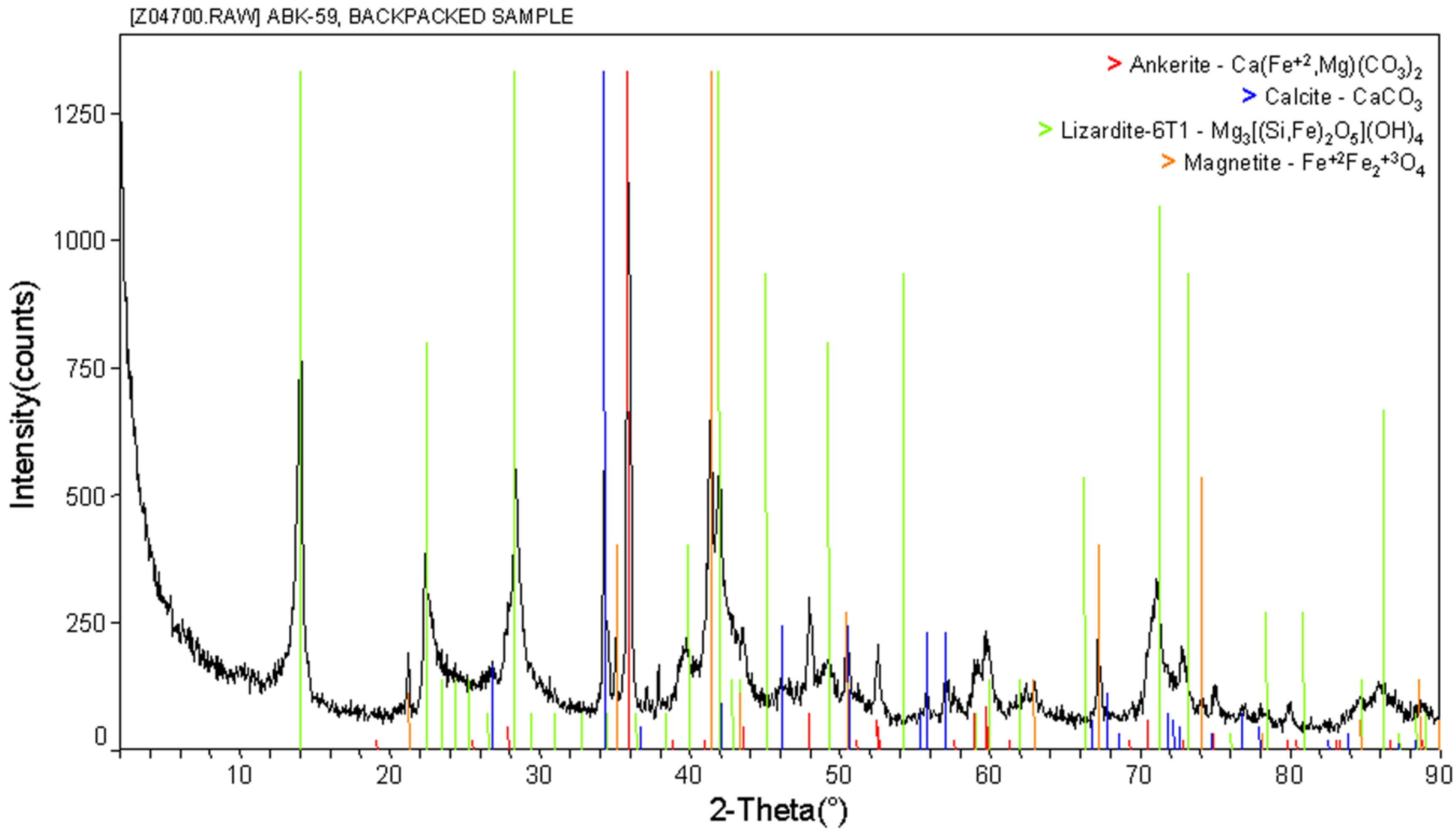

Figure 31. X-ray diffractogram for sample ABK-59, Legend kimberlite, Birch Mountains.

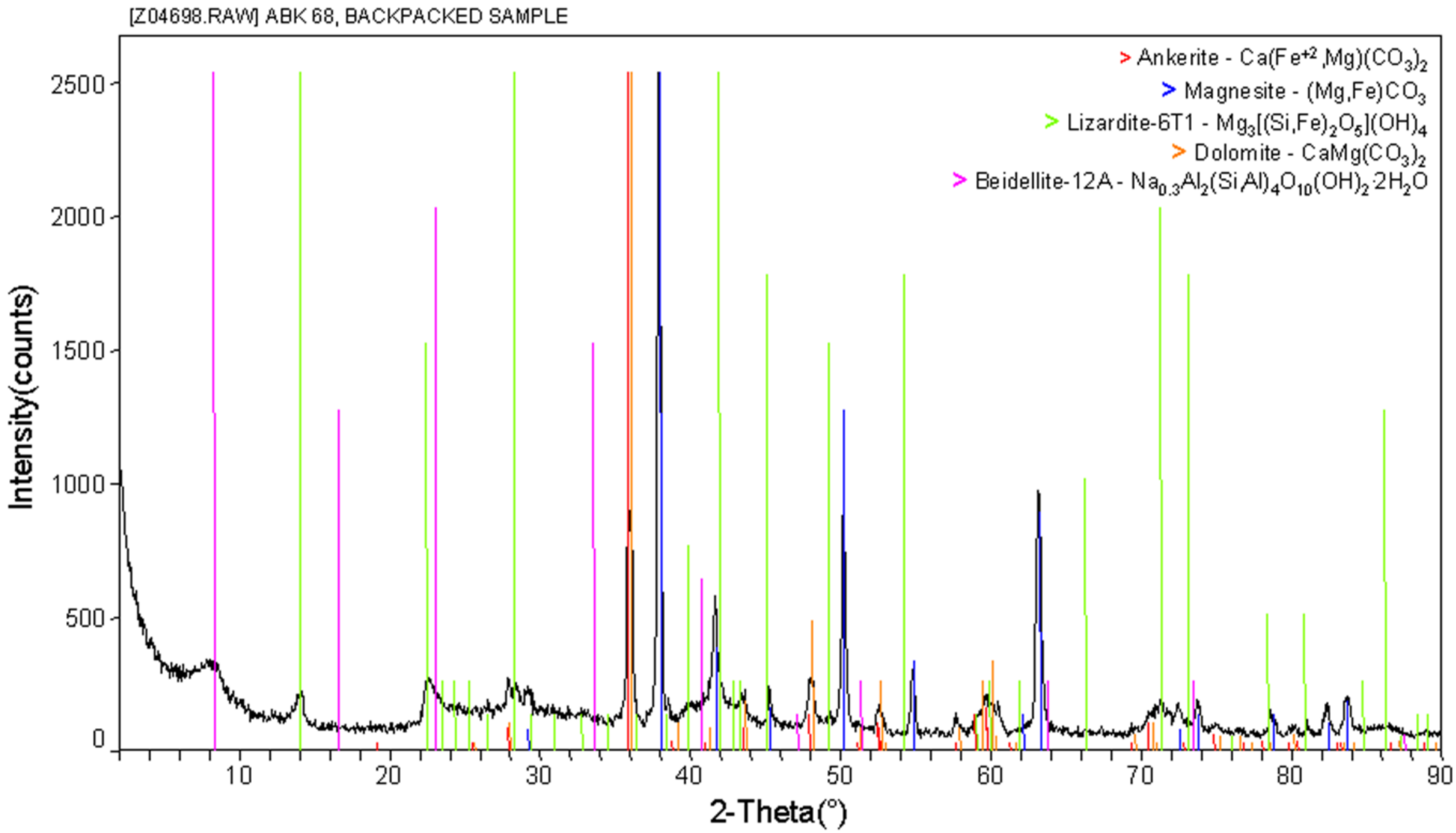

Figure 32. X-ray diffractogram for sample ABK-68, Legend kimberlite, Birch Mountains.

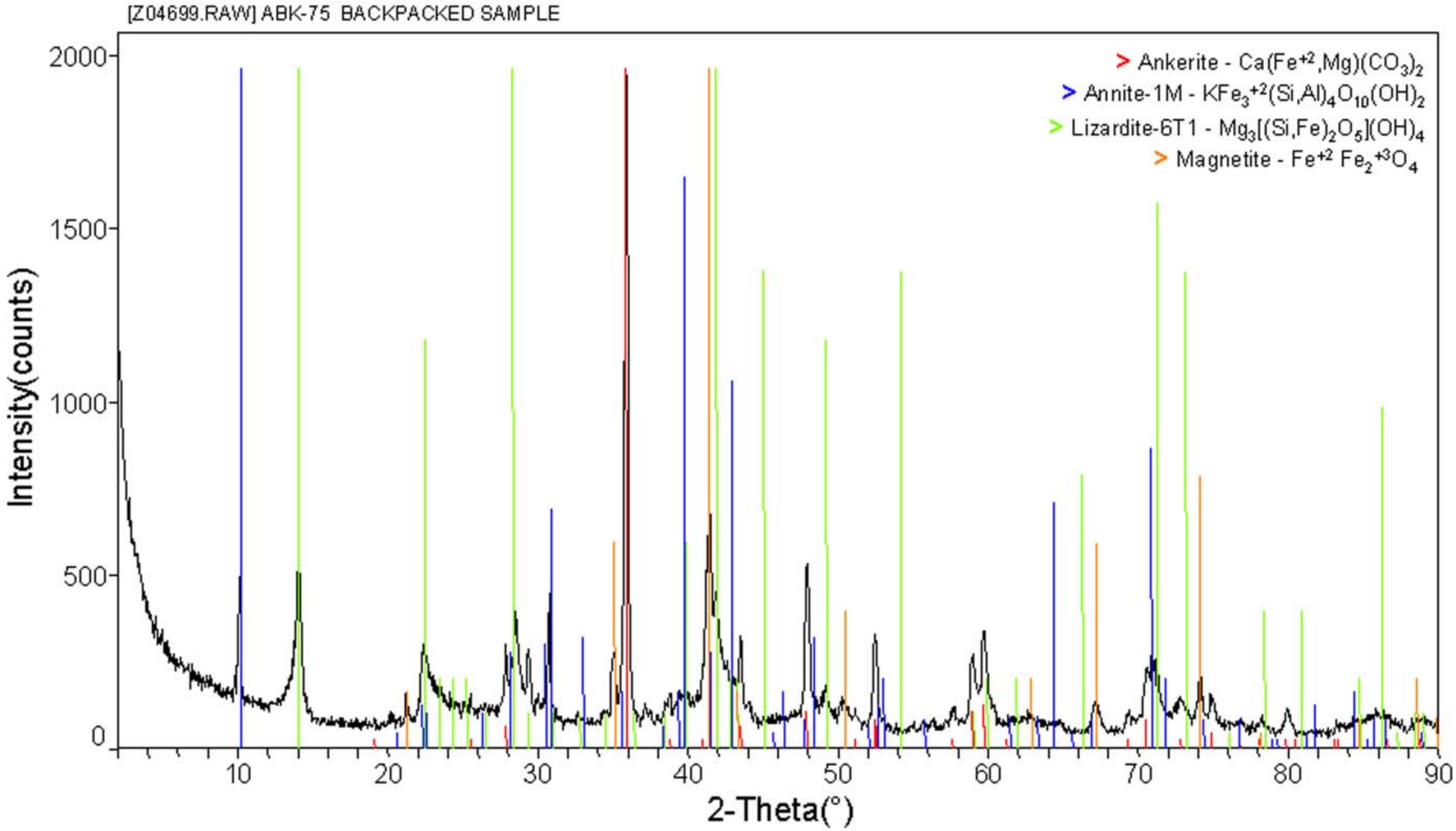

Figure 33. X-ray diffractogram for sample ABK-75, Phoenix kimberlite, Birch Mountains.

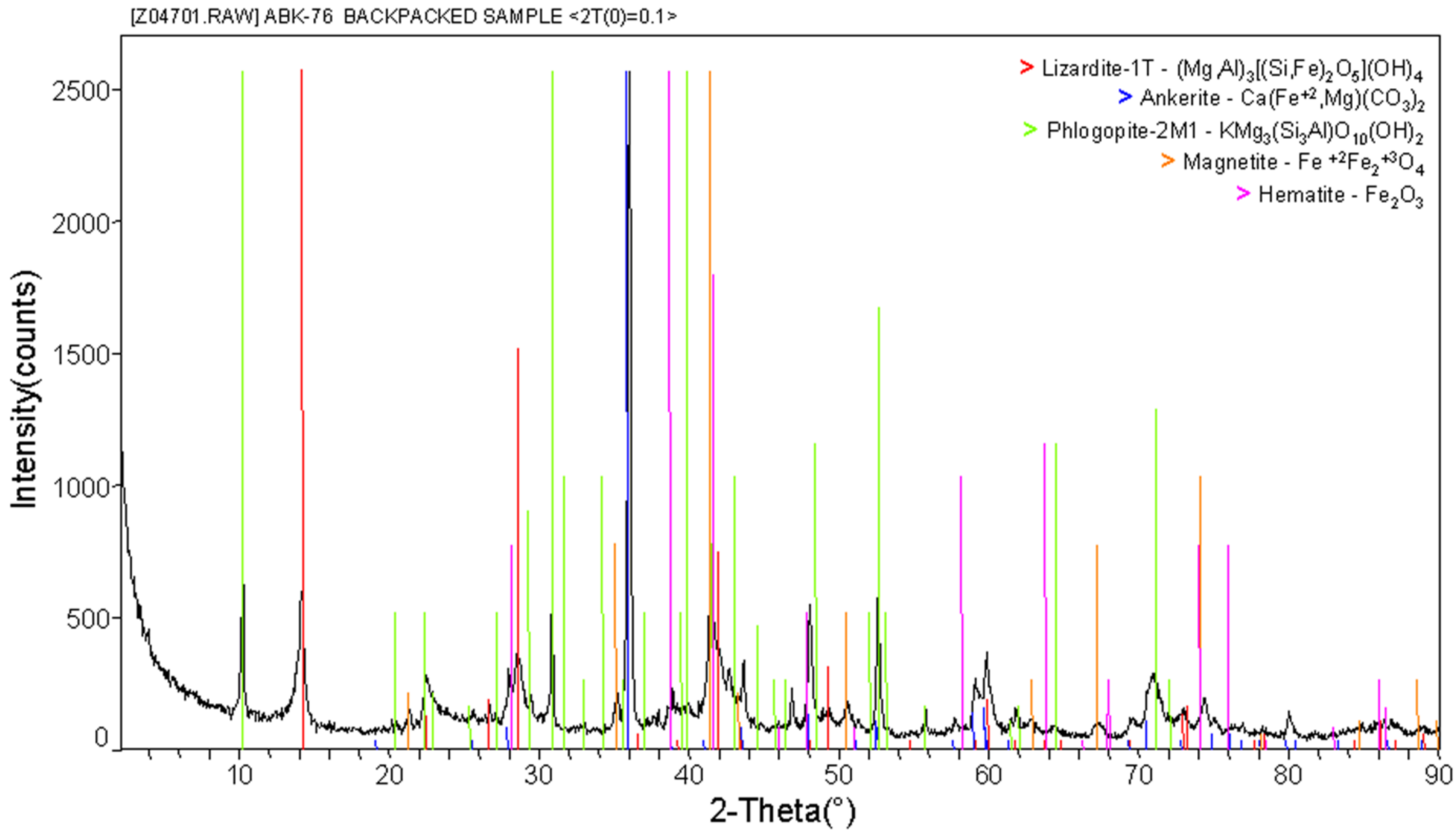

Figure 34. X-ray diffractogram for sample ABK-76, Phoenix kimberlite, Birch Mountains.

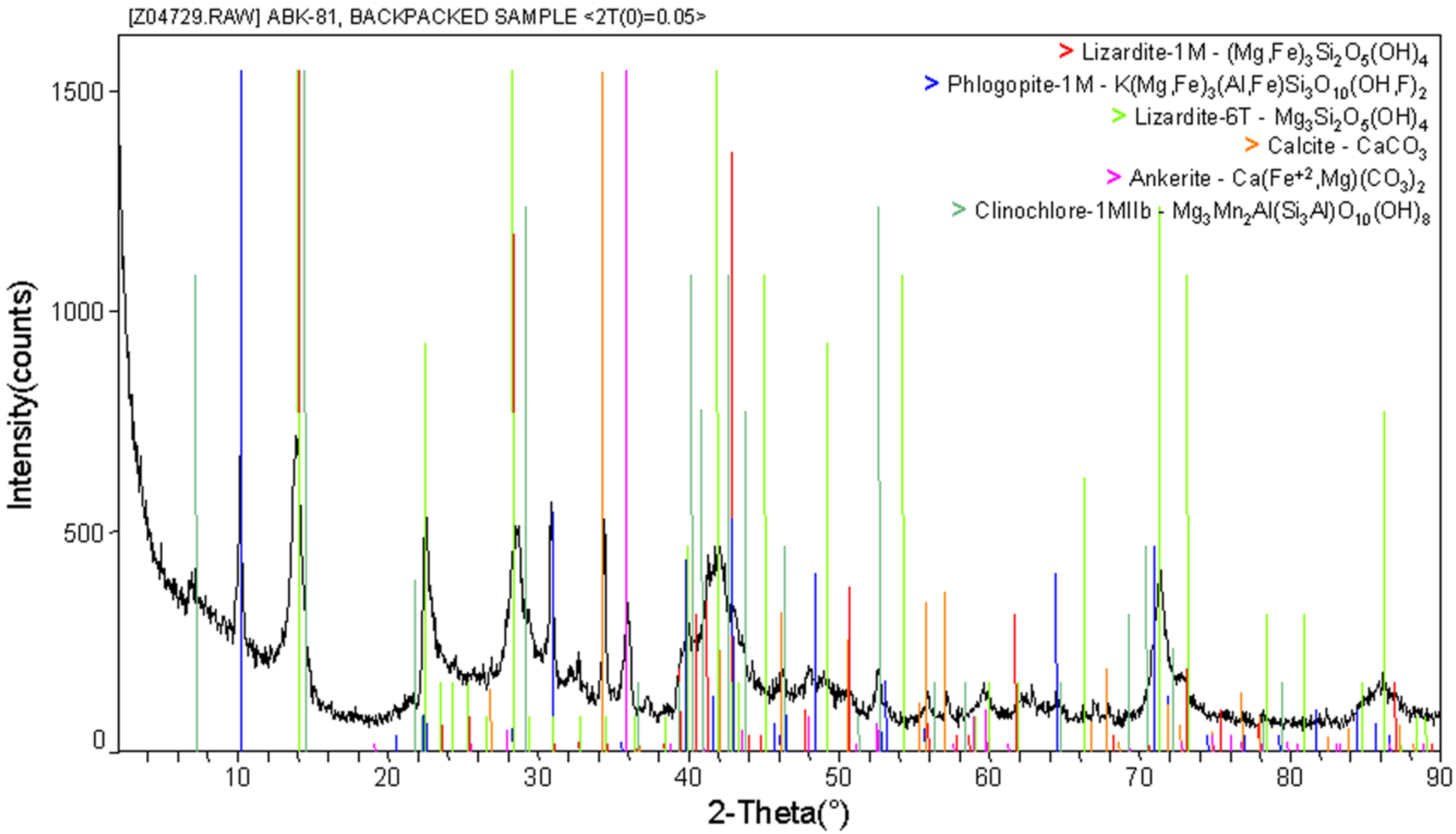

Figure 35. X-ray diffractogram for sample ABK-81, Kendu kimberlite, Birch Mountains.

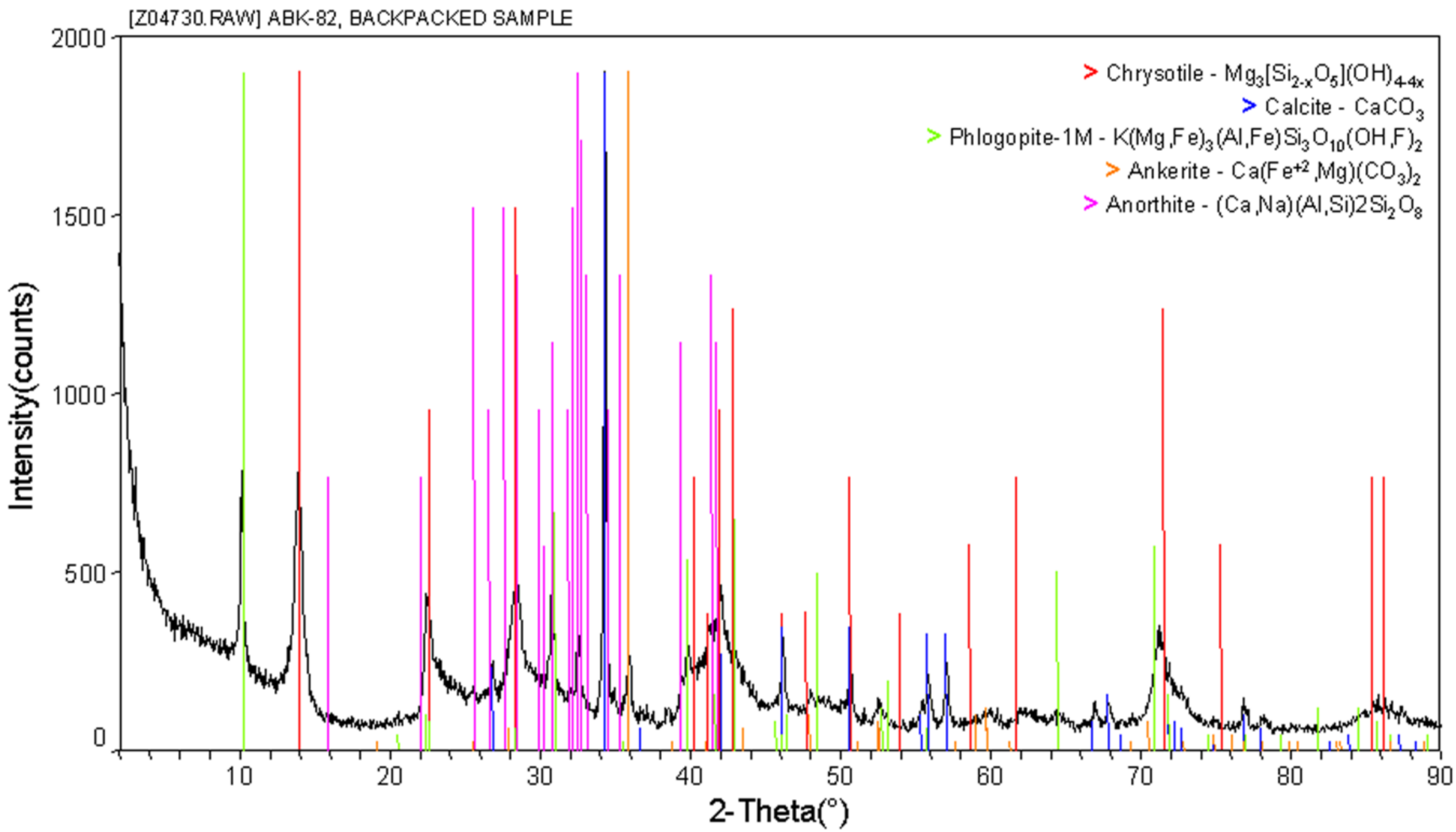

Figure 36. X-ray diffractogram for sample ABK-82, Kendu kimberlite, Birch Mountains.